ISSN 1881-7831 Online ISSN 1881-784X

DD&T

Drug Discoveries & Therapeutics

Volume 17, Number 6
December, 2023

IRCA BSSA

IACMHR

www.ddtjournal.com

DD&T
Drug Discoveries & Therapeutics

ISSN: 1881-7831
Online ISSN: 1881-784X
CODEN: DDTRBX
Issues/Year: 6
Language: English
Publisher: IACMHR Co., Ltd.

Drug Discoveries & Therapeutics is one of a series of peer-reviewed journals of the International Research and Cooperation Association for Bio & Socio-Sciences Advancement (IRCA-BSSA) Group. It is published bimonthly by the International Advancement Center for Medicine & Health Research Co., Ltd. (IACMHR Co., Ltd.) and supported by the IRCA-BSSA.

Drug Discoveries & Therapeutics publishes contributions in all fields of pharmaceutical and therapeutic research such as medicinal chemistry, pharmacology, pharmaceutical analysis, pharmaceutics, pharmaceutical administration, and experimental and clinical studies of effects, mechanisms, or uses of various treatments. Studies in drug-related fields such as biology, biochemistry, physiology, microbiology, and immunology are also within the scope of this journal.

Drug Discoveries & Therapeutics publishes Original Articles, Brief Reports, Reviews, Policy Forum articles, Case Reports, Communications, Editorials, News, and Letters on all aspects of the field of pharmaceutical research. All contributions should seek to promote international collaboration in pharmaceutical science.

Editorial Board

Editorial and Head Office:

Pearl City Koishikawa 603,
2-4-5 Kasuga, Bunkyo-ku,
Tokyo 112-0003, Japan
E-mail: office@ddtjournal.com

Drug Discoveries & Therapeutics

Editorial and Head Office

Pearl City Koishikawa 603, 2-4-5 Kasuga, Bunkyo-ku,
Tokyo 112-0003, Japan

E-mail: office@ddtjournal.com
URL: www.ddtjournal.com

Editorial Board Members

CONTENTS

Volume 17, Number 6, 2023

Review

Original Article

Brief Report

Correspondence

Review

DOI: 10.5582/ddt.2023.01086

Which biomarkers predict hard-to-heal diabetic foot ulcers? A scoping review

Qi Qin[1], Daijiro Haba[1,2], Gojiro Nakagami[1,2,*]

[1] Department of Gerontological Nursing/Wound Care Management, Graduate School of Medicine, The University of Tokyo, Tokyo, Japan;
[2] Global Nursing Research Center, Graduate School of Medicine, The University of Tokyo, Tokyo, Japan.

SUMMARY Diabetic foot ulcers (DFUs) often develop into hard-to-heal wounds due to complex factors. Several biomarkers capable of identifying those at risk of delayed wound healing have been reported. Controlling or targeting these biomarkers could prevent the progression of DFUs into hard-to-heal wounds. This scoping review aimed to identify the key biomarkers that can predict hard-to-heal DFUs. Studies that reported biomarkers related to hard-to-heal DFUs, from 1980 to 2023, were mapped. Studies were collected from the following databases: MEDLINE, CINAHL, EMBASE, and ICHUSHI (Japana Centra Revuo Medicina), search terms included "diabetic," "ulcer," "non-healing," and "biomarker." A total of 808 articles were mapped, and 14 (10 human and 4 animal studies) were included in this review. The ulcer characteristics in the clinical studies varied. Most studies focused on either infected wounds or neuropathic wounds, and patients with ischemia were usually excluded. Among the reported biomarkers for the prediction of hard-to-heal DFUs, the pro-inflammatory cytokine CXCL-6 in wound fluid from non-infected and non-ischemic wounds had the highest prediction accuracy (area under the curve: 0.965; sensitivity: 87.27%; specificity: 95.56%). CXCL-6 levels could be a useful predictive biomarker for hard-to-heal DFUs. However, CXCL6, a chemoattractant for neutrophilic granulocytes, elicits its chemotactic effects by combining with the chemokine receptors CXCR1 and CXCR2, and is involved in several diseases. Therefore, it's difficult to use CXCL6 as a prevention or treatment target. Targetable specific biomarkers for hard-to-heal DFUs need to be determined.

Keywords Delayed wound healing, prediction, prevention, treatment target

1. Introduction

Diabetic foot ulcer (DFU) is one of the major complications of diabetes mellitus, and one of the main causes of hard-to-heal wounds (*1*). A large-scale study conducted by the U.S. Wound Registry reported that within a 1-year follow-up period, around 33% of the DFUs failed to heal and developed into hard-to-heal wounds (*2*). Although the definition of a "hard-to-heal wound" varies, it can be broadly described as one that fails to heal with standard therapy in an orderly and timely manner (*3*). Hard-to-heal DFUs require sophisticated therapies that account for a large proportion of medical resources, with an average cost of $10,472 per episode (*4*). Despite the use of advanced treatments, this cohort experiences a greater risk of lower extremity amputations and mortality (*5,6*). Therefore, predicting the outcome early and replacing standard therapy with advanced therapies to return hard-to-heal wounds to a healing trajectory could be a useful approach to improving efficiency in wound care and minimizing the enormous burden on medical resources.

Wound healing is a dynamic and complex biological process that can be divided into four partly overlapping phases: hemostasis, inflammation, proliferation, and remodeling. These phases involve multiple functional cells, as well as cytokines, growth factors, and enzymes (*7,8*). Diabetes causes impaired wound healing by affecting one or more biological mechanisms that are triggered by hyperglycemia, micro- and macro-circulatory dysfunction, and tissue hypoxia (*9*). Therefore, to predict wound outcomes, two types of approaches have been adopted in previous studies, clinical and molecular biomarker assessments, which involve the macroscopic changes in the wound and the microscopic changes underneath during the wound healing process. Clinical assessment usually includes data such as the patients' basic characteristics, assessment of inflammatory signs, the efficiency of blood supply, and wound status. However, the prediction

rate is unsatisfactory, as a recent study has reported a prediction model using bedside assessment data with a 0.77 area under the curve (AUC) (*10*). In contrast, studies using molecular biomarkers such as C-X-C motif chemokine ligand 6 (CXCL6) exhibited a higher accuracy in predicting wound healing (*11*). However, patients with severe ischemia were not included in that study, so whether its results can be applied to people with angiopathy remains unknown. Several studies have extensively investigated dysregulated biomarkers related to wound healing, such as serpin family B member 3 (SERPINB3), miR-155, CXCL5, *etc.*, to elucidate the mechanism involved in delayed wound healing (*12-14*). The sensitivity and specificity of these biomarkers are unknown, and it is uncertain whether they can serve as predictive indicators for hard-to-heal DFUs in patients with any type of difficult-to-heal wounds.

We aimed to map biomarkers related to wound healing and identify the specific biomarkers that can be used to predict the progression of hard-to-heal DFUs, and answer the following research questions: (1) Which specific population among patients with DFUs was studied? (2) What is the definition of hard-to-heal DFUs in most studies? Or, how do most studies define a DFU exhibiting delayed healing? (3) What type of specimen was used to detect the biomarkers? (4) Which methods have been used to detect the biomarkers related to hard-to-heal DFUs? (5) Which analytical techniques were used to detect the biomarkers? (6) Which biomarkers were found to attribute to delayed wound healing in DFUs? (7) Can the detected biomarkers be used for the prediction of hard-to-heal wounds and what level of accuracy is provided by them?

2. Methods

2.1. Protocol

This scoping review was conducted by following the steps outlined in the Preferred Reporting Items for Systematic Reviews and Meta-Analyses (PRISMA)-ScR extension for scoping reviews (*15*).

2.2. Eligibility criteria

Population: People with DFUs, or diabetic animal models. Concept: Hard-to-heal wounds or wounds exhibiting delayed healing. Studies comparing delayed healing with non-diabetic wounds were excluded. Context: Delayed wound healing-related biomarkers. Original studies that reported molecular biomarkers related to hard-to-heal DFUs regardless of design, including clinical or animal experimental studies, were included in this scoping review. Both experimental and quasi-experimental study designs, including randomized controlled trials, non-randomized controlled trials, and before-and-after studies were considered. However, review papers were excluded. Since the definition of hard-to-heal wounds varied between studies, and many studies described hard-to-heal wounds as impaired wound healing, delayed wound healing, non-healing wounds, or poorly healed wounds; hence, we included all studies related to wound healing. The following studies were excluded: (1) Studies that addressed biomarkers that promote wound healing or are related to rapid healing. However, if the study reported the determination of biomarkers related to delayed wound healing and further experimentally confirmed their inhibitory effect on wound healing, they were included. (2) Studies that did not include people with diabetes or diabetic animal models, or those that only included comparisons with non-diabetic wounds. (3) Studies that did not describe the criteria for defining "hard-to-heal" wounds. (4) Studies that did not describe the biomarker sampling methods. (5) Studies not published in English or Japanese.

2.3. Information sources

The following electronic databases were searched and data from the inception of the database until the date on which the searches were performed (Oct 20, 2023) were included in the search: MEDLINE (PubMed interface), Cumulative Index to Nursing and Allied Health Literature (CINAHL), EMBASE, and ICHUSHI (Japan Medical Abstracts Society). These databases were searched using the following keywords: "diabetic foot" OR "diabetes mellitus" AND "wounds and injuries" AND "foot ulcer" OR "diabetic ulcer" OR "diabetic foot ulcer" OR "diabetic wound") AND "delayed wound healing" OR "non-healing" OR "impaired wound healing" OR "hard to heal" OR "poor wound healing" AND "biomarkers" OR "RNA" OR "proteins" OR "DNA".

2.4. Selection of sources of evidence

All the articles from the different databases were uploaded to a reference management software. Duplicate articles were removed. Two reviewers screened the titles and abstracts and excluded irrelevant studies, separately, based on the inclusion criteria. After screening the titles and abstracts, the full text of the articles was assessed and considered for review by two independent reviewers; the articles that matched the exclusion criteria were rejected and the reasons are shown in the flow chart. Next, the included studies were quantitatively synthesized. The whole process was conducted by two reviewers to screen the studies independently, and any lack of consensus was discussed with a third reviewer.

2.5. Data charting process

Data from eligible studies were charted by two

independent reviewers, using a data collection form developed by the authors.

2.6. Data items

We charted the following variables: study population and sample size, study design, patient/animal demographic data, wound characteristics (wound size, wound age, severity, and evaluation method), criteria of hard-to-heal DFUs, specimen-related information (sample type, collection method, collection timing, sample process, and sample storage conditions), targeted biomarkers (up-regulation/down-regulation and type of biomarker) and prediction accuracy.

The results were separated into two tables based on the subjects: human subject studies and animal subject studies, as shown in Table 1. Tables were produced to allow the comparison of the different collection techniques based on the key characteristics of the extracted data. One reviewer summarized it while the other reviewer double-checked the contents. Any lack of consensus was discussed with a third reviewer.

3. Results

3.1. Search flow (Figure 1)

The scoping review process is visually summarized in the flow diagram. Initially, a total of 808 records were identified from various databases, including CINAHL, EMBASE, MEDLINE, and ICHUSHI. After eliminating 86 duplicate records, the remaining 722 records underwent initial screening. Among these, 672 were excluded as they did not meet the specified inclusion criteria. In the subsequent screening phase, 50 reports were selected for retrieval. However, 21 of these reports could not be obtained due to various reasons, such as limited access to full-text articles or disparities in terms of population, concept, or context. During the eligibility assessment phase, 29 reports were thoroughly evaluated, resulting in the exclusion of 15 reports primarily due to their lack of alignment with the desired population and research concept. Ultimately, 14 studies were considered suitable for inclusion in the review, comprising 10 clinical studies and 4 animal studies.

3.2. Clinical studies (Table 1)

3.2.1. Which specific population among patients with DFUs was studied?

Among the nine clinical studies, six focused on diabetic neuropathic wounds, and one focused on infected wounds. Most studies focused on patients with diabetes aged between 18-90 years, presenting with neuropathic ulcers graded under the Texas Grading System, ranging from grades 2 to 3 (*11,13,16-19*). The majority of the patients were admitted to the inpatient department, and some studies had specific exclusion criteria for infection, such as systemic infection, being under microbial treatments, or other immunological disorders that might affect inflammatory markers (*11,16,19,20*). One study focused on patients with ischemic diabetic ulcers that required transluminal angioplasty and foot surgery (*21*), while MacDonald *et al.* focused on only infected diabetic foot ulcers (*22*).

3.2.2. What is the definition of hard-to-heal DFUs in most studies?

The definition of hard-to-heal or non-healing DFUs varied across studies. Common definitions included ulcers persisting or increasing in size, development of new ulcers, requirement of amputations, or patient death. Most studies defined non-healing as ulcers that did not heal or enlarged within a specific timeframe, commonly between three and six months, with six months being the most frequent benchmark (*11,13,16,17*). Some studies considered a wound size reduction of over 50% within four weeks as a healing ulcer (*18,19*), while others used a three-month period (*19,21*), and one study defined non-healing based on a one-year timeframe (*23*).

3.2.3. What type of specimen was used to detect the biomarkers?

Most studies utilized wound exudates, with some used serum (*18,21*), plasma (*17,23*), skin biopsies (*13,16*), or wound tissue samples (*19,22,23*). Wound exudates were mostly collected using the swabbing technique (*11,17,19,20*). These specimens were typically collected at the initial clinic visit or specific post-wounding time points in longitudinal studies.

3.2.4. Which methods and analytical techniques have been used to detect the biomarkers related to hard-to-heal DFUs?

The predominant method used for biomarker detection was Enzyme Linked Immunosorbent Assay (ELISA), since the studies primarily conducted protein analysis. Besides ELISA, studies employed techniques including proteomics analysis, protein arrays, multiplex immunoassay, real-time RT-PCR, and 16S rRNA genomic sequencing.

3.2.5. Which biomarkers were found to attribute to delayed wound healing in DFUs?

Several biomarkers were identified across the studies. These included downregulation of CXCL6 (*11*), ENA-78 (CXCL5) (*17*), SERPINB3, and upregulation of neutrophil elastase (*13,16*), citrullinates histone H3

Table 1. Clinical studies that reported potential biomarkers for predicting hard-to-heal DFUs

	Author, year, country	Wound characteristics	Definition of hard-to-heal	Specimen-related information	Analysis methods	Biomarkers	Accuracy of prediction
Protein	Wang *et al*., 2019, USA (*11*)	Diabetic neuropathic wounds Texas Grading System (grade 2–3) Exclusion: Ischemia, infection, and immunological disorder	Non-healing: Ulcer persisted or increased in size, new ulcers appeared, amputations were required, or the patient died.	Wound exudates (swab)	ELISA	CXCL6 ↓	AUC: 0.965 Cutoff value: 846.90 ng/mL Sensitivity: 87.27% Specificity: 95.56%
Protein	Li *et al*., 2019, China (*17*)	Diabetic neuropathic wounds Texas Grading System (grade 2–3)	Nonhealing: The ulcer persisted or was even enlarged, development of new ulcers, amputations, or death	Wound exudates (swab) and plasma	Protein array; candidate markers were then analyzed using ELISA	ENA-78↓	AUC: 0.705 (95% CI 0.608–0.801, $P < 0\,001$) Cutoff value: 1792.00 ng/mL Sensitivity:45.90% Specificity: 89.58%
Protein	Li *et al*., 2013, China (*18*)	Diabetic neuropathic wounds Texas Grading System (grade 1–3) Wound duration: 14 to 90 days Size: > 0.5 cm^2 Exclusion: Arteriopathy of the lower limbs	Poor healers: A decrease in wound area < 82% in 4 weeks	Serum samples at the first clinic visit and the end of 4-week treatment	ELISA for MMP-9, MMP-2, TIMP-1 and TIMP-2	MMP-9/TIMP-1 ratio↑	AUC:0.658 (Sensitivity: 63.6%; specificity: 58.6%)
Protein	Fadini *et al*., 2014, Italy (*13*)	Diabetic neuropathic wounds Exclusion: Ischemia, systematic infection	Non-healing: Ulcer persisted or was even enlarged in 6 months	Skin biopsy	Proteomics analysis, ELISA, Real-time RT-PCR	SerpinB3↓	AUC: 0.665 Sensitivity: 75%; Specificity: 62.5% Cutoff value: 1.13 ng/mL/ total protein μg/μl
Protein	Fadini *et al*., 2016, Italy (*16*)	Diabetic neuropathic wounds Exclusion: Ischemia, systematic infection	Non-healing: Ulcer persisted or was even enlarged in 6 months	Serum samples	ELISA (elastase, NGAL, lactoferrin, PR-3)	Neutrophil elastase↑	AUC: 0.815 (95% CI 0.686–0.944) (ulcer infection)
Protein	Yang *et al*., 2020, China (*23*)	Diabetic wounds Exclusion: Traumatic amputation, Buerger's disease, vasculitis, acute arterial occlusion	Non-healing: Did not heal in one year with multidisciplinary management of DFU	Peripheral blood plasma and wound tissues	ELISA (NET-related markers, elastase level)	CitH3↑, Neutrophil elastase↑	AUC: 0.84 [95% CI 0.76–0.90]
Protein	Loffle *et al*., 2011, Germany (*20*)	Diabetic ulcer located below the ankle Not receiving any antimicrobial treatments in 3 months	Healing: within no soft-tissue infection group: Healed within 6-month follow-up period	Wound fluid (swab)	Wound fluid lactate concentration	Lactate concentration↑	NA
Protein	Vieceli Dalla Sega *et al*., 2022, Italy (*21*)	Ischemic ulcer that requires percutaneous transluminal angioplasty and foot surgery	Optimal healing: healed at 3 months; Others: new limb revascularization, new lesions or recurrence	Peripheral blood serum	Multiplex immunoassay: sCD40L, IFN)-γ2, IFN-γ, 1RA, IL-2, IL-4, IL-5, IL-6, IL-10, IL-13, IL-18, TNF-α, Angiopoietin-2, Endoglin, Endothelin-1, sE-Selectin, Thrombomodulin, s-RAGE, sICAM-1, P-Selectin, sVCAM-1, and PAI-1; ELISA: vWF	Non-healing: sICAM-1 ↑, Endothelin-1↑ Revascularization: PAI-1↑, Endothelin-1↑ New lesions or recurrences: IL-10↑, IL1RA↑,sCD40L↑, Thrombomodulin↓	Decision tree accuracy for lower risk of new lesion: 0.812 (95% CI = 0.6192–0.937) (sCD40L < 18 pg/mL and thrombomodulin levels ≥ 2 pg/mL)

Table 1. Clinical studies that reported potential biomarkers for predicting hard-to-heal DFUs (continued)

	Author, year, country	Wound characteristics	Definition of hard-to-heal	Specimen-related information	Analysis methods	Biomarkers	Accuracy of prediction
Microbiome	MacDonald *et al.*, 2019, USA (22)	Infected diabetic foot ulcer	Persistent infections at week 12	Wound tissue debridement	16S rRNA genomic seq (microbial species) and qPCR (bacterial abundance)	Higher abundance of Bacteroidales and Streptococcaceae; Low level of Actinomycetales	NA
Microbiome	Min *et al.*, 2020, USA (*19*)	Vascularized plantar neuropathic DFU Duration; > 4 weeks Size: > 0.5 cm^2 Exclusion: Receiving antibiotics over 2 weeks	Non-healing wounds: < 50% closed by week 4	Plantar skin swab, ulcer debridement of the wound edge before wound cleansing.	16S rRNA next generation sequencing	Gram-positive anaerobic cocci ↑	NA

(citH3) (*23*), higher level of soluble intercellular adhesion molecule-1 (sICAM-1) and endothelin-1 (ET-1) (*21*), Gram-positive anaerobic cocci (*19*), and a higher abundance of Bacteroidales and Streptococcaceae and a lower level of Actinomycetales in non-healing wounds (*22*). In Vieceli Dalla Sega *et al*. study, they further mentioned that plasminogen activator inhibitor-1 (PAI-1) and ET-1 levels were associated with the need for revascularization within 12 months from the previous treatment. The levels of interleukin-10 (IL-10), IL1RA, and CD40L, were linked with an increased risk of developing new lesions or recurrences after DFU healing. Conversely, thrombomodulin levels were inversely associated with this risk (*21*).

3.2.6. Can the detected biomarkers be used for the prediction of hard-to-heal wounds and what level of accuracy is provided by them?

Several studies provided accuracy metrics for the biomarkers. For instance, CXCL6 exhibited a high level of predictive accuracy with an AUC of 0.965, indicating high sensitivity (87.27%) and specificity (95.56%) at a cutoff value of 846.90 ng/mL (*11*). ENA-78 had an AUC of 0.705 with a sensitivity of 45.90% and a specificity of 89.58% (*17*). SERPINB3 showed an AUC of 0.665 with a sensitivity of 75% and a specificity of 62.5% (*13*). Neutrophil elastase had an AUC of 0.815 (*16*), while CitH3 displayed an AUC of 0.84 (*23*). One study developed a decision tree for the endpoint of recurrences and new lesions based on sCD40L and thrombomodulin levels, which showed an accuracy of 0.812 (95% CI = 0.6192-0.937) for the outcome; however, the delayed wound healing prediction model was not shown (*21*). These metrics suggest that these biomarkers have potential predictive value for hard-to-heal DFUs.

3.3. Animal studies (Table 2)

3.3.1. Which specific population among animal models was studied?

The studies utilized various mouse models, including fibroblast growth factor-7 (FGF-7)-null diabetic mice (*24*), *p66Shc*-KO STZ-induced diabetic mice (*25*), *Flii*$^{+/-}$ mice (*26*), and *db/db* thrombospondin-2 (TSP2) KO mice (*27*).

3.3.2. What are the main findings?

Key findings included the significant delay in wound contraction and healing due to the absence of FGF-7 in diabetic mice (*24*), accelerated healing in *p66Shc* knockout diabetic mice (*25*), increased inflammation due to elevated Flii levels (*26*), and accelerated re-epithelialization in TSP2-deficient mice (*27*).

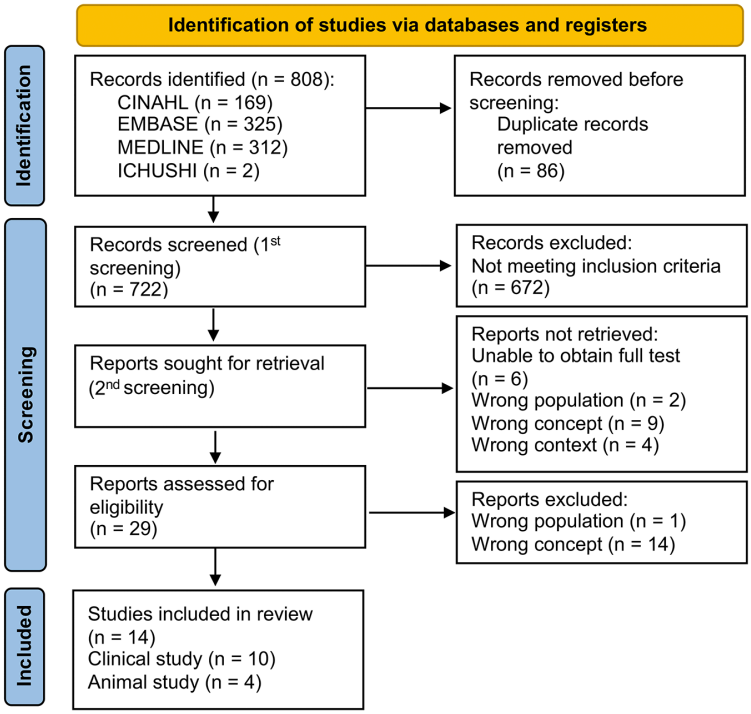

Figure 1. Scoping review flow diagram.

4. Discussion

The primary objective of this scoping review was to map biomarkers related to wound healing and to identify specific biomarkers that can predict the progression of hard-to-heal DFUs. Our findings provide a comprehensive overview of the current state of research in this area and highlight potential avenues for future investigations.

Our scoping review has identified several biomarkers associated with delayed wound healing in DFUs. The downregulation of CXCL6 in non-healing ulcers was highlighted by Wang *et al*. (2019) with high sensitivity and specificity, making it a potential promising biomarker for predicting hard-to-heal DFUs (*11*). CXCL6, a chemokine, is recognized for its involvement in various inflammatory processes. This finding underscores the central role inflammation plays in wound healing. Although our review did not find other studies directly supporting this observation, the significance of inflammation in wound healing is a recurring theme in the literature. While it exhibits high accuracy in predicting non-healing DFUs, it has also been implicated in various other diseases, including alcoholic liver disease (*28*), inflammatory bowel diseases and gastrointestinal tumors (*29*), neuro-inflammatory disease (*30*), and other inflammatory diseases (*31*). Because it is not specific to wounds, it might lead to false positives. Even if it could be used as a predictive measure, it might be a difficult treatment target. Li *et al*. (2019) reported the downregulation of ENA-78 in non-healing DFUs (*17*). ENA-78 plays a crucial role in neutrophil recruitment, further emphasizing the importance of inflammation in wound healing. This finding aligns with the broader understanding of inflammation's significance in wound healing, as seen in the studies by Wang *et al*. (2019) and Li *et al.* (2013) (*11,18*) which observed an increased matrix metalloproteinase (MMP-9)/TIMP-1 ratio in patients with poor wound healing. This balance between MMPs and TIMPs is essential for wound remodeling as described in many previous studies (*18,32-34*). While this observation is unique to their study, it offers a potential avenue for further research into the role of MMPs and TIMPs in wound healing. Loffle *et al.* (2011) found elevated lactate concentrations in the wound fluid of patients with soft-tissue infections. Lactate, a byproduct of anaerobic metabolism, can indicate tissue hypoxia or bacterial metabolism (*20*). Both factors can hinder wound healing. Fadini *et al*. (2014) noted a downregulation of SerpinB3 in rapidly healing ulcers (*13*). SerpinB3 is involved in various cellular processes, including apoptosis and inflammation. While this study suggests its potential protective role in wound healing, further studies are needed to confirm this observation and its implications. Levels of sICAM-1 and ET-1, both molecules expressed by the endothelium, were found to be inversely related to wound healing within three months in patients with critical limb ischemia (*21*). Elevated levels of these molecules are indicative of endothelial dysfunction. Elevated sICAM-1 levels are linked to inflammation and indicate either endothelial stimulation or damage. ET-1impacts vascular smooth muscle cells, serving as a powerful vasoconstrictor.

Table 2. Biomarkers of delayed wound healing in diabetic animal models

Author, year, country	Animal type	Wound model	Definition of delayed wound healing (hard-to-heal)	Specimen-related information	Analysis method	Biomarkers	Main findings
Peng *et al.*, 2011, China (*24*)	11-12 weeks old FGF-7-null diabetic mice: FGF-7 -/- Lepr db/db; FGF-7 null mice: FGF-7 -/- Lepr +/+; Diabetic mice: FGF-7 +/+ Lepr db/db; Wide type: FGF-7 +/+ Lepr +/+;	φ10 mm full-thickness dorsal excisional wound	Wound contraction rate: Contraction/initial area of wound size; Epithelialization rate: re-epithelialization/ (Initial area of wound size – contraction); Open wound rate: Open wound/initial area of wound size	For histological analysis: Wound tissue on day 7 and day 14 For RNA analysis: Wound tissue on day 7	Immunohistochemistry for Ki67; Real time PCR (α-SMA, Col-Ia, TGF-β1, bFGF,EGF, IGF-1)	FGF-7	Lack of FGF-7 in diabetic mice significantly delayed wound contraction and wound healing, however, did not affect reepithelialization of cutaneous compared to diabetic mice
Fadini *et al.*, 2010, Italy (*25*)	p66Shc-KO STZ-induced diabetic mice with and without hind limb ischemia; non-diabetic mice with or without hind limb ischemia	Diabetes (blood glucose level > 300 mg/dl). Hind limb ischemia (2 weeks after femoral artery ligation and excision) φ 4 mm full-thickness skin wounds	Wound size Healing time Granulation area	Wound tissue at mid-closure time	Histological analyses (H&E, MT, IF (B4-isolectin))	p66Shc	p66Shc knockout accelerates healing of diabetic and ischemic wounds. p66Shc knockout rescues the impaired granulation tissue in diabetic wounds.
Ruzehaji *et al.*, 2013, Australia (*26*)	12-16 weeks old female BALB/c Flii +/– (low Flii); WT (normal) STZ-induced diabetic mice; Flii Tg/Tg (high Flii) STZ-induced diabetic mice; Non-diabetic group	Two φ 6 mm full-thickness skin wounds	Wound area on day 7	Wound tissue on day 7 post-wounding	Immunohistochemistry for Flii, TLR9, TLR4, MyD88 and NF-kB.	Flii	Increased levels of Flii in diabetic mouse wounds led to increased TLR4 and NF-KB production which led to excessive inflammation and chronicity.
Kunkemoeller *et al.*, 2019, USA (*27*)	10–12-week db/db,DKO, STZ, and wild-type (WT) mice. db/db TSP2 KO (DKO)	two φ 6 mm full-thickness skin wounds	Wound closure time	3 mm wound surrounding tissue on 7, 10, or 14-days post-wounding	IHC (TSP2 , vimentin, CD31) Quantitative RT-PCR and Western Blot (TSP2, HSP90, O-GlcNAc ,OGT, and p65)	TSP2	TSP2 deficiency in diabetic mice accelerated reepithelialization and increased granulation tissue formation, fibroblast migration, and blood vessel maturation.

Indeed, elevated levels of ET-1 correlate with disrupted vascular tone control in diabetes (*35*). This might indicate that the variations in these biomarkers are attributable to the specific population of the study group, specifically, individuals with critical limb ischemia. In animal studies, it has been highlighted that FGF-7 is important for keratinocyte activity, and another study emphasized the role of p66Shc in inflammation and oxidative stress. Additionally, TSP2 was identified as an inhibitor of angiogenesis, which is essential for wound healing (*24-26*). While these findings are based on animal research, they present potential therapeutic targets to enhance wound healing in humans, which need to be further confirmed through clinical studies. It's noteworthy that some biomarkers, such as neutrophil elastase, were recurrent in multiple studies, suggesting a shared pathway or mechanism in delayed wound healing. The consistent theme across these studies is inflammation's role, as highlighted by markers like CXCL6 and ENA-78. Therefore, targeting inflammation could be a key strategy in promoting wound healing in DFUs.

While these biomarkers present promising prospects for predicting hard-to-heal wounds, their seamless integration into clinical practice poses challenges. Notably, some of the identified biomarkers lack specificity for wounds, as they can be elevated due to other systemic conditions. Consequently, while they may serve as predictive measures, utilizing them as treatment targets or for prevention might be intricate. For instance, biomarkers like CXCL6 and neutrophil elastase, although associated with wound healing, are also implicated in various inflammatory conditions including alcoholic liver disease (*28*), inflammatory bowel diseases and gastrointestinal tumors (*29*), neuro-inflammatory disease (*30*), and other inflammatory diseases (*31*). Thus, relying solely on these biomarkers without considering the broader clinical context may not be advisable. In the studies included in this review, the primary approach employed was the assessment of proteins, and the predominant method for collecting wound exudate was swabbing. However, it is crucial to acknowledge that the components of exudate collected *via* swabs predominantly consist of fresh wound exudate, which may differ from exudate collected over extended periods (*36,37*).

The studies incorporated into this review primarily concentrated on wounds characterized by vascular impairments or infections, with a particular emphasis on specific types of DFUs. Consequently, the biomarkers identified in these studies may have a pathological basis. However, it's important to note that this focus could potentially constrain the applicability of the findings to other types of DFUs. Furthermore, the study designs exhibited variation, encompassing both cross-sectional and longitudinal approaches; however, biomarkers were measured at a single time point in all the studies, and their cutoff levels could vary across different wound healing phases, potentially affecting the preventive strategies. Additionally, in some studies, the sample sizes were relatively small, which could potentially impact the robustness and generalizability of the findings.

Given the inherent limitations and the dynamic nature of biomedical research, future investigations can substantially benefit from the pursuit of shared biomarkers by incorporating diverse populations of individuals with various types of DFUs and utilizing a broader range of animal hard-to-heal wound models. Furthermore, continuous evaluation, involving comprehensive protein or gene expression analyses of samples that reflect the real-time conditions of the wound, such as exudate or cells collected from wound dressings, may yield deeper insights into the cellular dynamics significant to the wound healing process and advance our comprehension of it. Additionally, the use of high-resolution techniques, like single-cell RNA sequencing, represents a promising avenue for further research. This advanced methodology offers superior resolution of cellular responses and holds the potential to reveal novel biomarkers or pathways crucial to wound healing. Embracing such mechanism-driven approaches can yield more precise and actionable insights for guiding clinical interventions.

This review provides a comprehensive overview of the current state of research on biomarkers associated with hard-to-heal DFUs. However, it is important to acknowledge that our review is constrained by the existing body of literature. There might be unpublished studies or ongoing research that could provide additional insights. Additionally, the heterogeneity in study designs and populations might affect the comparability of the findings.

5. Conclusion

In conclusion, this scoping review has scoped a range of biomarkers associated with delayed wound healing in DFUs. Although these findings hold promise for potential clinical interventions, the generalizability and specificity of these biomarkers must undergo further validation. In the future, the adoption of advanced, mechanism-based research approaches has the potential to yield more precise insights, thereby paving the way for targeted interventions aimed at addressing the challenges posed by hard-to-heal DFUs.

Funding: This work was supported by the Fusion Oriented REsearch for disruptive Science and Technology (FOREST) from the Japan Science and Technology Agency (Grant No. JPMJFR205H) and JSPS KAKENHI (Grant No. 23KJ0482).

Conflict of Interest: The authors have no conflicts of interest to disclose.

References

1. van Netten JJ, Bus SA, Apelqvist J, Lipsky BA, Hinchliffe RJ, Game F, Rayman G, Lazzarini PA, Forsythe RO, Peters EJG, Senneville É, Vas P, Monteiro-Soares M, Schaper NC, International Working Group on the Diabetic Foot. Definitions and criteria for diabetic foot disease. Diabetes Metab Res Rev. 2020; 36(Suppl 1):e3268.
2. Fife CE, Horn SD, Smout RJ, Barrett RS, Thomson B. A predictive model for diabetic foot ulcer outcome: The wound healing index. Adv Wound Care (New Rochelle). 2016; 5:279-287.
3. Atkin L, Bućko Z, Conde Montero E, Cutting K, Moffatt C, Probst A, Romanelli M, Schultz GS, Tettelbach W. Implementing TIMERS: the race against hard-to-heal wounds inflammation/infection social factors edge regeneration moisture tissue. J Wound Care. 2019; 28:S1-S50.
4. Chan B, Cadarette S, Wodchis W, Wong J, Mittmann N, Krahn M. Cost-of-illness studies in chronic ulcers: A systematic review. J Wound Care. 2017; 26:S4-S14.
5. Armstrong DG, Swerdlow MA, Armstrong AA, Conte MS, Padula W V, Bus SA. Five-year mortality and direct costs of care for people with diabetic foot complications are comparable to cancer. J Foot Ankle Res. 2020; 13:16.
6. Boulton AJM, Armstrong DG, Kirsner RS, Attinger CE, Lavery LA, Lipsky BA, Mills JL Sr, Steinberg JS. Diagnosis and management of diabetic foot complications. In: ADA Clinical Compendia. Arlington, VA, 2018; pp.1-20.
7. Stolzenburg-Veeser L, Golubnitschaja O. Mini-encyclopaedia of the wound healing - Opportunities for integrating multi-omic approaches into medical practice. J Proteomics. 2018; 18:71-84.
8. Barrientos S, Stojadinovic O, Golinko MS, Brem H, Tomic-Canic M. Growth factors and cytokines in wound healing. Wound Repair Regen. 2008; 16:585-601.
9. Baltzis D, Eleftheriadou I, Veves A. Pathogenesis and treatment of impaired wound healing in diabetes mellitus: new insights. Adv Ther. 2014; 31:817-836.
10. Bender C, Cichosz SL, Pape-Haugaard L, Hartun Jensen M, Bermark S, Laursen AC, Hejlesen O. Assessment of simple bedside wound characteristics for a prediction model for diabetic foot ulcer outcomes. J Diabetes Sci Technol. 2020; 15:1161-1167.
11. Wang X, Li J, Wang Z, Deng A. Wound exudate CXCL6: A potential biomarker for wound healing of diabetic foot ulcers. Biomark Med. 2019; 13:167-174.
12. Botusan IR, Sunkari VG, Savu O, Catrina AI, Grünler J, Lindberg S, Pereira T, Ylä-Herttuala S, Poellinger L, Brismar K, Catrina SB. Stabilization of HIF-1α is critical to improve wound healing in diabetic mice. Proc Natl Acad Sci U S A. 2008; 105:19426-19431.
13. Fadini GP, Albiero M, Millioni R, Poncina N, Rigato M, Scotton R, Boscari F, Brocco E, Arrigoni G, Villano G, Turato C, Biasiolo A, Pontisso P, Avogaro A. The molecular signature of impaired diabetic wound healing identifies serpinB3 as a healing biomarker. Diabetologia. 2014; 57:1947-1956.
14. Mori R, Tanaka K, Shimokawa I. Identification and functional analysis of inflammation-related miRNAs in skin wound repair. Dev Growth Differ. 2018; 60:306-315.
15. Tricco AC, Lillie E, Zarin W, *et al*. PRISMA extension for scoping reviews (PRISMA-ScR): Checklist and explanation. Ann Intern Med. 2018; 169:467-473.
16. Fadini GP, Menegazzo L, Rigato M, *et al.* NETosis delays diabetic wound healing in mice and humans. Diabetes. 2016; 65:1061-1071.
17. Li JY, Wang ZJ, Deng AP, Li YM. ENA-78 is a novel predictor of wound healing in patients with diabetic foot ulcers. J Diabetes Res. 2019; 2019:2695436.
18. Li Z, Guo S, Yao F, Zhang Y, Li T. Increased ratio of serum matrix metalloproteinase-9 against TIMP-1 predicts poor wound healing in diabetic foot ulcers. J Diabetes Complications. 2013; 27:380-382.
19. Min KR, Galvis A, Baquerizo Nole KL, Sinha R, Clarke J, Kirsner RS, Ajdic D. Association between baseline abundance of *Peptoniphilus*, a Gram-positive anaerobic coccus, and wound healing outcomes of DFUs. PLoS One. 2020; 15:e0227006.
20. Löffler M, Zieker D, Weinreich J, Löb S, Königsrainer I, Symons S, Bühler S, Königsrainer A, Northoff H, Beckert S. Wound fluid lactate concentration: A helpful marker for diagnosing soft-tissue infection in diabetic foot ulcers? Preliminary findings. Diabetic Med. 2011; 28:175-178.
21. Vieceli Dalla Sega F, Cimaglia P, Manfrini M, Fortini F, Marracino L, Bernucci D, Pompei G, Scala A, Trichilo M, De Carolis B, Dalla Paola L, Ferrari R, Rizzo P, Campo G. Circulating biomarkers of endothelial dysfunction and inflammation in predicting clinical outcomes in diabetic patients with critical limb ischemia. Int J Mol Sci. 2022; 23:10641.
22. MacDonald A, Brodell JD, Daiss JL, Schwarz EM, Oh I. Evidence of differential microbiomes in healing versus non-healing diabetic foot ulcers prior to and following foot salvage therapy. J Orthop Res. 2019; 37:1596-1603.
23. Yang S, Gu Z, Lu C, Zhang T, Guo X, Xue G, Zhang L. Neutrophil extracellular traps are markers of wound healing impairment in patients with diabetic foot ulcers treated in a multidisciplinary setting. Adv Wound Care (New Rochelle). 2020; 9:16-27.
24. Peng C, Chen B, Kao HK, Murphy G, Orgill DP, Guo L. Lack of FGF-7 further delays cutaneous wound healing in diabetic mice. Plast Reconstr Surg. 2011; 128:673e-684e.
25. Fadini GP, Albiero M, Menegazzo L, Boscaro E, Pagnin E, Iori E, Cosma C, Lapolla A, Pengo V, Stendardo M, Agostini C, Pelicci PG, Giorgio M, Avogaro A. The redox enzyme p66Shc contributes to diabetes and ischemia-induced delay in cutaneous wound healing. Diabetes. 2010; 59:2306-2314.
26. Ruzehaji N, Mills SJ, Melville E, Arkell R, Fitridge R, Cowin AJ. The influence of Flightless I on Toll-like-receptor-mediated inflammation in a murine model of diabetic wound healing. Biomed Res Int. 2013; 2013:389792.
27. Kunkemoeller B, Bancroft T, Xing H, Morris AH, Luciano AK, Wu J, Fernandez-Hernando C, Kyriakides TR. Elevated thrombospondin 2 contributes to delayed wound healing in diabetes. Diabetes. 2019; 68:2016-2023.
28. Jiang Y, Xi Y, Li Y, Zuo ZH, Zeng CY, Fan J, Zhang D, Tao HL, Guo YC. Ethanol promoting the upregulation of C-X-C Motif Chemokine Ligand 1 (CXCL1) and C-X-C Motif Chemokine Ligand 6 (CXCL6) in models of early alcoholic liver disease. Bioengineered. 2022; 13:4688-4701.
29. Singh UP, Singh NP, Murphy EA, Price RL, Fayad R, Nagarkatti M, Nagarkatti PS. Chemokine and cytokine

levels in inflammatory bowel disease patients. Cytokine. 2016; 77:44-49.
30. Lepennetier G, Hracsko Z, Unger M, Van Griensven M, Grummel V, Krumbholz M, Berthele A, Hemmer B, Kowarik MC. Cytokine and immune cell profiling in the cerebrospinal fluid of patients with neuro-inflammatory diseases. J Neuroinflammation. 2019; 16:219.
31. Russo RC, Garcia CC, Teixeira MM, Amaral FA. The CXCL8/IL-8 chemokine family and its receptors in inflammatory diseases. Expert Rev Clin Immunol. 2014; 10:593-619.
32. Muller M, Trocme C, Lardy B, Morel F, Halimi S, Benhamou PY. Matrix metalloproteinases and diabetic foot ulcers: The ratio of MMP-1 to TIMP-1 is a predictor of wound healing. Diabetic Med. 2008; 25:419-426.
33. Sonamuthu J, Cai Y, Liu H, Kasim MSM, Vasanthakumar VR, Pandi B, Wang HX, Yao JM. MMP-9 responsive dipeptide-tempted natural protein hydrogel-based wound dressings for accelerated healing action of infected diabetic wound. Int J Biol Macromol. 2020; 153:1058-1069.
34. Luanraksa S, Jindatanmanusan P, Boonsiri T, Nimmanon T, Chaovanalikit T, Arnutti P. An MMP/TIMP ratio scoring system as a potential predictive marker of diabetic foot ulcer healing. J Wound Care. 2018; 27:849-855.
35. Mather KJ, Mirzamohammadi B, Lteif A, Steinberg HO, Baron AD. Endothelin contributes to basal vascular tone and endothelial dysfunction in human obesity and type 2 diabetes. Diabetes. 2002; 51:3517-3523.
36. Fivenson DP, Faria DT, Nickoloff BJ, Poverini PJ, Kunkel S, Burdick M, Strieter RM. Chemokine and inflammatory cytokine changes during chronic wound healing. Wound Repair Regen. 1997; 5:310-322.
37. Schmohl M, Beckert S, Joos TO, Königsrainer A, Schneiderhan-Marra N, Löffler MW. Superficial wound swabbing: A novel method of sampling and processing wound fluid for subsequent immunoassay analysis in diabetic foot ulcerations. Diabetes Care. 2012; 35:2113-2120.

Received October 24, 2023; Revised December 11, 2023; Accepted December 13, 2023.

*Address correspondence to:
Gojiro Nakagami, Department of Gerontological Nursing/ Wound Care Management, Graduate School of Medicine, The University of Tokyo, 7-3-1 Hongo, Bunkyo-Ku, Tokyo 113-0033, Japan.
E-mail: gojiron@g.ecc.u-tokyo.ac.jp

Released online in J-STAGE as advance publication December 22, 2023.

Review

DOI: 10.5582/ddt.2023.01096

Polycystic ovary syndrome and adverse pregnancy outcomes: Potential role of decidual function

Lisha Li[1,2,3,§], Hanting Ge[4,§], Jing Zhou[1,2,3], Jing Wang[1,2,3,*], Ling Wang[1,2,3,*]

[1] Laboratory for Reproductive Immunology, Obstetrics and Gynecology Hospital of Fudan University, Shanghai, China;
[2] The Academy of Integrative Medicine of Fudan University, Shanghai, China;
[3] Shanghai Key Laboratory of Female Reproductive Endocrine-related Diseases, Shanghai, China;
[4] Reproductive Medicine Center, The Fourth Affiliated Hospital Zhejiang University School of Medicine, Yiwu, Zhejiang, China.

SUMMARY Polycystic ovary syndrome (PCOS) is a common endocrine disorder affecting fertility and mental health among women of reproductive age. In addition to anovulation and hyperandrogenism, patients also experience metabolic issues, such as insulin resistance, obesity, and dyslipidemia, as well as chronic low-grade inflammation throughout the body. Recent studies have shown that even with assisted reproductive technology to treat anovulatory issues, patients with PCOS still have higher rates of adverse pregnancy outcomes and abortion compared to normal pregnancies. These findings suggest that PCOS may impair the endometrium and disrupt the onset and maintenance of healthy pregnancies. Decidualization is a crucial step in the process of healthy pregnancy, during which endometrial stromal cells (ESCs) differentiate into secretory decidual stromal cells (DSCs) regulated by hormones and local metabolism. This article comprehensively reviews the pathological processes of PCOS and the mechanisms involved in its impaired decidualization. In addition, we explore how PCOS increases the incidence of adverse pregnancy outcomes (APO). By gaining a better understanding of the adverse effects of PCOS on pregnancy and its specific mechanisms, we hope to provide a theoretical basis for reducing APO and improving the live birth rate among women with PCOS.

Keywords polycystic ovary syndrome, decidualization, adverse pregnancy outcomes, insulin resistance, inflammation

1. Introduction

Polycystic ovarian syndrome (PCOS) is the most prevalent reproductive endocrinopathy affecting women of reproductive age, with a predicted prevalence of 6%-10%, based on diagnostic criteria (*1*). PCOS is known for causing fertility-related challenges such as decreased fecundity, anovulation or oligo-ovulation, reduced oocyte competence, and impaired endometrial receptivity (*1-3*). The increased risk of adverse pregnancy outcomes and iatrogenic ovarian hyperstimulation syndromes are linked to PCOS patients' greater prevalence of assisted reproductive technologies (ARTs) (*4*). Additionally, pregnant women with PCOS are more likely to experience pregnancy- and neonatal-related problems (*5,6*). Research has shown that pregnant women with PCOS experience a 3 to 4 times higher incidence of gestational hypertension (GHTN), pre-eclampsia (PE), and gestational diabetes mellitus (GDM) compared to healthy women (*6-8*). Studies showed greater risk of miscarriage, preterm delivery, and intrauterine growth restriction (IUGR) among women who experience these adverse pregnancy outcomes (*9*). These unfavorable effects are thought to be caused by PCOS-affected women's aberrant hormone levels and metabolic malfunction. Previous systematic reviews and meta-analyses have linked PCOS in pregnancy with higher fasting blood glucose (FBG) levels, decreased levels of high-density lipoprotein (HDL), and high levels of serum androgen (*10,11*). As pregnancy progresses, mothers experience a natural increase in insulin resistance (IR) and androgen levels to supply energy to the growing fetus (*12*) and regulate critical processes during pregnancy and childbirth (*13*). However, in women with PCOS, the imbalance of beneficial and adverse effects of endocrine changes can lead to pathological alterations, resulting in an overexpression of metabolic pathways and potentially causing adverse outcomes for the pregnancy, fetal growth, and neonatal health (*14*).

Establishing the maternal-fetal interface as well as sustaining and growing the placenta depend on the decidualization of endometrial stromal cells (*15*). Due

to the heterogeneous phenotype of PCOS patients and multiple confounding factors, the pathogenic mechanisms of PCOS for adverse pregnancy outcomes are difficult to identify with precision. However, new literature reports progressively point to negative effects of PCOS on endometrial stromal cell decidualization impairment during the first trimester of pregnancy. This review summarizes current knowledge on PCOS-related decidualization impairment and discusses the role of decidualization in adverse pregnancy outcomes for women with PCOS.

2. The impact of PCOS on pregnancy

2.1. PCOS

PCOS is a complex and heterogeneous disease. The Rotterdam criteria requires the presence of at least two out of three features: oligo- or anovulation, hyperandrogenism (HA), and polycystic ovary morphology observed *via* ultrasound (*16*). The condition is lifelong and can have origins in fetal life, often being associated with intrauterine growth retardation or post-term birth (*17*). PCOS is characterized by reduced reproductive capacity and endocrine disturbances. The former includes infertility and adverse pregnancy outcomes, and the latter involves alteration in the levels of sex hormones as well as their stimulating hormones and clinical or laboratorial metabolic disorders such as IR, type II diabetes, dyslipidemia and a higher risk of cardiovascular disease. We hypothesized that the hormonal and metabolic disorders presented in PCOS patients may be the intrinsic pathological factors causing pregnancy disorders. We focus on the decidualization process in particular since it is essential for the creation and maintenance of pregnancy. And the specific molecular mechanisms of which will be described in detail later.

2.2. Pathogenic factors of PCOS

HA is a defining characteristic of PCOS, contributing to hormonal dysregulation and the development of small follicles in the ovaries. IR is a common metabolic disturbance in PCOS, characterized by impaired insulin sensitivity and elevated insulin levels. HA and IR influence each other, exacerbating PCOS symptoms. The interplay between IR and HA serves to accelerate the progression of PCOS symptoms in affected women (*18*). IR has been shown to contribute to androgen excess in PCOS through various mechanisms, including the upregulation of Gonadotropin-releasing hormone (GnRH) expression and enhancing the stimulating effects of Luteinizing hormone (LH) (*19*), inhibition of Sex Hormone-Binding Globulin (SHBG) release from the liver (*20*), and upregulation of aldo-keto reductase type 3 (*AKR1C3*), increasing adipose tissue testosterone production (*21*). Contrarily, the HA found in PCOS patients has been demonstrated to alter the phosphorylation patterns of Akt and protein kinase C (PKC), as well as reduce the production of the proteins glucose transporter type 4 (GLUT4) and insulin receptor substrate 1 (IRS-1) associated to tumor necrosis factor α (TNF-α) and interleukin 6 (IL-6) (*22-24*). Obesity and dyslipidemia are closely linked to PCOS, with obesity playing an integral role in its development. Dyslipidemia, characterized by abnormal lipid levels in the blood, promotes IR. Dyslipidemia in PCOS is characterized by the impaired inhibition of free fatty acid (FFA) release in response to insulin, increasing levels of low-density lipoprotein cholesterol (LDL-C)/triglycerides (TG) with decreasing high-density lipoprotein cholesterol (HDL-C) (*25*). PCOS is also recognized as a chronic low-grade inflammatory disease, with elevated levels of inflammatory markers. HA and IR stimulate the inflammatory pathway, leading to oxidative stress and chronic inflammation.

In summary, PCOS is characterized by hyperandrogenism, IR, obesity-related dyslipidemia, and chronic inflammation. These factors interact and contribute to the pathophysiology of this syndrome (Figure 1).

2.3. The impact of PCOS on pregnancy outcomes

PCOS and its manifestations potentially infer high-risk pregnancies, leading to a series of adverse maternal outcomes (*26*). The two main adverse maternal outcomes are hypertensive disorders during pregnancy (HDP) and GDM. Meta-analyses have reported higher risks for GDM and HDP in women with PCOS, especially PE compared to normal controls (*27,28*). Studies have shown that GDM is independently associated with PE in singleton pregnancies, and we speculate that there may be a common pathogenic factor of GDM and PE in women with PCOS.

The effects of PCOS on fetal growth have been linked to meconium aspiration, very preterm birth, and low Apgar scores (< 7) at five minutes (*29*). Large for gestational age (LGA) and small for gestational age (SGA) infants were more likely to be born to moms with PCOS. Animal experiments have demonstrated that IR and hyperinsulinemia are able to cause increased fetal size (*30*). It is also suspected to lead to higher LGA birth risk in human with PCOS. Although some studies have not detected fetuses with IUGR in PCOS patients (*31*), others have claimed that women with PCOS had higher rates of IUGR and SGA than women without the condition who are the same age and body mass index (BMI) (*28*). The decrease of nutrients such as amino acids required by the fetus due to placental malperfusion may be one of the causes.

HDP may stem in part from the direct and indirect effects of insulin on vasoconstriction (*32*). In addition, insulin stimulates various growth factors promoting

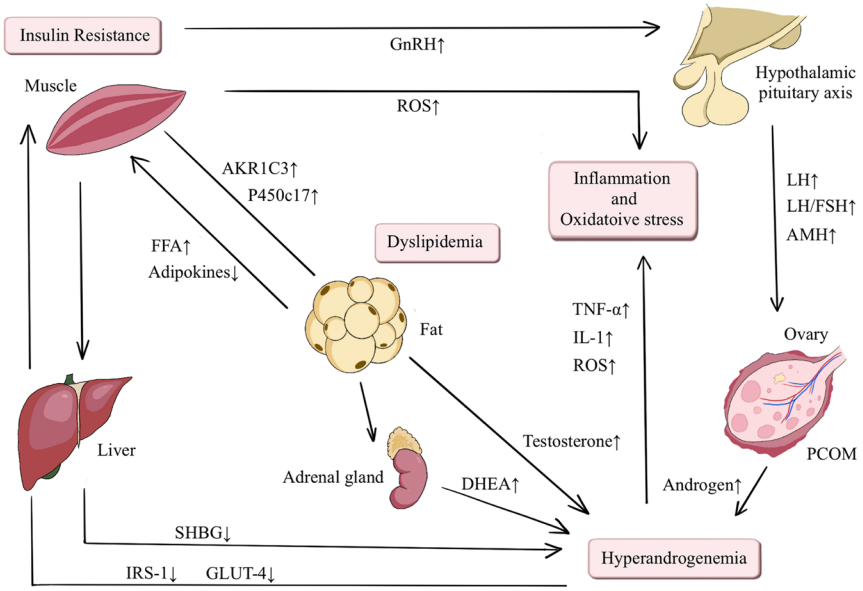

Figure 1. Characteristic manifestations of PCOS and their interaction. Hyperandrogenemia may be due to insulin resistance and dyslipidemia that induces the production of additional androgens through a variety of mechanisms (*e.g.*, increased hypothalamic-pituitary-gonadal axis release, increased adipose tissue and adrenal gland synthesis), which can in turn exacerbate insulin resistance. In addition to directly or indirectly acting on adrenal androgen production, lipid metabolism disorders can also promote insulin resistance through up-regulation of fatty acids (FFA) and down-regulation of Adipokines. In addition, hyperandrogenemia, lipid metabolism disorders, chronic inflammation and oxidative stress in patients with insulin resistance and PCOS are also closely related and mutually reinforcing.

thrombosis and fibrosis as well as up-regulates blood pressure response to sodium intake (*33,34*). Hormonal imbalance and HA may also play a role here. Animal experiments demonstrated that testosterone-treated mice exhibited increased vascular resistance and hypertension (*35*).

Placental dysfunction caused by impaired maternal-fetal interface is widely known as a vital cause of pregnancy complications and adverse fetal outcomes (*36*). Therefore, we hypothesized that the characteristic manifestations of PCOS, such as IR, HA, abnormal lipid metabolism and inflammation may contribute to adverse pregnancy outcomes (APO) by influencing decidualization, one of the most essential parts in maternal-fetal interface.

3. Impaired decidualization in adverse pregnancy outcomes

PCOS is commonly associated with APO, leading to greater use of ART compared to women without PCOS (*29*). APO refers to a range of short- and long-term complications related to pregnancy and delivery that impact both the mother and the fetus. APOs related to maternal PCOS include preeclampsia, gestational diabetes, gestational hypertension, and recurrent miscarriage. The process of becoming pregnant is intricate and irreversible, involving a number of separate steps, such as implantation, decidualization, placentation, and ultimately, birth. Any interference with these processes can result in adverse pregnancy outcomes. In humans, decidualization is initiated not by the blastocyst signal but by the menstrual cycle, and it occurs simultaneously with the development of the fertilized egg. Decidualization not only plays a critical role in implantation but also regulates placentation, making it of utmost importance during pregnancy. This review aims to examine and summarize the relationship between impaired decidualization and APO, as well as the specific mechanisms involved (Figure 2).

4. The role of PCOS in decidualization impaired APO

4.1. The role of decidualization in the progress of pregnancy

Decidualization of the human endometrium is the process of remodeling post-ovulation in preparation for pregnancy. This procedure includes vascular remodeling, the development of secretory uterine glands, and the influx of specialized uterine natural killer cells (uNKs) (*37,38*). More specifically, human endometrial stromal cells (ESCs) undergo morphological and functional differentiation known as decidualization (*39*). It is initiated mainly by hormones, particularly estrogen estradiol (E2) and progesterone (P4) secreted by the corpus luteum post-ovulation. In pregnancy, trophoblast cells produce human chorionic gonadotropin (hCG), which helps maintain progesterone levels. A regulatory loop is then established between hormones such as relaxin and corticotropin-releasing hormone (CRH), along with hCG, to increase intracellular

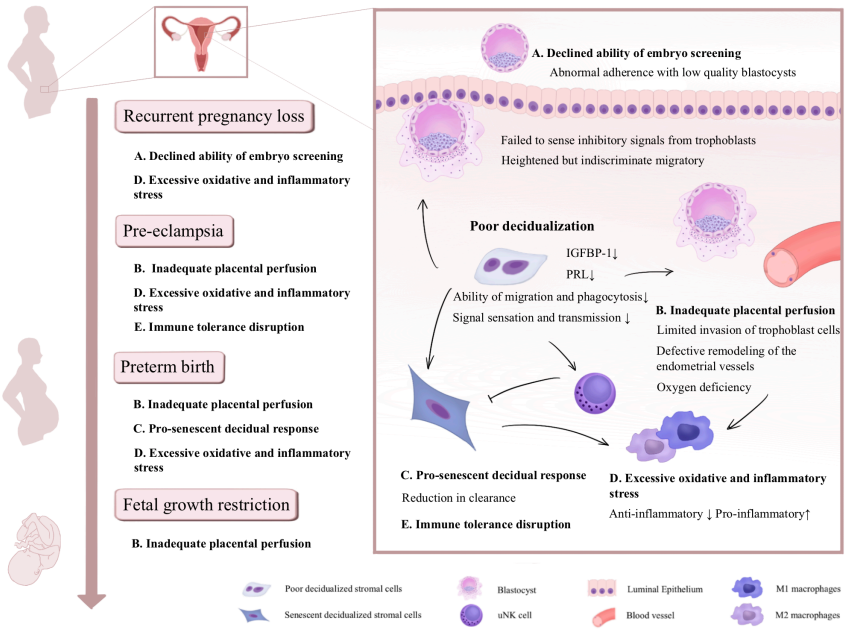

Figure 2. The role poor decidualization played in adverse pregnancy outcome in women with PCOS. Endometrial stromal cells with imperfect decidualization in the maternal-fetal interface have adverse effects on the normal physiology of surrounding cells, including embryonic trophoblast cells, immune cells, *etc*. Resulting in declined ability of embryo screening, inadequate placental perfusion, pro-senescent decidual response, excessive oxidative and inflammatory stress and immune tolerance. These phenomena affect the mother and fetus at different periods respectively, contributing to adverse pregnancy outcomes.

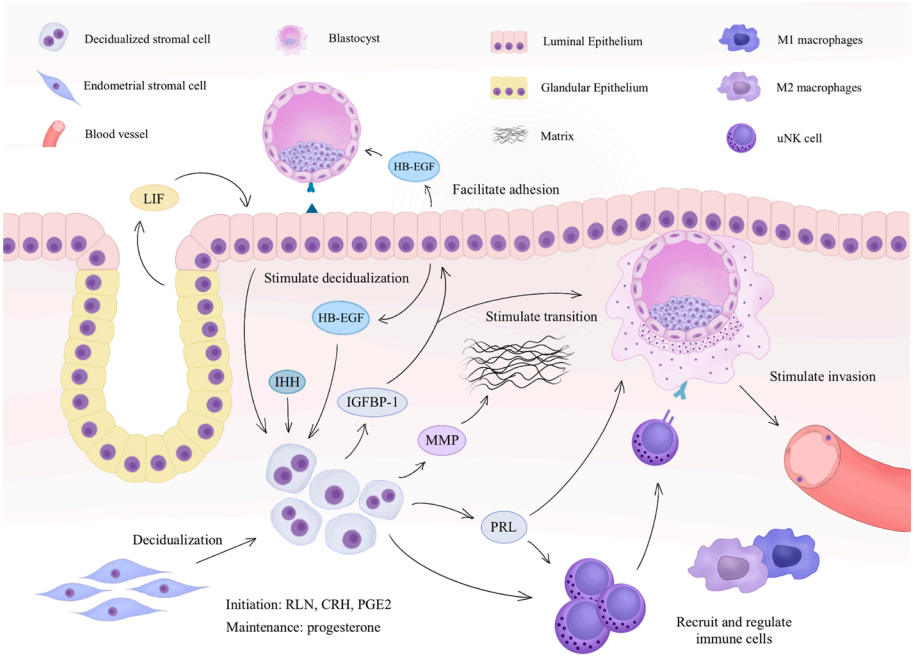

Figure 3. Communication between decidualized stromal cells and other cells in maternal-fetal interface. Successful decidualization is regulated by multiple factors, including contact between blastocyst and epithelium, changes in hormone levels and other factors in the body. At the same time, normal decidualized stromal cells (DSCs) also promote the invasion of blastocyst trophoblast cells and vascular reconstruction through multiple ways, such as promoting stromal decomposition, promoting endometrial NK cell recruitment and recognition of blastocyst.

cyclic adenosine monophosphate (cAMP) levels and promote decidualization. Prolactin (PRL) and insulin-like growth factor binding protein 1 (IGFBP1), which have been frequently employed as markers of decidual cells, are examples of particular molecules secreted by decidualized ESCs (Figure 3).

4.2. The regulation of dysdecidualization in APO

In addition to discrete events like implantation, decidualization, placentation, and childbirth, pregnancy is a difficult, irreversible process. Interference in any of these steps may lead to adverse pregnancy

outcomes. Decidualization in humans is initiated not by the blastocyst signal but the menstrual cycle (*15*). Decidualization of the endometrium and the development of the fertilized egg go on simultaneously and it is not only related to implantation but also regulates placentation, which plays an extremely essential role during pregnancy. Therefore, the purpose of this review is to study and summarize the relationship between impaired decidualization and APO and the specific mechanisms involved. Recurrent pregnancy loss (RPL) is considered a disease as compared to sporadic pregnancy loss. Although embryo aneuploidy is a common cause of pregnancy loss, studies have shown that RPL patients with PCOS have a decreased rate of embryo aneuploidy, suggesting a potentially greater role for endometrial disorders in RPL (*40*).

Numerous studies have established a link between PRL and deficient endometrial decidualization, with reduced expression of decidualization markers, including PRL, tissue factor (TF), and signal transducer and activator of transcription 5 (Stat5), detected in such patients. However, it is yet unclear how PRL affects the expression of IGFBP-1 (*41-43*). Studies on the mechanism of improper decidualization leading to RPL primarily focus on two aspects: reduced embryo screening ability and premature, excessive oxidative and inflammatory stress. Women with RPL often show prolonged, heightened inflammatory endometrial reactions which may be linked to defective endometrial vessel remodeling and disrupted oxygen supply (*44,45*). In women with RPL, all genes in the interleukin 8 (IL-8) pathway are upregulated, while those in the interleukin 1 (IL-1) pathway are downregulated (*46*). Oxidative and inflammatory stress, such as heightened tumor necrosis factor α (TNF-α) and nucleotide oligomerization domain (NOD)-like receptor thermal protein domain associated protein 3 (NLRP3) secretion, can induce stromal cell senescence and deplete endometrial mesenchymal stem cells (eMSCs) (*47-49*). RPL has also been linked to a variety of genes, intracellular signaling pathways, and metabolic dysregulation (*50-53*).

4.3. The relationship between PCOS pathological factors and dysdecidualization

Numerous studies have yielded compelling evidence supporting the association between PCOS characteristics and adverse pregnancy outcomes, irrespective of the phenotype, including metabolic and hormonal disorders and the ensuing inflammatory response (*54*). Of these factors, endometrial factors have been increasingly cited, with a greater emphasis on decidualization. To address this topic, our review focuses on investigating the mechanisms through which PCOS directly affects the differentiation and function of endometrial stromal cells by disrupting endocrine balance. Additionally, epithelial cell growth and the attraction of immune cells can both be negatively impacted by a number of variables, leading to epithelial-mesenchymal communication disorders that ultimately undermine ESC decidualization. The above content is an important elaboration of our review.

4.3.1. Insulin resistance impairs the energy uptake in ESC through the insulin signaling pathway

The impairment in insulin signal pathway contributes to the improper decidualization of women with PCOS by downregulating the expression of variety of important secretion factors. Neff *etc*. has reported a reduced expression of IR stimulated by hyper-insulinemic conditions led to impaired decidualization (*55*). Insulin receptor substrate 2 (IRS2) induced by progesterone bridges receptor tyrosine kinases such as insulin-like growth factor 1 receptor (IGF1R) and IR to downstream phosphoinositide 3-kinase (PI3K)/AKT and mitogen-activated protein kinases (MAPK) pathways. EDCs with abnormal PI3K/AKT and MAPK activation had less glucose transporter type 1 (GLUT1) and GLUT4 accumulating in the cell membrane, which may lead to an energy deficiency during decidualization considering an obviously increased uptake in decidual stromal cells (DSCs) and a booming necessity of energy during decidualization (*56*). Thus, IR and declined progesterone in women with PCOS are supposed to have negative impact on MAPK and PI3K/AKT signal pathway. IGFBP1, bone morphogenetic protein 2 (BMP2), Wnt family member 4 (WNT4), and heart and neural crest derivatives expressed 2 (HAND2) (but not PRL) expression in human ESC has been reported to be dramatically reduced by IRS-2 loss. IGFBP1 and PRL expression were considerably reduced after treatment with an ERK1/2 (member of the MAPK pathway) inhibitor, and the activation of known extracellular regulated protein kinases 1/2 (ERK1/2) target genes FOS, mitogen- and stress-activated kinase 1 (MSK1), signal transducerand activator of transcription 1 (STAT1), and signal transducerand activator of transcription 3 (STAT3) was also blocked, which verified the importance of MAPK pathway in decidualization (*57*). Increased nuclear accumulation and forkhead box O1 (FOXO1) transcriptional activity require PI3K/AKT activation, which is exhibited to promote decidual procession by increasing PRL promoter activity (*58*).

Insulin resistance is also found significantly up-regulated Prokineticin 1 (PROK1) mRNA and protein levels in human decidualized endometrial stromal cells through hypoxia-inducible factor-1α (HIF1α) and PI3K pathways, which impacted trophoblast migration and invasion as well as endometrial stromal cell migration (*59*).

4.3.2. Elevated androgens and increased androgen receptor expression in PCOS patients may disrupt the decidualization

In uterus of normal pregnant women, the abundance of

androgen receptor (AR) in pregnancy phase is down-regulated, but for PCOS, AR is reported overexpressed both in endometrium epithelial and stromal cells compared to fertile controls (*60*). This upregulation of AR' s expression may be attributed to the chronic elevation of estrogen and androgens in women with PCOS (*61*). Numerous researches have shown endometrial androstenedione concentrations in women with PCOS are three times greater than in normal women and dramatically promote cell proliferation in ESC cultures because AR is colocalized with Ki-67. Androgen and progesterone work together to promote PRL secretion, and can be inhibited by the specific AR competitive inhibitor flutamide. *In-vitro* experiments showed a decreased proliferation of ESC cells collected from both PCOS patients and normal pregnant women treated with dihydrotestosterone (DHT), which can be partially compensated by treatment with dexamethasone (*60*). And the decreased expression of PRL has also been exhibited, suggesting that ESC decidualization was impaired.

A recent study found that melanoma-associated antigen 11 (MAGEA11), a cAMP-induced AR coregulator, was delayed in up-regulation and expressed less in ESC cells from PCOS patients. Furthermore, AR chromatin immunoprecipitation research revealed that Krüppel-like factor (KLF)-9 and 13 transcription factors (KLF9/KLF13) are both important targets of androgen receptor. Researchers postulated that aberrant MAGEA11 expression may induce delayed or incorrect decidualization by interfering with normal signal transduction from AR to the target KLF9/13 and its downstream component *BMP2*. Furthermore, the promyelocytic leukemia zinc finger transcription factor (PLZF)-related pathway may play a role in the poor decidualization process. AR overexpression and activation appear to mediate mis-expression of these transcriptional regulators required for transcriptional programming (*62*).

The up-regulation of B-cell lymphoma-2 (*Bcl-2*) in PCOS samples with hyperandrogenemia showed signs of early apoptosis and delayed cell cycle. And a higher p27 protein expression also shows that cell cycle regulation may be compromised (*63*). Apoptosis is delayed in PCOS; overexpression and hyperactivation of AR may be the cause of this. Gene ontology analysis showed that AR targets were primarily involved in processes linked to the positive control of cell death.

4.3.3. Disorders of lipid metabolism may directly affect the synthesis and breakdown of cellular lipids required during decidualization

Lipids and their derivatives are increasingly being identified to be crucial in the decidualization of endometrial stromal cells in research. Cholesterol-derived steroid hormones E2 and P4 are essential for the maintenance of decidualization of stromal cells. Up-regulated by E2 and stimulated by P4, the progesterone receptors (PGRs) directly activate transcription factors such as FOXO1 and homeobox A10 (HOXA10), which leads to the procession of decidualization and the secretion of DSCs markers such as IGFBP-1 and PRL (*64-66*). E2 and P4 expression in the circulation and estrogen receptor (ER) and PGR observed in the endometrium of PCOS patients are both vary from that in normal women. More intriguingly, the findings showed that a subset of PCOS-affected women had ESCs that showed a reduced decidualization response to E2P4 therapy, which is also called "progesterone resistance" (*67*).

Adipocytes synthesize and secrete adipokines, such as leptin and adiponectin. Leptin is involved in the pro-inflammatory process, while adiponectin has protective effects such as anti-inflammatory and increasing insulin sensitivity. Some studies have found that the level of circulating adiponectin is decreased in PCOS patients, and there is abnormal expression of adiponectin system genes in granulosa cells (*68,69*). Investigators have identified adiponectin expression in endometrial ESCs of PCOS patients and reported that adiponectin is a component of correct endometrial decidualization and embryo implantation (*70*). Adiponectin treatment of stromal cells was found to up-regulate the expression of leukemia inhibitory factor (*LIF*) and glutathione peroxidase 3 (*GPX3*), and down-regulate the expression of interleukin 15 (*IL-15*) and mucin 1 (*MUC1*), indicating that the presence of adiponectin promotes stromal cell decidualization and is anti-inflammatory and anti-oxidative and creating a favorable endometrial environment (*71*). In addition, adiponectin can inhibit the excessive invasion of trophoblast cells, the effect of which may be related to the decreased activity of matrix metalloproteinase 2 (MMP-2) and matrix metalloproteinase 9 (MMP-9) and the up-regulated expression of tissue inhibitor of metalloproteinase 3 (*TIMP-3*) mRNA, a tissue inhibitor of metalloproteinases in ESCs (*72,73*). Therefor we can conclude that the decreased expression of adiponectin in PCOS patients has an adverse effect on decidualization of ESCs.

Additionally, high levels of advanced glycation end products (AGEs) affect the function of endometrial epithelial cells and endometrial stromal cells, stress endoplasmic reticulum (ER) in ESCs and impair decidualization, compromise the implantation of blastocyst mimics, and inhibit trophoblast invasion (*74*).

4.3.4. Imbalance of pro- and anti-inflammatory factors interferes with signal transduction, apoptosis and cell cycle regulation in ESC

Inflammation is prevalent in women with PCOS: Serum levels of TNF-α, IL-1, IL-6 and IL-18, adhesion molecules, follistatin and C-reactive protein (CRP) were widely observed elevated. Microarray analysis revealed

that ESCs in women with PCOS showed upregulation of inflammatory genes (*C4A/B*, *CCL2*, *ICAM1*, *TNFAIP3*) (*75,76*). Inflammation is closely related to metabolic disorders, immune cell dysfunction and even oxidative stress, and leading to a definite disruption on decidualization procession. In addition, some inflammatory cytokines themselves can directly damage the decidualization process of ESCs through Intracellular pathways.

TNF-α was significantly increased in PCOS patients. On the one hand, TNF-α levels interfere with the insulin signal pathway by lowering adiponectin signaling and GLUT-4 protein, which in turn interferes with the activation of the *IRS-1* gene in the ESCs of PCOS women. This will further exacerbate the disruption of insulin signaling pathway, which is especially common in obese PCOS women (*69,77*). On the other hand, infertile PCOS patients with increased levels of the inflammatory cytokines TNF-α and IFN-α increase NF-κB and STAT1 protein recruitment to osteopontin (OPN) and CD44 promoters. This overexpression of NF-κB p65 (Rel A) is positively correlated with serum insulin levels and hyperandrogenism in overweight PCOS women (*78*). Thus, we can infer that TNF-α could profoundly damage decidualization by promoting IR and HA decidua.

It has been found that the cytotoxic cytokine IL-1β blocks human ESCs differentiation and automatically upregulates its synthesis and secretion through independent signaling pathways. Uterine gap junction protein connexin 43 (Cx43) and two other ESCs differentiation markers: PRL and vascular endothelial growth factors (VEGF) are inhibited by IL-1β activation. This may be handled through the ERK1/2 and p38 MAPK cascades. Furthermore, IL-1β has been suggested to inhibit the expression of estrogen receptor-α, progesterone receptor-a and progesterone receptor-b in ESCs (*79*).

Studies have demonstrated that PCOS patients' endometrium expresses more IL-6 and IL-8, which may be due to the influence of insulin and androgen (*80*). These inflammatory factors secreted by the DSCs plays the chemotaxis of white blood cells (WBC) in endometrium, coordination of sertoli cell invasion, and so on. But do these cytokines have an effect on the differentiation of ESCs themselves? A recent study found *in vitro* experiment that the addition of IL-6 and IL-8 to ESCs cells derived from PCOS patients did not affect their decidual morphology or reduce the expression of their secreted production IGFBP-1. This may imply IL-6 and IL-8 have no significant effect on decidualization of endometrial ESCs from PCOS patients (*81*).

Excepting the upregulation of inflammatory factors, the downregulation of anti-inflammatory factors is also be found in PCOS patients. A pro-survival factor called stoniocalcin-1 (STC-1) shields tissues from stresses including inflammation and hypoxia. In the nonpregnant state, *STC-1* gene expression is restricted to the uterine luminal epithelium, while during implantation, *STC-1* gene expression is observed to be exhibited and increased in DSCs in the superficial layer of endometrium (*82*). Expression of *STC-1* is found reduced in women with PCOS when facing stress that may cause deficits, possibly because of a diminished STC-1 response to stressors in ESCs of PCOS patients (*83*). This reflects that STC-1 may affect the decidualization of ESCs in PCOS patients through inflammation and oxidative stress pathways. A recent study constructing endometrial organoids reported that treatment of ESCs *in vitro* with STC-1 alone had no effect on decidualization (84) (Figure 4). We suggest more future experiments are needed to verify this conclusion.

5. Conclusions and prospects

PCOS is a global health concern with serious and long-term adverse effects on the physical and mental health of women in their reproductive age, studies have found woman with PCOS suffering a higher rate of APO. However, the study of the increased incidence of APO in PCOS patients is still in its early stages, with multiple essential pathological mechanisms yet to be uncovered and clinically verified. Decidualization plays a crucial role in pregnancy and any dysfunction leading to poor decidualization can result in catastrophic adverse pregnancy outcomes. Through our review of recent literature, we have discovered that decidualization of stromal cells in PCOS patients is not only impacted by low progesterone levels caused by ovulation disorders, but also influenced by changes in biochemical and metabolic signals, such as hyperandrogenism, obesity, IR, and hyperinsulinemia. These pathological processes impair decidualization of endometrial stromal cells at the cellular signaling and gene expression levels mediated by cytokines, inflammatory factors, and oxidative stress. Dysfunctional secretion and phagocytosis further contribute to poor function and excessive pro-senescence, resulting in various APO, including RPL, preterm birth (PTB), PE, and IUGR. It is apparent that the changes in biochemical and metabolic signals caused by PCOS not only affect stromal cells, but also impact other components of the endometrium, including epithelial cells and immune cells. These effects may directly impair decidual function or indirectly damage stromal cell decidualization through intercellular crosstalk. However, space limitations prohibit us from exploring this aspect in this review. Similarly, due to the wide range of biochemical and metabolic signal changes and types of APO associated with PCOS, we have focused on discussing 4 representative features and diseases. Furthermore, the subject of PCOS and its impact on decidualization and APO is still a topic of debate, and the effects and outcomes may vary depending on the patient's phenotypic presentation and pathophysiological processes. Therefore, in this review, we have not

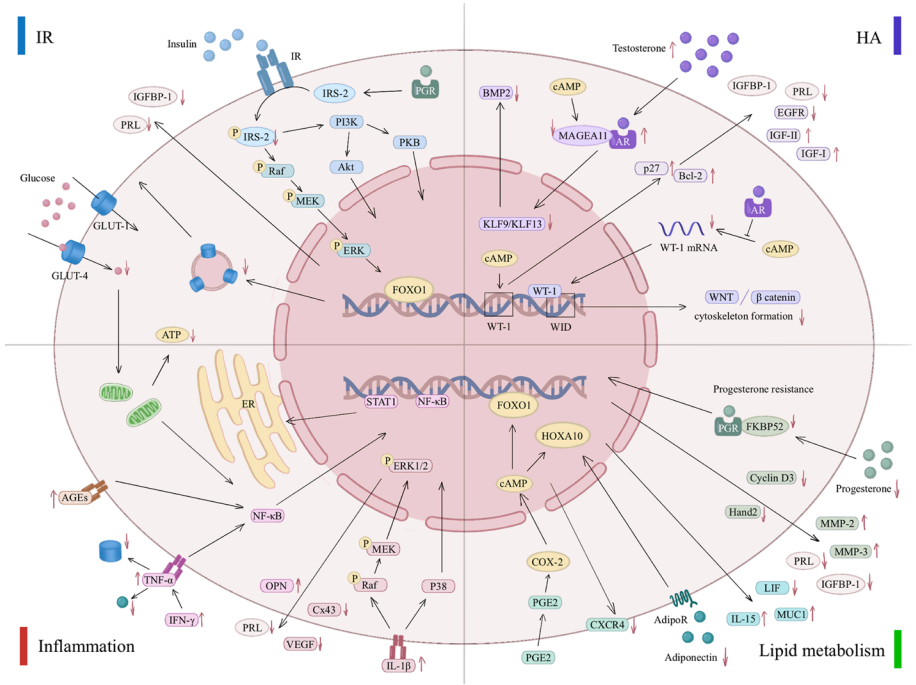

Figure 4. Mechanism of poor decidualization caused by PCOS. IR (insulin resistance) affects ESC decidualization through pathways such as insulin receptor MAPK and reduced glucose transport, shown in blue in the upper left box. HA (hyperandrogenemia) affecting receptor cofactors MAGEA11 and WT-1 pathways, which are highlighted in purple in the upper right box. The inflammatory NF-κB pathway as well as inflammatory cytokines and oxidative stress are highlighted in red at the lower left corner. The mechanisms of lipid disorders are highlighted in green in the bottom right box.

differentiated between different PCOS phenotypes.

Our aim was to link PCOS to APO through decidualization, which is a novel approach to our knowledge. We have outlined a range of signaling pathways and cytokines that could serve as potential therapeutic targets for the treatment of PCOS or improving live birth rates for pregnant PCOS patients. Our summary of the pathological mechanisms linking gynecological endocrine diseases and adverse obstetric outcomes may assist clinicians in gaining a better understanding of the impact of PCOS on pregnancies, and pave the way for further in-depth research in this field.

Funding: This work was supported by grants from a project under the Scientific and Technological Innovation Action Plan of the Shanghai Natural Science Fund (grant no. 20ZR1409100 to L Wang), a project of the Chinese Association of Integration of Traditional and Western Medicine special foundation for Obstetrics and Gynecology-PuZheng Pharmaceutical Foundation (grant no. FCK-PZ-08 to L Wang), a project for hospital management of the Shanghai Hospital Association (grant no. X2021046 to L Wang), a clinical trial project of the Special Foundation for Healthcare Research of the Shanghai Municipal Health Commission (grant no. 202150042 to L Wang).

Conflict of Interest: The authors have no conflicts of interest to disclose.

References

1. Lizneva D, Suturina L, Walker W, Brakta S, Gavrilova-Jordan L, Azziz R. Criteria, prevalence, and phenotypes of polycystic ovary syndrome. Fertil Steril. 2016; 106:6-15.
2. Al Wattar BH, Fisher M, Bevington L, Talaulikar V, Davies M, Conway G, Yasmin E. Clinical practice guidelines on the diagnosis and management of polycystic ovary syndrome: A systematic review and quality assessment study. J Clin Endocrinol Metab. 2021; 106:2436-2446.
3. Huddleston HG, Dokras A. Diagnosis and treatment of polycystic ovary syndrome. JAMA. 2022; 327:274-275.
4. Cai H, Mol BW, Gordts S, Wang H, Wang T, Li N, Shi J. Early and late pregnancy loss in women with polycystic ovary syndrome undergoing IVF/ICSI treatment: A retrospective cohort analysis of 21,820 pregnancies. BJOG. 2021; 128:1160-1169.
5. Yang H, Wang G, Liu C, Ding L, Li Y, Chen Y, Teng Y, Xu Z, Ye Z, Zhao Y, Mu L. Elevated serum uric acid level is associated with adverse reproductive outcomes in women with polycystic ovary syndrome undergoing *in vitro* fertilization or intracytoplasmic sperm injection embryo transfer cycles: A retrospective cohort study. Am J Obstet Gynecol. 2023; 228:324 e321-324 e310.
6. Wang Q, Wang H, Li P, Li X, Wang Z, Yan L, Shi Y. Association of polycystic ovary syndrome phenotypes with adverse pregnancy outcomes after *in-vitro* fertilization/intracytoplasmic sperm injection. Front Endocrinol (Lausanne). 2022; 13:889029.
7. Zhao J, Chen Q, Xue X. An update on the progress of endometrial receptivity in women with polycystic ovary syndrome. Reprod Sci. 2022; 29:2136-2144.
8. Bahri Khomami M, Joham AE, Boyle JA, Piltonen T,

Silagy M, Arora C, Misso ML, Teede HJ, Moran LJ. Increased maternal pregnancy complications in polycystic ovary syndrome appear to be independent of obesity-A systematic review, meta-analysis, and meta-regression. Obes Rev. 2019; 20:659-674.
9. Lin J, Guo H, Wang B, Chen Q, Zhu Q. Neonatal outcomes in women with polycystic ovary syndrome after frozen-thawed embryo transfer. Fertil Steril. 2021; 115:447-454.
10. Cooney LG, Dokras A. Beyond fertility: Polycystic ovary syndrome and long-term health. Fertil Steril. 2018; 110:794-809.
11. Osibogun O, Ogunmoroti O, Michos ED. Polycystic ovary syndrome and cardiometabolic risk: Opportunities for cardiovascular disease prevention. Trends Cardiovasc Med. 2020; 30:399-404.
12. Palomba S, Falbo A, Chiossi G, Muscogiuri G, Fornaciari E, Orio F, Tolino A, Colao A, La Sala GB, Zullo F. Lipid profile in nonobese pregnant women with polycystic ovary syndrome: A prospective controlled clinical study. Steroids. 2014; 88:36-43.
13. Ryan EA. Hormones and insulin resistance during pregnancy. Lancet. 2003; 362:1777-1778.
14. Gan Y, Lu D, Yan C, Zhang J, Zhao J. Maternal polycystic ovary syndrome and offspring birth weight: A mendelian randomization study. J Clin Endocrinol Metab. 2022; 107:1020-1029.
15. Meng X, Chen C, Qian J, Cui L, Wang S. Energy metabolism and maternal-fetal tolerance working in decidualization. Front Immunol. 2023; 14:1203719.
16. Ortiz-Flores AE, Luque-Ramirez M, Escobar-Morreale HF. Polycystic ovary syndrome in adult women. Med Clin (Barc). 2019; 152:450-457.
17. Robinson SL, Yeung EH. Polycystic ovary syndrome and preterm birth-what's going on? Fertil Steril. 2021; 115:326-327.
18. Sadeghi HM, Adeli I, Calina D, Docea AO, Mousavi T, Daniali M, Nikfar S, Tsatsakis A, Abdollahi M. Polycystic ovary syndrome: A comprehensive review of pathogenesis, management, and drug repurposing. Int J Mol Sci. 2022; 23:583.
19. Wang J, Wu D, Guo H, Li M. Hyperandrogenemia and insulin resistance: The chief culprit of polycystic ovary syndrome. Life Sci. 2019; 236:116940.
20. Qu X, Donnelly R. Sex hormone-binding globulin (SHBG) as an early biomarker and therapeutic target in polycystic ovary syndrome. Int J Mol Sci. 2020; 21:8191.
21. Paulukinas RD, Mesaros CA, Penning TM. Conversion of classical and 11-oxygenated androgens by insulin-induced AKR1C3 in a model of human PCOS adipocytes. Endocrinology. 2022; 163:bqac068.
22. Cabrera-Cruz H, Orostica L, Plaza-Parrochia F, Torres-Pinto I, Romero C, Vega M. The insulin-sensitizing mechanism of myo-inositol is associated with AMPK activation and GLUT-4 expression in human endometrial cells exposed to a PCOS environment. Am J Physiol Endocrinol Metab. 2020; 318:E237-E248.
23. Stepto NK, Hiam D, Gibson-Helm M, Cassar S, Harrison CL, Hutchison SK, Joham AE, Canny BJ, Moreno-Asso A, Strauss BJ, Hatzirodos N, Rodgers RJ, Teede HJ. Exercise and insulin resistance in PCOS: muscle insulin signalling and fibrosis. Endocr Connect. 2020; 9:346-359.
24. Glueck CJ, Goldenberg N. Characteristics of obesity in polycystic ovary syndrome: Etiology, treatment, and genetics. Metabolism. 2019; 92:108-120.
25. Paoli A, Mancin L, Giacona MC, Bianco A, Caprio M. Effects of a ketogenic diet in overweight women with polycystic ovary syndrome. J Transl Med. 2020; 18:104.
26. Bahri Khomami M, Boyle JA, Tay CT, Vanky E, Teede HJ, Joham AE, Moran LJ. Polycystic ovary syndrome and adverse pregnancy outcomes: Current state of knowledge, challenges and potential implications for practice. Clin Endocrinol (Oxf). 2018; 88:761-769.
27. Li X, Zhang W, Lin J, Liu H, Yang Z, Teng Y, Duan S, Lin X, Xie Y, Li Y, Xie L, Peng Q, Xia L. Risk factors for adverse maternal and perinatal outcomes in women with preeclampsia: Analysis of 1396 cases. J Clin Hypertens (Greenwich). 2018; 20:1049-1057.
28. Farland LV, Stern JE, Liu CL, Cabral HJ, Coddington CC, Diop H, Dukhovny D, Hwang S, Missmer SA. Polycystic ovary syndrome and risk of adverse pregnancy outcomes: A registry linkage study from Massachusetts. Hum Reprod. 2022; 37:2690-2699.
29. Dehghani Firoozabadi A, Dehghani Firouzabadi R, Eftekhar M, Sadat Tabatabaei Bafghi A, Shamsi F. Maternal and neonatal outcomes among pregnant women with different polycystic ovary syndrome phenotypes: A cross-sectional study. Int J Reprod Biomed. 2020; 18:339-346.
30. Mumm H, Jensen DM, Sorensen JA, Andersen LL, Ravn P, Andersen M, Glintborg D. Hyperandrogenism and phenotypes of polycystic ovary syndrome are not associated with differences in obstetric outcomes. Acta Obstet Gynecol Scand. 2015; 94:204-211.
31. Elkholi DGEY, Nagy HM. The effects of adipocytokines on the endocrino-metabolic features and obstetric outcome in pregnant obese women with polycystic ovary syndrome. Middle East Fertil Soc J. 2014; 19:293-302.
32. Aktun HL, Yorgunlar B, Acet M, Aygun BK, Karaca N. The effects of polycystic ovary syndrome on gestational diabetes mellitus. Gynecol Endocrinol. 2016; 32:139-142.
33. Ding PF, Zhang HS, Wang J, Gao YY, Mao JN, Hang CH, Li W. Insulin resistance in ischemic stroke: Mechanisms and therapeutic approaches. Front Endocrinol (Lausanne). 2022; 13:1092431.
34. Wójcik M, Kozioł-Kozakowska A. Obesity, sodium homeostasis, and arterial hypertension in children and adolescents. Nutrients. 2021; 13:4032.
35. Chinnathambi V, Yallampalli C, Sathishkumar K. Prenatal testosterone induces sex-specific dysfunction in endothelium-dependent relaxation pathways in adult male and female rats. Biol Reprod. 2013; 89:97.
36. Kelley AS, Smith YR, Padmanabhan V. A narrative review of placental contribution to adverse pregnancy outcomes in women with polycystic ovary syndrome. J Clin Endocrinol Metab. 2019; 104:5299-5315.
37. Ng SW, Norwitz GA, Pavlicev M, Tilburgs T, Simon C, Norwitz ER. Endometrial decidualization: The primary driver of pregnancy health. Int J Mol Sci. 2020; 21:4092.
38. Gellersen B, Brosens IA, Brosens JJ. Decidualization of the human endometrium: Mechanisms, functions, and clinical perspectives. Semin Reprod Med. 2007; 25:445-453.
39. Okada H, Tsuzuki T, Murata H. Decidualization of the human endometrium. Reprod Med Biol. 2018; 17:220-227.
40. Wang Q, Luo L, Lei Q, Lin MM, Huang X, Chen MH, Zeng YH, Zhou CQ. Low aneuploidy rate in early pregnancy loss abortuses from patients with polycystic

ovary syndrome. Reprod Biomed Online. 2016; 33:85-92.
41. Larsen EC, Christiansen OB, Kolte AM, Macklon N. New insights into mechanisms behind miscarriage. BMC Med. 2013; 11:154.
42. Lucas ES, Vrljicak P, Muter J, Diniz-da-Costa MM, Brighton PJ, Kong CS, Lipecki J, Fishwick KJ, Odendaal J, Ewington LJ, Quenby S, Ott S, Brosens JJ. Recurrent pregnancy loss is associated with a pro-senescent decidual response during the peri-implantation window. Commun Biol. 2020; 3:37.
43. Pirtea P, Cicinelli E, De Nola R, de Ziegler D, Ayoubi JM. Endometrial causes of recurrent pregnancy losses: Endometriosis, adenomyosis, and chronic endometritis. Fertil Steril. 2021; 115:546-560.
44. El-Azzamy H, Dambaeva SV, Katukurundage D, Salazar Garcia MD, Skariah A, Hussein Y, Germain A, Fernandez E, Gilman-Sachs A, Beaman KD, Kwak-Kim J. Dysregulated uterine natural killer cells and vascular remodeling in women with recurrent pregnancy losses. Am J Reprod Immunol. 2018; 80:e13024.
45. Windsperger K, Vondra S, Lackner AI, Kunihs V, Haslinger P, Meinhardt G, Dietrich B, Dekan S, Fiala C, Knofler M, Saleh L, Pollheimer J. Densities of decidual high endothelial venules correlate with T-cell influx in healthy pregnancies and idiopathic recurrent pregnancy losses. Hum Reprod. 2020; 35:2467-2477.
46. Krieg SA, Fan X, Hong Y, Sang QX, Giaccia A, Westphal LM, Lathi RB, Krieg AJ, Nayak NR. Global alteration in gene expression profiles of deciduas from women with idiopathic recurrent pregnancy loss. Mol Hum Reprod. 2012; 18:442-450.
47. Lucas ES, Dyer NP, Murakami K, *et al*. Loss of endometrial plasticity in recurrent pregnancy loss. Stem Cells. 2016; 34:346-356.
48. Zeng S, Liang Y, Lai S, Bi S, Huang L, Li Y, Deng W, Xu P, Liu M, Xiong Z, Chen J, Tu Z, Chen D, Du L. TNFalpha/TNFR1 signal induces excessive senescence of decidua stromal cells in recurrent pregnancy loss. J Reprod Immunol. 2023; 155:103776.
49. Tersigni C, Vatish M, D'Ippolito S, Scambia G, Di Simone N. Abnormal uterine inflammation in obstetric syndromes: Molecular insights into the role of chemokine decoy receptor D6 and inflammasome NLRP3. Mol Hum Reprod. 2020; 26:111-121.
50. Devesa-Peiro A, Sebastian-Leon P, Garcia-Garcia F, Arnau V, Aleman A, Pellicer A, Diaz-Gimeno P. Uterine disorders affecting female fertility: what are the molecular functions altered in endometrium? Fertil Steril. 2020; 113:1261-1274.
51. Bunnewell SJ, Honess ER, Karia AM, Keay SD, Al Wattar BH, Quenby S. Diminished ovarian reserve in recurrent pregnancy loss: A systematic review and meta-analysis. Fertil Steril. 2020; 113:818-827 e813.
52. Zhou Q, Xiong Y, Qu B, Bao A, Zhang Y. DNA Methylation and recurrent pregnancy loss: A mysterious compass? Front Immunol. 2021; 12:738962.
53. Saha B, Ganguly A, Home P, Bhattacharya B, Ray S, Ghosh A, Rumi MAK, Marsh C, French VA, Gunewardena S, Paul S. TEAD4 ensures postimplantation development by promoting trophoblast self-renewal: An implication in early human pregnancy loss. Proc Natl Acad Sci U S A. 2020; 117:17864-17875.
54. Palomba S, Piltonen TT, Giudice LC. Endometrial function in women with polycystic ovary syndrome: A comprehensive review. Hum Reprod Update. 2021; 27:584-618.
55. Neff AM, Yu J, Taylor RN, Bagchi IC, Bagchi MK. Insulin signaling *via* progesterone-regulated insulin receptor substrate 2 is critical for human uterine decidualization. Endocrinology. 2020; 161:bqz021.
56. Frolova AI, Moley KH. Quantitative analysis of glucose transporter mRNAs in endometrial stromal cells reveals critical role of GLUT1 in uterine receptivity. Endocrinology. 2011; 152:2123-2128.
57. Lee CH, Kim TH, Lee JH, Oh SJ, Yoo JY, Kwon HS, Kim YI, Ferguson SD, Ahn JY, Ku BJ, Fazleabas AT, Lim JM, Jeong JW. Extracellular signal-regulated kinase 1/2 signaling pathway is required for endometrial decidualization in mice and human. PLoS One. 2013; 8:e75282.
58. Ujvari D, Jakson I, Babayeva S, Salamon D, Rethi B, Gidlof S, Hirschberg AL. Dysregulation of *in vitro* decidualization of human endometrial stromal cells by insulin *via* transcriptional inhibition of forkhead box protein O1. PLoS One. 2017; 12:e0171004.
59. Ujvari D, Jakson I, Oldmark C, Attarha S, Alkasalias T, Salamon D, Gidlof S, Hirschberg AL. Prokineticin 1 is up-regulated by insulin in decidualizing human endometrial stromal cells. J Cell Mol Med. 2018; 22:163-172.
60. Freis A, Renke T, Kammerer U, Jauckus J, Strowitzki T, Germeyer A. Effects of a hyperandrogenaemic state on the proliferation and decidualization potential in human endometrial stromal cells. Arch Gynecol Obstet. 2017; 295:1005-1013.
61. Zhou R, Li S, Liu J, Wu H, Yao G, Sun Y, Chen ZJ, Li W, Du Y. Up-regulated FHL2 inhibits ovulation through interacting with androgen receptor and ERK1/2 in polycystic ovary syndrome. EBioMedicine. 2020; 52:102635.
62. Younas K, Quintela M, Thomas S, Garcia-Parra J, Blake L, Whiteland H, Bunkheila A, Francis LW, Margarit L, Gonzalez D, Conlan RS. Delayed endometrial decidualisation in polycystic ovary syndrome; the role of AR-MAGEA11. J Mol Med (Berl). 2019; 97:1315-1327.
63. Lahav-Baratz S, Ben-Izhak O, Sabo E, Ben-Eliezer S, Lavie O, Ishai D, Ciechanover A, Dirnfeld M. Decreased level of the cell cycle regulator p27 and increased level of its ubiquitin ligase Skp2 in endometrial carcinoma but not in normal secretory or in hyperstimulated endometrium. Mol Hum Reprod. 2004; 10:567-572.
64. Bi Y, Huang W, Yuan L, Chen S, Liao S, Fu X, Liu B, Yang Y. HOXA10 improves endometrial receptivity by upregulating E-cadherindagger. Biol Reprod. 2022; 106:992-999.
65. Grund S, Grummer R. Direct cell(-)cell interactions in the endometrium and in endometrial pathophysiology. Int J Mol Sci. 2018; 19.
66. Lessey BA, Young SL. What exactly is endometrial receptivity? Fertil Steril. 2019; 111:611-617.
67. Ye X. Uterine luminal epithelium as the transient gateway for embryo implantation. Trends Endocrinol Metab. 2020; 31:165-180.
68. Chrousos GP, MacLusky NJ, Brandon DD, Tomita M, Renquist DM, Loriaux DL, Lipsett MB. Progesterone resistance. Adv Exp Med Biol. 1986; 196:317-328.
69. Dehghan R, Saidijam M, Mehdizadeh M, Shabab N, Yavangi M, Artimani T. Evidence for decreased expression of APPL1 associated with reduced insulin and adiponectin receptors expression in PCOS patients. J Endocrinol Invest. 2016; 39:1075-1082.

70. Orostica L, Garcia P, Vera C, Garcia V, Romero C, Vega M. Effect of TNF-alpha on molecules related to the insulin action in endometrial cells exposed to hyperandrogenic and hyperinsulinic conditions characteristics of polycystic ovary syndrome. Reprod Sci. 2018; 25:1000-1009.
71. Bannigida DM, Nayak SB, Vijayaragavan R. Serum visfatin and adiponectin - markers in women with polycystic ovarian syndrome. Arch Physiol Biochem. 2020; 126:283-286.
72. Gamundi-Segura S, Serna J, Oehninger S, Horcajadas JA, Arbones-Mainar JM. Effects of adipocyte-secreted factors on decidualized endometrial cells: Modulation of endometrial receptivity *in vitro*. J Physiol Biochem. 2015; 71:537-546.
73. Duval F, Dos Santos E, Moindjie H, Serazin V, Swierkowski-Blanchard N, Vialard F, Dieudonne MN. Adiponectin limits differentiation and trophoblast invasion in human endometrial cells. J Mol Endocrinol. 2017; 59:285-297.
74. Antoniotti GS, Coughlan M, Salamonsen LA, Evans J. Obesity associated advanced glycation end products within the human uterine cavity adversely impact endometrial function and embryo implantation competence. Hum Reprod. 2018; 33:654-665.
75. Dabravolski SA, Nikiforov NG, Eid AH, Nedosugova LV, Starodubova AV, Popkova TV, Bezsonov EE, Orekhov AN. Mitochondrial dysfunction and chronic inflammation in polycystic ovary syndrome. Int J Mol Sci. 2021; 22:3923.
76. Long X, Li R, Yang Y, Qiao J. Overexpression of IL-18 in the proliferative phase endometrium of patients with polycystic ovary syndrome. Reprod Sci. 2017; 24:252-257.
77. Orostica L, Poblete C, Romero C, Vega M. Pro-inflammatory markers negatively regulate IRS1 in endometrial cells and endometrium from women with obesity and PCOS. Reprod Sci. 2020; 27:290-300.
78. Koc O, Ozdemirici S, Acet M, Soyturk U, Aydin S. Nuclear factor-kappaB expression in the endometrium of normal and overweight women with polycystic ovary syndrome. J Obstet Gynaecol. 2017; 37:924-930.
79. Yu J, Berga SL, Zou W, Taylor RN. Interleukin-1beta inhibits estrogen receptor-alpha, progesterone receptors A and B and biomarkers of human endometrial stromal cell differentiation: implications for endometriosis. Mol Hum Reprod. 2019; 25:625-637.
80. Velez LM, Seldin M, Motta AB. Inflammation and reproductive function in women with polycystic ovary syndromedagger. Biol Reprod. 2021; 104:1205-1217.
81. Piltonen TT, Chen JC, Khatun M, Kangasniemi M, Liakka A, Spitzer T, Tran N, Huddleston H, Irwin JC, Giudice LC. Endometrial stromal fibroblasts from women with polycystic ovary syndrome have impaired progesterone-mediated decidualization, aberrant cytokine profiles and promote enhanced immune cell migration *in vitro*. Hum Reprod. 2015; 30:1203-1215.
82. Xiao LJ, Yuan JX, Song XX, Li YC, Hu ZY, Liu YX. Expression and regulation of stanniocalcin 1 and 2 in rat uterus during embryo implantation and decidualization. Reproduction. 2006; 131:1137-1149.
83. Khatun M, Arffman RK, Lavogina D, Kangasniemi M, Laru J, Ahtikoski A, Lehtonen S, Paulson M, Hirschberg AL, Salumets A, Andersson LC, Piltonen TT. Women with polycystic ovary syndrome present with altered endometrial expression of stanniocalcin-1dagger. Biol Reprod. 2020; 102:306-315.
84. Fitzgerald HC, Kelleher AM, Ranjit C, Schust DJ, Spencer TE. Basolateral secretions of human endometrial epithelial organoids impact stromal cell decidualization. Mol Hum Reprod. 2023; 29:gaad007.

Received October 12, 2023; Revised December 22, 2023; Accepted December 25, 2023.

[§]These authors contributed equally to this work.
**Address correspondence to:*
Ling Wang and Jing Wang, Laboratory for Reproductive Immunology, Obstetrics and Gynecology Hospital of Fudan University, 419 Fangxie Road, Shanghai, China 200011. China. mail: dr.wangling@fudan.edu.cn (LW); wjsunny2776@163.com (JW)

Released online in J-STAGE as advance publication December 27, 2023.

Review

DOI: 10.5582/ddt.2023.01065

Impact of anesthesia on postoperative breast cancer prognosis: A narrative review

Yi Tang[1,2], Shanshan Guo[1,2], Yao Chen[1], Li Liu[1], Minqiang Liu[1], Renliang He[1], Qiang Wu[1,*]

[1] Department of Anesthesiology, Shenzhen Third People's Hospital, Shenzhen, Guangdong, China;
[2] Medical Department of Shenzhen University, Shenzhen, Guangdong, China.

SUMMARY The incidence of breast cancer has exhibited an annually increasing trend, and the disease has become the most common malignant tumour worldwide. Currently, the primary treatment for breast cancer is surgical resection. However, metastatic recurrence is the main cause of cancer-related death in this patient population. Various factors are associated with breast cancer prognosis, and anaesthesia-induced changes in the tumour microenvironment have attracted increasing attention. To date, however, it remains unclear whether anaesthetic drugs have a positive or negative impact on cancer outcomes after surgery. The present article reviews the effects of different anaesthetics on the postoperative prognosis of breast cancer surgery to guide the choice of anaesthetic technique(s) and agents for such patients.

Keywords breast cancer, metastatic recurrence, anesthesia, techniques, agents

1. Introduction

Breast cancer is one of the primary causes of cancer-related death among females (*1*). Although surgical resection of breast cancer is the first-line treatment, other therapies, such as chemotherapy and radiation therapy, continue to play important roles (*2*). Mortality associated with breast cancer is attributable to recurrence and distant organ metastasis, with five-year survival rates ranging from 69.5% to 93.8% (*3,4*). Perioperative interventions produce substantial biological perturbations associated with the risk for recurrence after cancer surgery. Whether tumours recur or metastasise depends on the balance between immune capacity of the host and the progression of residual disease. Studies have shown that surgical stress and intraoperative anaesthesia impair host immunity (*5*). Previous studies have suggested that general anaesthetics can affect cancer progression (*6,7*). Several preclinical models have demonstrated that inhaled anaesthetics inhibit natural killer (NK) cell- and T lymphocyte-mediated immunity, resulting in increased metastasis (*8*). The present article reviews the effect of anaesthetics used during breast cancer surgery on breast cancer recurrence and survival and discusses the current status and future prospects of anaesthesia in breast cancer.

2. Inhalation anaesthesia

Inhalational anaesthetics are inhaled into the lungs through the respiratory tract to induce general anaesthesia (GA). Inhalational halogenated hydrocarbon anaesthetics, including isoflurane and sevoflurane, are known to provide a degree of cytoprotection to organs, including the heart, brain, and kidneys, and to reduce both infarct size and functional impairment in models of ischaemia-reperfusion injury (*9,10*).

However, animal and *in vitro* studies have shown that the use of volatile anaesthesia in cancer surgery may be associated with poorer cancer outcomes. In anaesthesia-induced immunosuppression, inhalation anaesthetics, such as sevoflurane, suppress cell-mediated immunity and promote tumour cell proliferation and angiogenesis. Sevoflurane induces the apoptosis of T lymphocytes and upregulates the expression of hypoxia-inducible factor-1a (HIF-1a) *in vitro*, whereas other inhalation anaesthetics, including isoflurane and desflurane, upregulate HIF-1a expression *in vitro* and *in vivo* (*11,12*) (Figure 1). In an *in-vitro* model of breast cancer cell function, sevoflurane increased proliferation, migration, and invasion in estrogen receptor (ER)-positive MCF7 cells, and increased proliferation and migration, but not invasion, in ER-negative cells (*13*). Jaura *et al.* found that serum from patients administered sevoflurane anaesthesia and opioids for primary breast cancer surgery reduced apoptosis in ER-negative breast cancer cells to a greater extent than serum from those administered propofol paravertebral anaesthesia (*14*). Similarly, clinical studies have reported that survival after cancer surgery is worse in patients who receive

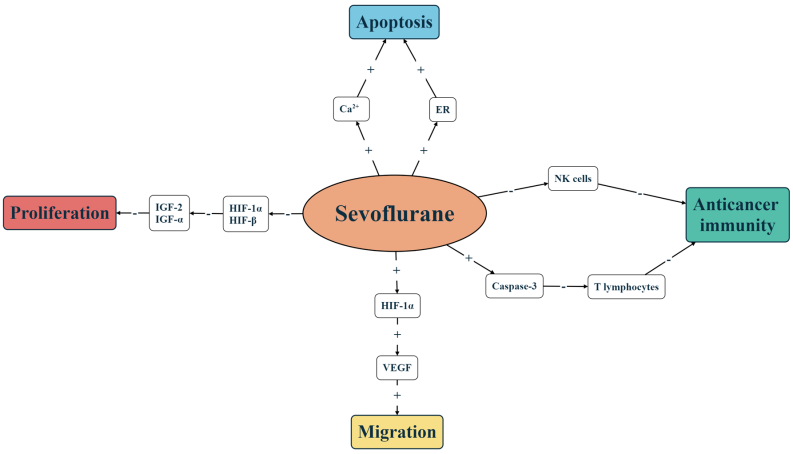

Figure 1. Mechanisms of sevoflurane on anticancer immunity, breast cancer cell proliferation, migration and apoptosis (*11-13*)**.** ER, endoplasmic reticulum; NK cells, natural killer cells; IGF, insulin-like growth factor; HIF, hypoxia inducible factor; VEGF, vascular endothelial growth factor.

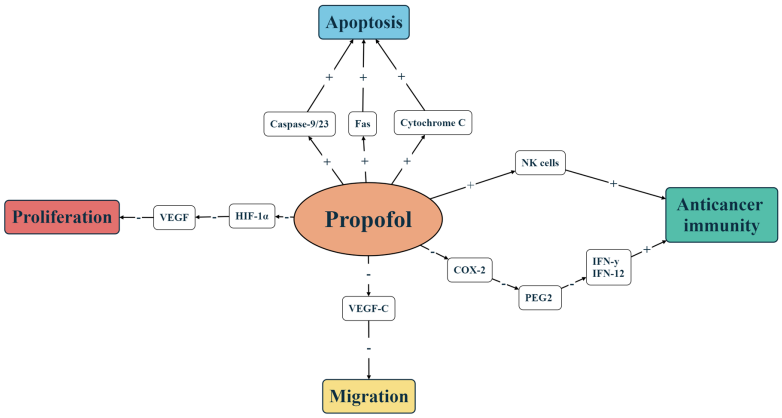

Figure 2 Mechanisms of propofol on anticancer immunity, breast cancer cell proliferation, migration and apoptosis (*23,24,26*)**.** Fas, a cell surface death receptor; NK cells, natural killer cells; VEGF, vascular endothelial growth factor; HIF, hypoxia inducible factor; COX-2, cyclooxygenase-2; PGE2, prostaglandin E2; IFN, interferon.

inhalation anaesthesia than in those who receive total intravenous anesthesia (TIVA) (*15*). Buckley also found that volatile inhalation anaesthesia and propofol had different effects on NK cell function in patients undergoing breast cancer surgery, with the former being shown to result in significant reductions (*16*). At the same time, relevant clinical studies have also confirmed that, in terms of survival rate after breast cancer surgery, the use of sevoflurane is not superior to propofol-based anaesthesia (*17,18*).

Paradoxically, inhalation anaesthesia does not always lead to worse prognosis in those with breast cancer. In a study investigating the effect of anaesthesia techniques on circulating tumour cell counts in breast cancer, the type of anaesthesia did not affect circulating tumour cell counts over time, although the administration of sevoflurane resulted in a significant increase in postoperative maximum tumour cell counts (*19*). Moreover, different inhalation anaesthetic gases are associated with varying prognoses after breast cancer surgery. Compared with sevoflurane, xenon reduces cell migration and secretion of proangiogenic factors in breast adenocarcinoma cells, thereby reducing the recurrence rate of tumour metastasis after breast cancer surgery (*20*). Relevant studies have also confirmed no significant difference in postoperative survival between different anaesthesia methods, whether inhalation or intravenous (*21,22*).

3. Intravenous anaesthesia

Anaesthetic drugs that are injected intravenously into the body and act on the central nervous system through the blood circulation to produce general anaesthetic effects are known as intravenous anaesthetics. Commonly used intravenous anaesthetics include thiopentone, ketamine, etomidate and propofol. A recent study confirmed the high priority of propofol in oncological surgery, and may also be a promising immunomodulatory drug for tumour therapy (*23*).

Studies have shown that propofol exerts antitumour effects through various mechanisms, including the inhibition of tumour viability, tumour progression, and cancer cell invasion (*24,25*) (Figure 2). For example, propofol-induced apoptosis has been observed in murine leukaemia RAW264.7 cells *in vitro* through altered levels of apoptosis-associated proteins, resulting in the induction of apoptotic gene expression and inhibition of cell growth (*26*). In *in vitro* models of breast cancer, 10% serum from patients receiving propofol anaesthesia reduced cancer cell proliferation, but not migration, compared with that from patients receiving sevoflurane anaesthesia (*27*). *In vitro* model breast cancer cells are highly aggressive and have a worse overall prognosis than ER-positive breast cancer. Therefore, the ability to attenuate proliferation or migration of this highly aggressive cell line by safely and easily altering the

manner in which anaesthesia is administered during primary cancer surgery has strong clinical implications (*27*). A retrospective analysis revealed that propofol may have a survival advantage over sevoflurane in patients with breast cancer (*28*). Propofol-based TIVA for breast cancer surgery may reduce the risk for recurrence within the first five years after modified radical mastectomy (*29*). Compared with sevoflurane inhalation anaesthesia, propofol TIVA can effectively inhibit the release of vascular endothelial growth factor-C (VEGF-C) induced by breast cancer surgery, thereby inhibiting tumour growth and metastasis (*30*).

However, in some studies, there was no significant difference in prognosis after breast cancer surgery between the two drugs. In patients undergoing primary breast cancer surgery, the use of either sevoflurane or propofol without regional anaesthesia did not appear to affect the risk for recurrence after one year (*31*). In a study investigating breast cancer surgery, Huang *et al*. (*32*) reported that propofol-based TIVA did not improve postoperative survival. This may be related to the fact that anaesthetics have little effect on perioperative immune activity during cancer surgery (*33*). The same situation occurred in a study by Kim *et al.*, in which five-year overall survival after breast cancer surgery was not associated with the choice of general anaesthetic (*34*). Results comparing the effect of anaesthetics (mainly propofol versus sevoflurane) on prognosis after breast cancer surgery are summarised in Table 1. These inconsistent results may be explained by the fact that multiple factors affecting cancer surgery prognosis must be considered.

4. Opioids

Opioids are commonly used in combination with inhalation anaesthetics as analgesics and sedatives for GA. However, non-synthetic and synthetic opioids can suppress cell-mediated immunity depending on the dose and duration of use (*35*). For example, morphine stimulates the growth of tumour cells *in vitro*, and synthetic opioids, such as fentanyl and remifentanil, inhibit cell-mediated immunity. Most opioids inhibit T lymphocyte proliferation (*36*).

In particular, data from animal and *in vitro* models suggest a role for opioids in the promotion of tumour cell survival and angiogenesis. In immune cells, stimulation of m-opioid receptors reduces the release of cytokines and decreases macrophage and lymphocyte proliferation (*37*). Opioids have been shown to drive breast cancer metastasis through δ-opioid receptors and oncogenic signal transducer and activator of transcription 3 (STAT3) (*38*). At clinically relevant doses, morphine has been associated with microvascular endothelial cell proliferation, angiogenesis, and vascularisation of human breast tumour xenografts in mouse models (*39*). *In vivo* studies investigating breast cancer xenograft models

Table 1. Studies comparing effects of propofol versus sevoflurane on prognosis of breast cancer

Research Type	Country	Cancer	Anesthetic Technique	Number of patients	Evaluations	Outcomes
Retrospective clinical studies	Korea, 2016 (*29*)	Breast cancer	Propofol *vs.* sevoflurane	363 (173 *vs.* 152)	Rate of cancer recurrence; overall survival rate.	Propofol was superior to sevoflurane; no difference.
Retrospective clinical studies	Sweden, 2014 (*17*)	Breast cancer	Propofol *vs.* sevoflurane	1,837 (620 *vs.*1217)	One-year and 5-year survival rate.	One-year survival rate: propofol was superior to sevoflurane; 5-year survival rate: no difference.
Retrospective clinical studies	UK, 2016 (*18*)	Mixed cancer	Total intravenous anesthesia (TIVA) *vs.* volatile inhalational anesthesia (INHA)	7,030 (3,714 *vs.* 3,316) (2,607 in each group after PS matching)	One-year survival rate and overall mortality rate.	TIVA was superior to INHA.
Retrospective clinical studies	Korea, 2015 (*22*)	Breast cancer	Propofol *vs.* sevoflurane	325 (173 *vs.* 152)	Five year-recurrence-free survival and overall survival.	Five year-recurrence-free survival: propofol was superior to sevoflurane; 5 year-overall survival: no difference.
Retrospective clinical studies	Sweden, 2020 (*28*)	Breast cancer	Propofol *vs.* sevoflurane	6,305 (3,096 *vs.* 3,209)	Five-year survival rate.	Propofol was superior to sevoflurane.
Retrospective clinical studies	Japan, 2020 (*31*)	Breast cancer	Propofol *vs.* sevoflurane	1,034 (814 *vs.* 220)	One-year survival rate.	No difference.
Retrospective clinical studies	Taiwan China, 2019 (*32*)	Breast cancer	Propofol *vs.* desflurane	976 (344 *vs.* 632)	Mortality rate; 5-year survival rate.	No difference.
Randomized controlled trials	Switzerland, 2020 (*19*)	Breast cancer *in vitro*	Propofol *vs.* sevoflurane	210 (103 *vs.*107)	Circulating tumor cell counts at three time points postoperatively (0, 48, and 72 h)	There was no difference between these two groups with respect to circulating tumor cell counts.
Randomized controlled trials	Ireland, 2009 (*27*)	Breast cancer *in vitro*	Propofol/paravertebral *vs.* sevoflurane/opioid	22 (11 *vs.* 11)	The proliferation/migration of MDA-MB-231 cells	Propofol/paravertebral anesthesia for breast cancer surgery inhibited proliferation, but not migration.
Randomized controlled trials	Ireland, 2014 (*20*)	Breast cancer *in vitro*	Sevoflurane *vs.* xenon	/	Cell viability; migration at 24h	Xenon was superior to sevoflurane.

Notes: PS, propensity scores

(using human MCF-7 and MDA-MB-231 cells) revealed that prolonged application of subcutaneous morphine sulfate at therapeutic doses accelerated breast tumour growth and increased tumour growth vascularisation (*40*).

However, the association between opioids and breast cancer progression remains controversial. Preclinical studies have suggested that high-dose morphine and other opioids have antiangiogenic and proapoptotic properties (*41*). An *in vitro* study reported that papaverine radio-sensitizes lung and breast cancer cells by targeting mitochondrial complex-1 (*42*). In a cohort study from Denmark, there was no association between opioids and breast cancer recurrence, regardless of opioid type, intensity, duration of use, or cumulative dose (*43*). Studies have confirmed that intraoperative opioids have a protective effect on recurrence-free survival in triple-negative breast cancer (*44*). Another study indicated that fentanyl plays an antitumour role by inducing apoptosis and reducing the number of cancer stem cells in human breast adenocarcinoma cells (*45*). In a study by Boudreau *et al.*, involving 4,216 females with a history of breast cancer, chronic opioid consumption, defined as opioid consumption over a 150-day period, did not increase the risk for new secondary breast cancers during a median follow-up of six years (*46*). Tramadol is an atypical opioid analgesic that has demonstrated antitumour effects in breast cancer cells both *in vitro* and *in vivo* (*47,48*). A retrospective analysis revealed that tramadol use was associated with reduced breast cancer recurrence and mortality rates in patients who underwent breast cancer surgery(*47*).

Therefore, further observational studies are warranted. Currently, there is no clear evidence suggesting that opioid use should be avoided in patients with breast cancer due to concerns about the risk for breast cancer recurrence (*49*).

5. GA adjuvants

Dexmedetomidine (DEX) is a selective a_2-adrenergic receptor agonist that exerts analgesic and antiemetic effects and can be used as an anaesthetic adjuvant in cancer surgery. As an adjuvant to anaesthetics, it reduces the use of analgesics, such as tramadol, morphine, and fentanyl, prolongs the time to first analgesic request, and relieves postoperative pain (*50*). Furthermore, DEX administration has been shown to enhance host protective immunity, including increases in NK and CD4-positive(+) cells and CD4/CD8 and T-helper cell (Th)1/Th2 ratios *via* suppression of the hypothalamic-pituitary-adrenal (HPA) axis and sympathetic nervous system (SNS) stimulation of the surgical stress response during cancer surgery (*51*) To a certain extent, this is beneficial in cancer surgery to prevent tumour recurrence and metastasis. However, DEX has also been reported to exert tumour-promoting effects. *In vitro* studies have shown that it promotes the proliferation, migration, and invasion of breast cancer cells by activating the A2B adrenergic receptor/ERK signalling pathway (*52*). Similar results were obtained in an *in vitro* study (*53*).

Nonsteroidal anti-inflammatory drugs (NSAIDs) are increasingly used to treat postoperative pain and are also commonly used in female breast surgery (*54*). In patients undergoing mastectomy, postoperative analgesia using flurbiprofen axetil combined with fentanyl was associated with decreases in serum concentrations of VEGF-C, tumour necrosis factor-alpha, and interleukin-1β compared with patients receiving fentanyl only (*55*). Relevant studies have shown that flurbiprofen can reduce the serum concentrations of these factors, most likely due to its ability to reduce the use of opioids (*56*). Opioids have been shown to exert some immunosuppressive effects. Recent evidence suggests that perioperative NSAIDs (flurbiprofen axetil and ketorolac) may be associated with decreased breast cancer recurrence by inhibiting proinflammatory and protumourigenic factors in patients undergoing surgery (*57*), consistent with a previous view by Forget *et al.* (*58*).

6. Other anaesthesia techniques

Regional anaesthesia has been consistently shown to attenuate the neuroendocrine response to surgery and, therefore, perioperative immunosuppression (*59,60*). It may also reduce the amount of GA required intraoperatively, provide excellent analgesia, and reduce opioid consumption. Compared with GA, regional (spinal) anaesthesia attenuates tumour metastasis in rats inoculated with a strain of breast adenocarcinoma (*61*). In breast cancer, VEGF-C, transforming growth factor-β, placental growth factor, and fibroblast growth factor (acidic and basic) promote angiogenesis and metastases (*62*). A propofol-paravertebral anaesthetic (PPA) technique would attenuate postoperative changes in these angiogenic factors to a greater extent than balanced GA and morphine analgesia in females undergoing surgery for primary breast cancer (*63*). These findings suggest that patients who received PPA anaesthesia had higher NK cell activity than those in the GA trial arm (*16*). Serum inoculated into the endoplasmic reticulum of the ER-negative MDA-MB-231 breast cancer cell line induced less apoptosis in the GA group than in the PPA group (*63*). However, in some cases, regional anaesthesia does not always have a positive effect. Regional anaesthesia analgesia (paravertebral block and propofol) did not reduce breast cancer recurrence after potentially curative surgery compared with volatile anaesthesia (sevoflurane) and opioids (*64*).

To some extent, local anaesthesia also controls breast cancer metastasis through the principle of local anaesthetics, such as lidocaine, which blocks voltage-gated sodium channels (*65-67*). This was also confirmed by *in vitro* experiments (*68*), which demonstrated the benefits of local anaesthesia in breast cancer surgery.

7. Conclusion

Current randomised controlled studies do not provide sufficient evidence to suggest that anaesthesia techniques are associated with recurrence rates or long-term outcomes in patients undergoing breast cancer surgery. Both preclinical and clinical studies have provided conflicting data regarding the effects of inhalation anaesthetics, propofol, and opioids on immune response and breast cancer growth. There is a strong correlation between patient underlying condition (*69,70*), cancer grade, risk for cancer recurrence, and postoperative death (*4*). Interestingly, in the clinical studies reviewed here, it was found that the same anaesthetic drug exhibited inconsistent associated prognosis in different types of cancer surgery. A simple comparison of sevoflurane and propofol in breast cancer surgery does not clearly indicate which of the two is superior. Furthermore, other GA adjuvant drugs also demonstrate bilateral effects, and only local anaesthesia can more clearly indicate its ability to improve prognosis in breast cancer surgery. However, due to the lack of multicentre or multi-country large clinical trials, it is not possible to draw definitive conclusions regarding which anaesthetic is more favourable for the long-term effect of breast cancer recurrence and metastasis. The above comparison results present certain challenges for anaesthesiologists in selecting appropriate anaesthetic drugs for breast cancer surgery. It is worth exploring whether the different effects of drugs on breast tumour subtypes should be considered while assessing the basic situation of patients and whether there are inconsistent signalling pathway mechanisms. As such, it cannot be ruled out that all perioperative factors comprehensively affect prognosis after breast cancer surgery.

Acknowledgements

We thank Shenzhen Science and Technology Innovation Commission for its support.

Funding: This work was supported by a grant from Shenzhen Science and Technology Innovation Commission, Basic Research (General Project), JCYJ20210324131410029.

Conflict of Interest: The authors have no conflicts of interest to disclose.

References

1. Siegel RL, Miller KD, Wagle NS, Jemal A. Cancer statistics, 2023. CA Cancer J Clin. 2023; 73:17-48.
2. Gralow JR, Burstein HJ, Wood W, Hortobagyi GN, Gianni L, von Minckwitz G, Buzdar AU, Smith IE, Symmans WF, Singh B, Winer EP. Preoperative therapy in invasive breast cancer: Pathologic assessment and systemic therapy issues in operable disease. J Clin Oncol. 2008; 26:814-819.
3. Chen CS, Liu TC, Lin HC, Lien YC. Does high surgeon and hospital surgical volume raise the five-year survival rate for breast cancer? A population-based study. Breast Cancer Res Treat. 2008; 110:349-356.
4. Yoo S, Lee HB, Han W, Noh DY, Park SK, Kim WH, Kim JT. Total intravenous anesthesia versus inhalation anesthesia for breast cancer surgery: A retrospective cohort study. Anesthesiology. 2019; 130:31-40.
5. Kim R. Anesthetic technique and cancer recurrence in oncologic surgery: Unraveling the puzzle. Cancer Metastasis Rev. 2017; 36:159-177.
6. Yuki K, Eckenhoff RG. Mechanisms of the immunological effects of volatile anesthetics: A review. Anesth Analg. 2016; 123:326-335.
7. Buggy DJ. Anesthesia, analgesia, and perioperative intervention in cancer surgery: The potential to influence outcome. Int Anesthesiol Clin. 2016; 54:1-3.
8. Melamed R, Bar-Yosef S, Shakhar G, Shakhar K, Ben-Eliyahu S. Suppression of natural killer cell activity and promotion of tumor metastasis by ketamine, thiopental, and halothane, but not by propofol: Mediating mechanisms and prophylactic measures. Anesth Analg. 2003; 97:1331-1339.
9. Wu L, Zhao H, Wang T, Pac-Soo C, Ma D. Cellular signaling pathways and molecular mechanisms involving inhalational anesthetics-induced organoprotection. J Anesth. 2014; 28:740-758.
10. Pagel PS, Crystal GJ. The discovery of myocardial preconditioning using volatile anesthetics: A history and contemporary clinical perspective. J Cardiothorac Vasc Anesth. 2018; 32:1112-1134.
11. Tavare AN, Perry NJS, Benzonana LL, Takata M, Ma D. Cancer recurrence after surgery: Direct and indirect effects of anesthetic agents. Int J Cancer. 2012; 130:1237-1250.
12. Loop T, Dovi-Akue D, Frick M, Roesslein M, Egger L, Humar M, Hoetzel A, Schmidt R, Borner C, Pahl HL, Geiger KK, Pannen BHJ. Volatile anesthetics induce caspase-dependent, mitochondria-mediated apoptosis in human T lymphocytes *in vitro*. Anesthesiology. 2005; 102:1147-1157.
13. Ecimovic P, McHugh B, Murray D, Doran P, Buggy DJ. Effects of sevoflurane on breast cancer cell function *in vitro*. Anticancer Res. 2013; 33:4255-4260.
14. Jaura AI, Flood G, Gallagher HC, Buggy DJ. Differential effects of serum from patients administered distinct anaesthetic techniques on apoptosis in breast cancer cells *in vitro*: A pilot study. Br J Anaesth. 2014; 113 Suppl 1:i63-67.
15. Lee JH, Kang SH, Kim Y, Kim HA, Kim BS. Effects of propofol-based total intravenous anesthesia on recurrence and overall survival in patients after modified radical mastectomy: A retrospective study. Korean J Anesthesiol. 2016; 69:126-132.
16. Buckley A, McQuaid S, Johnson P, Buggy DJ. Effect of anaesthetic technique on the natural killer cell anti-tumour activity of serum from women undergoing breast cancer surgery: A pilot study. Br J Anaesth. 2014; 113 Suppl 1:i56-62.
17. Enlund M, Berglund A, Andreasson K, Cicek C, Enlund A, Bergkvist L. The choice of anaesthetic--sevoflurane or propofol--and outcome from cancer surgery: A retrospective analysis. Ups J Med Sci. 2014; 119:251-261.
18. Wigmore TJ, Mohammed K, Jhanji S. Long-term survival for patients undergoing volatile versus IV anesthesia for

cancer surgery: A retrospective analysis. Anesthesiology. 2016; 124:69-79.
19. Hovaguimian F, Braun J, Z'graggen BR, Schläpfer M, Dumrese C, Ewald C, Dedes KJ, Fink D, Rölli U, Seeberger M, Tausch C, Papassotiropoulos B, Puhan MA, Beck-Schimmer B. Anesthesia and circulating tumor cells in primary breast cancer patients: A randomized controlled trial. Anesthesiology. 2020; 133:548-558.
20. Ash SA, Valchev GI, Looney M, Ni Mhathuna A, Crowley PD, Gallagher HC, Buggy DJ. Xenon decreases cell migration and secretion of a pro-angiogenesis factor in breast adenocarcinoma cells: Comparison with sevoflurane. Br J Anaesth. 2014; 113 Suppl 1:i14-21.
21. Kim MH, Kim DW, Kim JH, Lee KY, Park S, Yoo YC. Does the type of anesthesia really affect the recurrence-free survival after breast cancer surgery? Oncotarget. 2017; 8:90477-90487.
22. Hong B, Lee S, Kim Y, Lee M, Youn AM, Rhim H, Hong SH, Kim YH, Yoon SH, Lim C. Anesthetics and long-term survival after cancer surgery-total intravenous versus volatile anesthesia: A retrospective study. BMC Anesthesiol. 2019; 19:233.
23. Gu L, Pan X, Wang C, Wang L. The benefits of propofol on cancer treatment: Decipher its modulation code to immunocytes. Front Pharmacol. 2022; 13:919636.
24. Kim R. Effects of surgery and anesthetic choice on immunosuppression and cancer recurrence. J Transl Med. 2018; 16:8.
25. Crone V, Hasselager RP, Fransgaard T, Gögenur I. Anaesthetic technique and outcomes after colorectal cancer surgery. Dan Med J. 2020; 67:A04190255.
26. Wu RSC, Liu KC, Tang NY, Chung HK, Ip SW, Yang JS, Chung JG. cDNA microarray analysis of the gene expression of murine leukemia RAW 264.7 cells after exposure to propofol. Environ Toxicol. 2013; 28:471-478.
27. Deegan CA, Murray D, Doran P, Ecimovic P, Moriarty DC, Buggy DJ. Effect of anaesthetic technique on oestrogen receptor-negative breast cancer cell function *in vitro*. Br J Anaesth. 2009; 103:685-690.
28. Enlund M, Berglund A, Ahlstrand R, Walldén J, Lundberg J, Wärnberg F, Ekman A, Sjöblom Widfeldt N, Enlund A, Bergkvist L. Survival after primary breast cancer surgery following propofol or sevoflurane general anesthesia-A retrospective, multicenter, database analysis of 6305 Swedish patients. Acta Anaesthesiol Scand. 2020; 64:1048-1054.
29. Lee JH, Kang SH, Kim Y, Kim HA, Kim BS. Effects of propofol-based total intravenous anesthesia on recurrence and overall survival in patients after modified radical mastectomy: A retrospective study. Korean J Anesthesiol. 2016; 69:126-132.
30. Yan T, Zhang GH, Wang BN, Sun L, Zheng H. Effects of propofol/remifentanil-based total intravenous anesthesia versus sevoflurane-based inhalational anesthesia on the release of VEGF-C and TGF-β and prognosis after breast cancer surgery: A prospective, randomized and controlled study. BMC Anesthesiol. 2018; 18:131.
31. Shiono S, Shibata SC, Kabata D, Shintani A, Ikeda T, Fujino Y. Comparison of 1-year recurrence-free survival between sevoflurane and propofol use for general anesthesia management in primary breast cancer surgery. J Anesth. 2020; 34:694-701.
32. Huang YH, Lee MS, Lou YS, Lai HC, Yu JC, Lu CH, Wong CS, Wu ZF. Propofol-based total intravenous anesthesia did not improve survival compared to desflurane anesthesia in breast cancer surgery. PloS One. 2019; 14:e0224728.
33. Oh CS, Lee J, Yoon TG, Seo EH, Park HJ, Piao L, Lee SH, Kim SH. Effect of equipotent doses of propofol versus sevoflurane anesthesia on regulatory T cells after breast cancer surgery. Anesthesiology. 2018; 129:921-931.
34. Kim R, Kawai A, Wakisaka M, Kin T. Current status and prospects of anesthesia and breast cancer: Does anesthetic technique affect recurrence and survival rates in breast cancer surgery? Front Oncol. 2022; 12:795864.
35. Yardeni IZ, Beilin B, Mayburd E, Alcalay Y, Bessler H. Relationship between fentanyl dosage and immune function in the postoperative period. J Opioid Manag. 2008; 4:27-33.
36. Sacerdote P, Bianchi M, Gaspani L, Manfredi B, Maucione A, Terno G, Ammatuna M, Panerai AE. The effects of tramadol and morphine on immune responses and pain after surgery in cancer patients. Anesth Analg. 2000; 90:1411-1414.
37. Wang J, Barke RA, Ma J, Charboneau R, Roy S. Opiate abuse, innate immunity, and bacterial infectious diseases. Arch Immunol Ther Exp (Warsz). 2008; 56:299-309.
38. Tripolt S, Neubauer HA, Knab VM, Elmer DP, Aberger F, Moriggl R, Fux DA. Opioids drive breast cancer metastasis through the δ-opioid receptor and oncogenic STAT3. Neoplasia. 2021; 23:270-279.
39. Gupta K, Kshirsagar S, Chang L, Schwartz R, Law PY, Yee D, Hebbel RP. Morphine stimulates angiogenesis by activating proangiogenic and survival-promoting signaling and promotes breast tumor growth. Cancer Res. 2002; 62:4491-4498.
40. Bimonte S, Barbieri A, Rea D, Palma G, Luciano A, Cuomo A, Arra C, Izzo F. Morphine promotes tumor angiogenesis and increases breast cancer progression. Biomed Res Int. 2015; 2015:161508.
41. Weingaertner IR, Koutnik S, Ammer H. Chronic morphine treatment attenuates cell growth of human BT474 breast cancer cells by rearrangement of the ErbB signalling network. PloS One. 2013; 8:e53510.
42. Benej M, Hong X, Vibhute S, Scott S, Wu J, Graves E, Le QT, Koong AC, Giaccia AJ, Yu B, Chen CS, Papandreou I, Denko NC. Papaverine and its derivatives radiosensitize solid tumors by inhibiting mitochondrial metabolism. Proc Natl Acad Sci U S A. 2018; 115:10756-10761.
43. Cronin-Fenton DP, Heide-Jørgensen U, Ahern TP, Lash TL, Christiansen PM, Ejlertsen B, Sjøgren P, Kehlet H, Sørensen HT. Opioids and breast cancer recurrence: A Danish population-based cohort study. Cancer. 2015; 121:3507-3514.
44. Montagna G, Gupta HV, Hannum M, Tan KS, Lee J, Scarpa JR, Plitas G, Irie T, McCormick PJ, Fischer GW, Morrow M, Mincer JS. Intraoperative opioids are associated with improved recurrence-free survival in triple-negative breast cancer. Br J Anaesth. 2021; 126:367-376.
45. Kocak N, Ozen F, Yildirim IH, Duran Y. Fentanyl inhibits tumorigenesis from human breast stem cells by inducing apoptosis. Asian Pac J Cancer Prev. 2017; 18:735-739.
46. Boudreau DM, Chen L, Yu O, Bowles EJA, Chubak J. Risk of second breast cancer events with chronic opioid use in breast cancer survivors. Pharmacoepidemiol Drug Saf. 2019; 28:740-753.
47. Kim MH, Oh JE, Park S, Kim JH, Lee KY, Bai SJ, Song H, Hwang HJ, Kim DW, Yoo YC. Tramadol use is associated with enhanced postoperative outcomes in breast cancer

patients: A retrospective clinical study with *in vitro* confirmation. Br J Anaesth. 2019; 123:865-876.
48. Kim MH, Lee JR, Kim KJ, Jun JH, Hwang HJ, Lee W, Nam SH, Oh JE, Yoo YC. Identification for antitumor effects of tramadol in a xenograft mouse model using orthotopic breast cancer cells. Sci Rep. 2021; 11:22113.
49. Cronin-Fenton D. Opioids and breast cancer recurrence. Curr Opin Support Palliat Care. 2019; 13:88-93.
50. Liu C, Wang W, Shan Z, Zhang H, Yan Q. Dexmedetomidine as an adjuvant for patients undergoing breast cancer surgery: A meta-analysis. Medicine. 2020; 99:e23667.
51. Wang K, Wu M, Xu J, Wu C, Zhang B, Wang G, Ma D. Effects of dexmedetomidine on perioperative stress, inflammation, and immune function: systematic review and meta-analysis. Br J Anaesth. 2019; 123:777-794.
52. Xia M, Ji NN, Duan ML, Tong JH, Xu JG, Zhang YM, Wang SH. Dexmedetomidine regulate the malignancy of breast cancer cells by activating α2-adrenoceptor/ERK signaling pathway. Eur Rev Med Pharmacol Sci. 2016; 20:3500-3506.
53. Lavon H, Matzner P, Benbenishty A, Sorski L, Rossene E, Haldar R, Elbaz E, Cata JP, Gottumukkala V, Ben-Eliyahu S. Dexmedetomidine promotes metastasis in rodent models of breast, lung, and colon cancers. Br J Anaesth. 2018; 120:188-196.
54. Klifto KM, Elhelali A, Payne RM, Cooney CM, Manahan MA, Rosson GD. Perioperative systemic nonsteroidal anti-inflammatory drugs (NSAIDs) in women undergoing breast surgery. Cochrane Database Syst Rev. 2021; 11:CD013290.
55. Wen Y, Wang M, Yang J, Wang Y, Sun H, Zhao J, Liu W, Zhou Z, Deng H, Castillo-Pedraza C, Zhang Y, Candiotti KA. A comparison of fentanyl and flurbiprofen axetil on serum VEGF-C, TNF-α, and IL-1ß concentrations in women undergoing surgery for breast cancer. Pain Pract. 2015; 15:530-537.
56. Doleman B, Leonardi-Bee J, Heinink TP, Boyd-Carson H, Carrick L, Mandalia R, Lund JN, Williams JP. Pre-emptive and preventive NSAIDs for postoperative pain in adults undergoing all types of surgery. Cochrane Database Syst Rev. 2021; 6:CD012978.
57. Desmedt C, Demicheli R, Fornili M, Bachir I, Duca M, Viglietti G, Berlière M, Piccart M, Sotiriou C, Sosnowski M, Forget P, Biganzoli E. Potential benefit of intra-operative administration of ketorolac on breast cancer recurrence according to the patient's body mass index. J Natl Cancer Inst. 2018; 110:1115-1122.
58. Forget P, Bentin C, Machiels JP, Berliere M, Coulie PG, De Kock M. Intraoperative use of ketorolac or diclofenac is associated with improved disease-free survival and overall survival in conservative breast cancer surgery. Br J Anaesth. 2014; 113 Suppl 1:i82-87.
59. Buggy DJ, Smith G. Epidural anaesthesia and analgesia: Better outcome after major surgery?. Growing evidence suggests so. BMJ. 1999; 319:530-531.
60. Tsuchiya Y, Sawada S, Yoshioka I, Ohashi Y, Matsuo M, Harimaya Y, Tsukada K, Saiki I. Increased surgical stress promotes tumor metastasis. Surgery. 2003; 133:547-555.
61. Bar-Yosef S, Melamed R, Page GG, Shakhar G, Shakhar K, Ben-Eliyahu S. Attenuation of the tumor-promoting effect of surgery by spinal blockade in rats. Anesthesiology. 2001; 94:1066-1073.
62. Gisterek I, Matkowski R, Lacko A, Sedlaczek P, Szewczyk K, Biecek P, Halon A, Staszek U, Szelachowska J, Pudelko M, Bebenek M, Harlozinska-Szmyrka A, Kornafel J. Serum vascular endothelial growth factors a, C and d in human breast tumors. Pathol Oncol Res. 2010; 16:337-344.
63. Looney M, Doran P, Buggy DJ. Effect of anesthetic technique on serum vascular endothelial growth factor C and transforming growth factor β in women undergoing anesthesia and surgery for breast cancer. Anesthesiology. 2010; 113:1118-1125.
64. Sessler DI, Pei L, Huang Y, Fleischmann E, Marhofer P, Kurz A, Mayers DB, Meyer-Treschan TA, Grady M, Tan EY, Ayad S, Mascha EJ, Buggy DJ, Collaboration BCR. Recurrence of breast cancer after regional or general anaesthesia: A randomised controlled trial. Lancet. 2019; 394:1807-1815.
65. Baptista-Hon DT, Robertson FM, Robertson GB, Owen SJ, Rogers GW, Lydon EL, Lee NH, Hales TG. Potent inhibition by ropivacaine of metastatic colon cancer SW620 cell invasion and NaV1.5 channel function. Br J Anaesth. 2014; 113 Suppl 1:i39-i48.
66. Fraser SP, Diss JKJ, Chioni A-M, *et al.* Voltage-gated sodium channel expression and potentiation of human breast cancer metastasis. Clin Cancer Res. 2005; 11:5381-5389.
67. Lucchinetti E, Awad AE, Rahman M, Feng J, Lou PH, Zhang L, Ionescu L, Lemieux H, Thébaud B, Zaugg M. Antiproliferative effects of local anesthetics on mesenchymal stem cells: potential implications for tumor spreading and wound healing. Anesthesiology. 2012; 116:841-856.
68. Chang YC, Liu CL, Chen MJ, Hsu YW, Chen SN, Lin CH, Chen CM, Yang FM, Hu MC. Local anesthetics induce apoptosis in human breast tumor cells. Anesth Analg. 2014; 118:116-124.
69. Arendt LM, McCready J, Keller PJ, Baker DD, Naber SP, Seewaldt V, Kuperwasser C. Obesity promotes breast cancer by CCL2-mediated macrophage recruitment and angiogenesis. Cancer Res. 2013; 73:6080-6093.
70. Kolb R, Phan L, Borcherding N, *et al.* Obesity-associated NLRC4 inflammasome activation drives breast cancer progression. Nat Commun. 2016; 7:13007.

Received August 22, 2023; Revised October 20, 2023; Accepted October 21, 2023.

*Address correspondence to:
Qiang Wu, Department of Anesthesiology, Shenzhen Third People's Hospital, No. 29 Bujibulan Road, Longgang District, Shenzhen 518112, China.
E-mail: wuqiang@mail.sustech.edu.cn

Released online in J-STAGE as advance publication October 31, 2023.

Original Article

DOI: 10.5582/ddt.2023.01093

Lack of information on gender differences in the package inserts of prescription drugs in Japan

Narumi Maida[1,2], Shingo Kondo[1,2,*], Masanori Ogawa[3], Naoko Hayashi[2], Hiroki Iwata[1,2], Noriko Kobayashi[1,2], Katsunori Yamaura[1,2]

[1] Division of Social Pharmacy, Center for Social Pharmacy and Pharmaceutical Care Sciences, Faculty of Pharmacy, Keio University, Tokyo, Japan;
[2] Keio University Community Pharmacy, Tokyo, Japan;
[3] Medi Pharm Co., Ltd., Tokyo, Japan.

SUMMARY The package inserts of prescription drugs provide essential information for the proper administration of pharmacotherapy. The incidence of adverse reactions for several drugs is known to be higher in women than in men. However, no studies have examined whether information on gender differences is included in Japanese package inserts. Therefore, this study investigated information on gender differences in the package inserts of Japanese prescription drugs, using the drug information database JAMES provided by the Medical Information System Development Center and the Japan Pharmaceutical Information Center. Non-proprietary names of prescription drugs were yielded 1,679 in Japan. Of the 1,679 ingredients in package inserts of prescription drugs, 76 (4.5%) included information on gender differences. The number of inserts that contained information on gender differences in the "DOSAGE AND ADMINISTRATION," "ADVERSE REACTIONS," and "PHARMACOKINETICS" sections was 3, 16, and 62, respectively. Furthermore, in the "ADVERSE REACTIONS" section, 15 of the 16 inserts mentioned a higher frequency of adverse reactions in women compared with men. Importantly, most of the inserts with information on gender differences in the "PHARMACOKINETICS" section mentioned a higher area under the curve for women than for men. Most of the package inserts of prescription drugs with information on gender differences provide useful information aimed at preventing risks in women. However, there is an extreme lack of information on gender differences in the package inserts of prescription drugs in Japan, and we consider enhancing information on gender difference as an urgent issue.

Keywords gender-specific medicine, sex differences, adverse reaction, ethical drugs

1. Introduction

The incidence of adverse reactions for several drugs is known to be higher in women than in men (*1,2*). Gender differences in pharmacokinetics, including differences in drug absorption and metabolic enzyme expression rates between men and women, have also been reported (*3*).

In the 1950s and 1960s, thalidomide, which was initially administered as a hypnotic drug, caused numerous birth defects worldwide. In the 1970s, diethylstilbestrol, which was administered as an anti-miscarriage drug, resulted in numerous reports of reproductive disorders in mothers and their growing daughters. In response, the U.S. Food and Drug Administration (FDA) published guidelines in 1977 to exclude women from clinical trials (*4*). In 1985, physicians who were concerned about the lack of data on women's health suggested the need for biomedical research on women (*5*). In 1986, a notice was issued requesting the collection of data on women in clinical trials (*6,7*). Since 2000, there has been a growing awareness in Japan of the importance of gender-specific pharmacotherapy. The number of medical facilities with women's outpatient clinics is gradually increasing in Japan.

In the U.S., considering that adverse reactions of the hypnotic drugs zolpidem are more common in women, the FDA issued a notice setting the initial dosage of zolpidem at different doses for men and women (*8,9*). Since then, the package insert has indicated lower starting doses for women than for men, but the Japanese package insert has no such indication and the initial doses are the same for men and women.

The package inserts of prescription drugs provide

essential information for the proper administration of pharmacotherapy and are one of the most accessible sources of drug information for health care professionals in Japan. The Ministry of Health, Labour and Welfare has provided instructions regarding the sections and numbers that should be included in the package insert of prescription drugs in Japan (*10*).

Although the promotion of gender-specific medicine is critical, the actual state of information on gender differences in the "DOSAGE AND ADMINISTRATION," "ADVERSE REACTIONS," and "PHARMACOKINETICS" sections of the package inserts of prescription drugs in Japan is not known. Therefore, the purpose of this research was to investigate the actual state of information on gender differences in the package inserts of prescription drugs in Japan and to clarify issues from the viewpoint of information in promoting gender-specific medicine.

2. Materials and Methods

2.1. Methods for searching the package inserts of prescription drugs

We investigated information on gender differences in the package inserts of prescription drugs, using the drug information database JAMES provided by the Medical Information System Development Center and the Japan Pharmaceutical Information Center. The research was conducted using the data of prescription drug package inserts in Japan that were last revised before December 2022. The search terms were "gender," "gender difference," "men," and "women" in Japanese. The contents of package inserts that returned hits with the search terms in the "DOSAGE AND ADMINISTRATION," "ADVERSE REACTIONS," and "PHARMACOKINETICS" sections of the package inserts were reviewed, and drugs with information on gender differences were extracted. In addition, data on animal experiments were excluded from this study.

2.2. Methods for identifying the number of non-proprietary names in prescription drugs

The number of prescription drugs was calculated using the individual drug code, known as the "YJ code," in order to identify the number of non-proprietary names. The YJ code is a 12-digit alphanumeric code. Because the first 7 digits of the YJ code are identical for the same non-proprietary names, the number of prescription drugs with the same first 7-digits were counted as one non-proprietary name. When both brand-name and generic drugs were available, information from the package insert of the brand-name drug was used. Drugs with different YJ codes were counted as one component. As an exception, we visually confirmed and counted drugs with the same non-proprietary name but having different formulations as well as drugs with different salts (different non-proprietary name but the same active ingredient) and biosimilar drugs as one drug.

In this study, we excluded drugs classified as topical drugs for local action and ingredients for preparation (*e.g.*, white soft sugar for taste correction) because they have no systemic action. In addition, drugs containing multiple active ingredients, including combination products and infusion solutions, as well as blood products were excluded.

3. Results

3.1. Number of drugs with information on gender differences in package inserts

To explore the information on gender differences, we calculated the number of prescription drugs using the YJ code. Our study yielded 1,679 non-proprietary names of prescription drugs in Japan (Figure 1). Of these, there were 76 drugs (4.5%) with information on gender differences in the package inserts. The number of drugs

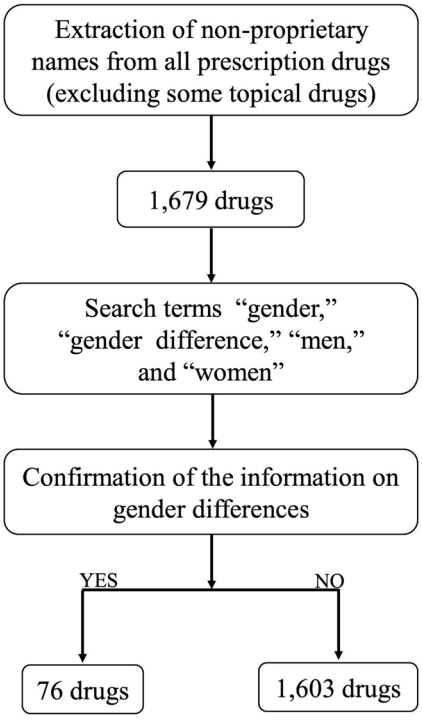

Figure 1. Process for extracting information on gender differences in the package inserts of prescription drugs. The number of prescription drugs was calculated using the YJ code. Excluded drugs were classified as topical drugs for local action and ingredients for preparation. In addition, drugs containing multiple active ingredients, including combination products and infusion solutions, as well as blood products were excluded. Non-proprietary names of prescription drugs were yielded 1,679 in Japan. The search terms were "gender," "gender difference," "men," and "women" in Japanese. The contents of package inserts that returned hits with the search terms were reviewed, and drugs with information on gender differences were extracted. Of these, there were 76 drugs with information on gender differences in the package inserts.

that included information on gender differences in the "DOSAGE AND ADMINISTRATION," "ADVERSE REACTIONS," and "PHARMACOKINETICS" sections was 3, 16, and 62, respectively (Figure 2). In addition, there were 4 drugs, ramosetron hydrochloride, pioglitazone hydrochloride, mirabegron, and nevirapine, with information on gender differences across multiple sections.

3.2. Drug package inserts describing gender differences in the "DOSAGE AND ADMINISTRATION" section

The package inserts of 3 drugs, metreleptin, pioglitazone hydrochloride, and ramosetron hydrochloride, mentioned gender differences in the "DOSAGE AND ADMINISTRATION" section (Table 1). Metreleptin, a leptin hormone with higher blood secretion levels

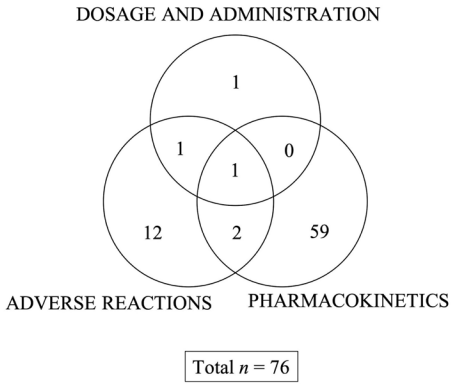

Figure 2. Venn diagram; breakdown of the 76 drugs and sections with information on gender differences in the drug package inserts. There were 76 drugs with information on gender differences in the package inserts. The number of drugs that included information on gender differences in the "DOSAGE AND ADMINISTRATION," "ADVERSE REACTIONS", and "PHARMACOKINETICS" sections was 3, 16, and 62, respectively. In addition, there were 4 drugs with information on gender differences across multiple sections.

in women than in men, was set at a higher dose in women than in men. Ramosetron hydrochloride was set at a lower dose for women than for men. In the "PRECAUTIONS CONCERNING DOSAGE AND ADMINISTRATION" section, it was recommended that the starting dosage of pioglitazone hydrochloride be lower in women than in men.

3.3. Drug package inserts describing gender differences in the "ADVERSE REACTIONS" section

The package inserts of 16 drugs mentioned gender differences in the "ADVERSE REACTIONS" section (Table 2). Fifteen of the 16 drugs were described as having a higher incidence of adverse reactions in women than in men. Antiviral drugs were the most common therapeutic category, with 6 drugs, while the others were 1 drug each. Severe lactic acidosis and severe hepatomegaly (fatty liver) due to fat deposition were the most frequently reported adverse reactions for antiviral drugs (5 drugs). An increased frequency of adverse reactions in women was noted in the package inserts of 4 drugs, emedastine fumarate, lansoprazole, sodium ferrous citrate, and theophylline. The only drug that was reported to have more adverse reactions in men than in women was the anti-arrhythmic drug verapamil hydrochloride.

3.4. Drug package inserts describing gender differences in the "PHARMACOKINETICS" section

The package inserts of 62 drugs mentioned gender differences in the "PHARMACOKINETICS" section (Table 3). Many of the drugs were described as having higher blood concentrations or lower clearance (CL) in women than in men. In addition, some package inserts stated that there were no differences in pharmacokinetics between men and women. We counted the number of medicines for these parameters. Of these, 31 drugs (50%)

Table 1. List of drugs with information on gender differences in the "DOSAGE AND ADMINISTRATION" section of the package inserts for prescription drugs (*n* = 3)

Non-proprietary name of drug	Therapeutic Category[a]	Dosages
metreleptin (genetical recombination)	other hormone preparations (including anti-hormone agents)	The usual dose of metreleptin is 0.04 mg/kg for men, 0.06 mg/kg for women under 18 years of age, and 0.08 mg/kg for women over 18 years of age by subcutaneous injection once daily.
pioglitazone hydrochloride	diabetes agent	Since edema has been reported relatively frequently in women, when administering to women, it is desirable to pay attention to the occurrence of edema and start administration at 15 mg once daily.
ramosetron hydrochloride	other gastrointestinal drugs	<Diarrhea-type irritable bowel syndrome in men> The usual adult male dosage is 5 μg of ramosetron hydrochloride administered orally once daily. The dosage may be adjusted according to the symptoms, but the maximum daily dose should not exceed 10 μg. <Diarrhea-type irritable bowel syndrome in women> The usual dose for adult women is 2.5 μg of ramosetron hydrochloride administered orally once daily. The dose can be increased if the effect is insufficient, but the maximum daily dose should not exceed 5 μg.

[a]For the medicinal efficacy classification of pharmaceutical ingredients, we used the "Therapeutic category number" used in Japan.

Table 2. List of drugs with information on gender differences in the "ADVERSE REACTIONS" section of the package inserts for prescription drugs (*n* = 16)

Non-proprietary name of drug	Therapeutic Category[a]	Incidence	Adverse reactions
abacavir sulfate	antiviral drug	W > M	Severe lactic acidosis and severe hepatomegaly (fatty liver) due to fat deposition
emedastine fumarate	other allergy medications	W > M	Frequency of adverse reactions
emtricitabine	antiviral drug	W > M	Severe lactic acidosis and severe hepatomegaly (fatty liver) due to fat deposition
lamivudine	antiviral drug	W > M	Severe lactic acidosis and severe hepatomegaly (fatty liver) due to fat deposition
lansoprazole	agent for peptic ulcer	W > M	Frequency of adverse reactions
mirabegron	other urogenital and anal medications	W > M	Prolongation of QTc interval
moxifloxacin hydrochloride	synthetic antibacterial agent	W > M	Prolongation of QT interval
nevirapine	antiviral drug	W > M	Development of rash or liver dysfunction
pioglitazone hydrochloride	diabetes agent	W > M	Edema, fractures
ramosetron hydrochloride	other gastrointestinal drugs	W > M	Constipation and hard stools
sodium ferrous citrate	inorganic preparations	W > M	Frequency of adverse reactions
temocapril hydrochloride	antihypertensive	W > M	Cough
tenofovir disoproxil fumarate	antiviral drug	W > M	Severe lactic acidosis and severe hepatomegaly (fatty liver) due to fat deposition
theophylline	bronchodilator	W > M	Frequency of adverse reactions
verapamil hydrochloride	antiarrhythmic drug	M > W	Decreased LH and testosterone levels in the blood
zidovudine	antiviral drug	W > M	Severe lactic acidosis and severe hepatomegaly (fatty liver) due to fat deposition

M, men; W, women; [a]For the medicinal efficacy classification of pharmaceutical ingredients, we used the "Therapeutic category number" used in Japan.

included information on gender differences in the area under the curve (AUC) (Figure 3). Next were 29 drugs (47%) for maximum blood concentration (C_{max}), 14 drugs (23%) for blood concentration half-life ($T_{1/2}$), 17 drugs (27%) for CL, 6 drugs (9.7%) for volume of distribution, and 6 drugs (9.7%) for protein binding as well as 8 drugs (13%) that referred to "overall pharmacokinetics." Many package inserts included information on gender differences in the pharmacokinetic parameters AUC, C_{max}, CL, and $T_{1/2}$. About half of the drugs provided AUC and C_{max} data. The number of coverages of information for each of the four pharmacokinetic parameters by component was confirmed by a Venn diagram, and it was found that only two drugs, nevirapine and tigecycline, included all four parameters, while 10 drugs included three parameters (Figure 4). The other 50 drugs included two or fewer pharmacokinetics parameters with information on gender differences.

4. Discussion

In this study, we investigated the status of information on gender differences in the package inserts of prescription drugs marketed in Japan on a non-proprietary name basis. Information on gender differences in the "DOSAGE AND ADMINISTRATION," "ADVERSE REACTIONS," and "PHARMACOKINETICS" sections was available for 76 drugs (Figure 1). This number represents approximately 4.5% of the 1,679 prescription drugs in Japan, indicating for the first time that there is an extreme lack of information on gender differences in the package inserts of prescription drugs in Japan.

In the "DOSAGE AND ADMINISTRATION" section of the package inserts, there were three drugs for which the dosages for men and women differed (Table 1). The dosages of ramosetron hydrochloride and pioglitazone hydrochloride were set lower because adverse reactions are more likely to occur in women than in men. In clinical studies of pioglitazone hydrochloride in Japan conducted up to the time of its approval (15 mg, 30 mg, or 45 mg of pioglitazone hydrochloride once daily), edema occurred in 3.9% (26/665) of men and 11.2% (72/643) of women who received the drug alone or in combination with other diabetes drugs excluding insulin (*11*). In addition, edema occurred in 13.6% (3/22) of men and 28.9% (11/38) of women when pioglitazone hydrochloride was administered with insulin. The information included in the pioglitazone hydrochloride package insert may reflect the results of this clinical trial.

In the "ADVERSE REACTIONS" section of the package inserts, it was found that the incidence of adverse reactions differed between men and women for 16 drugs. Of these, the incidence of adverse reactions was higher in women for the 15 drugs other than verapamil hydrochloride. Among them, "severe lactic acidosis and severe hepatomegaly (fatty liver) due to fat deposition" in the "antiviral drug" category was much more common among women. It has been reported that the probability of hepatic impairment with nevirapine is higher in women (*12*); this report has also been cited in the human immunodeficiency virus treatment guidelines in Japan (*13*). It is expected that as information on gender differences becomes more complete, it will be included in guidelines for the treatment of other diseases as well.

Table 3. List of drugs with information on gender differences in the "PHARMACOKINETICS" section of the package inserts for prescription drugs (n = 62)

Non-proprietary name of drug	Therapeutic Category[a]	Women/Men							
		AUC	C_{max} (C_{ss})	$T_{1/2}$	CL	Distribution volume	Protein binding rate	Overall pharmaco-kinetics	Remarks
apixaban	anticoagulant	1.15	1.18	-	-	-	-	-	
apremilast	metabolic drugs not elsewhere classified	1.31	1.08	-	-	-	-	-	
aripiprazole	psychoneurotic agent	-	-	-	-	-	-	M = W	
azithromycin hydrate	antibiotic preparation	-	-	1.68	-	-	-	-	
bevacizumab	other oncologic drugs	-	-	-	0.79	0.82	-	-	
bilastine	other allergy medications	M = W[c]	M = W[c]	-	-	-	-	-	
cabergoline	anti parkinsonian	1.06	0.09	1.16	-	-	-	-	
celecoxib	antipyretic analgesic anti-inflammatory agent	1.88	1.88	-	-	-	-	-	Elderly people
cetuximab	other oncologic drugs	-	-	-	0.75	-	-	-	
cinacalcet hydrochloride	metabolic drugs not elsewhere classified	-	-	-	-	-	0.99	-	Calculated from average
dabigatran etexilate methanesulfonate	anticoagulant	1.50 >	-	-	-	-	-	-	
darunavir ethanolate	antiviral agent	1.17	-	-	-	-	-	-	
dexmedetomidine hydrochloride	hypnotic sedative, anti-anxiety drug	-	-	-	-	-	M = W	-	
dolutegravir sodium	antiviral agent	-	-	-	-	-	-	1.2[b] >	
dotinurad	gout remedy	1.29	1.15	1.02	-	-	-	-	
eldecalcitol	vitamin A and D agents	-	-	-	M = W	-	M = W	-	
eltrombopag olamine	metabolic drugs not elsewhere classified	1.5[b]	-	-	-	-	-	-	
entecavir hydrate	antiviral agent	-	-	-	M = W	-	-	-	
febuxostat	gout remedy	1.12	1.24	-	-	-	-	-	
fesoterodine fumarate	other genitourinary and anal drugs	M = W	M = W	-	-	-	-	-	Elderly people
fluvoxamine maleate	psychoneurotic agent	2.97	2.61	-	0.33	-	-	-	6-11 years old, 50 mg/day[d]
gadobutrol	other diagnostic agents (excluding *in-vitro* diagnostic agents)	1.10[c]	-	0.91[c]	1.02[c]	-	-	-	Elderly people
gemcitabine hydrochloride	antimetabolite	-	-	2.08	0.34	-	-	-	
icatibant acetate	other allergy medications	1.26	1.26	-	-	-	-	-	
imidafenacin	other genitourinary and anal drugs	-	-	-	M = W	-	-	-	
lacosamide	antiepileptic drug	1.13[c]	1.19[c]	0.83[c]	-	-	-	-	Elderly people
leflunomide	metabolic drugs not elsewhere classified	-	(1.29)	-	-	-	-	-	(C_{ss})
linezolid	synthetic antibacterial agent	-	W > M	M = W	M ≥ W	M > W	-	-	
lorazepam	antiepileptic drugs	-	-	-	-	-	-	M = W	
maraviroc	antiviral agent	-	M = W	-	-	-	-	-	
mianserin hydrochloride	psychoneurotic agent	-	-	-	-	-	M = W	-	
midazolam	antiepileptic drugs	-	-	0.71	1.70	1.31	-	-	
minodronic acid hydrate	metabolic drugs not elsewhere classified	-	M = W	-	-	-	-	-	
mirabegron	other genitourinary and anal drugs	1.38	1.44	-	-	-	-	-	
mirtazapine	psychoneurotic agent	2.00	-	1.60	-	-	-	-	

AUC, area under the serum concentration-time; C_{max}: maximum serum concentration; C_{ss}, steady-state blood concentration; $T_{1/2}$, elimination half-life; CL, clearance; M, men; W, women; [a] For the medicinal efficacy classification of pharmaceutical ingredients, we used the "Therapeutic category number" used in Japan. [b] The number of digits after the decimal point conforms to the numerical value stated in the package insert. [c] For drugs with approximate pharmacokinetic descriptions for male and female in the package insert, detailed numerical information was calculated with reference to the "Interview Form," which is a comprehensive information form provided by the pharmaceutical company to supplement information that is inadequate in the prescription drug's package insert. [d] No gender differences were provided in adolescent data.

Table 3. List of drugs with information on gender differences in the "PHARMACOKINETICS" section of the package inserts for prescription drugs (n = 62) (continued)

Non-proprietary name of drug	Therapeutic Category[a]	Women/Men							
		AUC	C_{max} (C_{ss})	$T_{1/2}$	CL	Distribution volume	Protein binding rate	Overall pharmaco-kinetics	Remarks
nalfurafine hydrochloride	other central nervous system drugs	-	-	-	-	-	M = W	-	
naratriptan hydrochloride	vasoconstrictor	1.19 - 1.33	0.99 - 1.39	M = W	-	-	-	-	
nelarabine	antimetabolite	-	-	-	-	-	-	M = W	
nevirapine	antiviral agent	1.13	1.11	0.87	1.24	1.12	-	-	
olanzapine	psychoneurotic agent	-	-	-	M > W	-	-	-	
omarigliptin	diabetes agent	1.20	1.00	-	-	-	-	-	
oxaliplatin	other oncologic drugs	-	-	-	1.09	-	-	-	
oxycodone hydrochloride hydrate	opium alkaloids	1.40	1.40	-	-	-	-	-	
panitumumab	other oncologic drugs	-	-	-	-	M = W	-	-	
pralmorelin hydrochloride	functional test reagent	-	M = W	-	-	-	-	-	
propofol	general anesthetic	-	-	-	-	-	-	M = W	
ramosetron hydrochloride	other gastrointestinal drugs	1.72	1.48	-	-	-	-	-	
rasagiline mesilate	anti parkinsonian	-	-	-	-	-	0.98	-	Calculated from average
remifentanil hydrochloride	synthetic drug	-	-	-	-	0.60	-	M = W (Other than distribution volume)	
rosuvastatin calcium	hyperlipidemia agent	1.10	1.22	-	-	-	-	-	
sertraline hydrochloride	psychoneurotic agent	M = W	1.41	1.16	-	-	-	-	Elderly people
solifenacin succinate	other genitourinary and anal drugs	1.21	-	-	0.83	-	-	-	
sumatriptan succinate	vasoconstrictor	-	-	-	-	-	-	M = W	
telmisartan	antihypertensive agent	0.97, 1.69	1.18, 1.77	-	0.72 (40 mg)	-	-	-	40 mg, 80 mg
temozolomide	alkylating agent	-	-	-	0.95	-	-	-	
teriparatide	thyroid, parathyroid hormone	1.23	1.12	-	-	-	-	-	
thrombomodulin alfa	anticoagulant	-	-	-	-	-	-	M = W	
ticagrelor	other blood and body fluid drugs	1.52 (1.56)	1.37 (1.55)	-	-	-	-	-	(Main metabolite: AR-C124910XX)
tigecycline	antibiotic preparation	1.21	1.20	0.77	0.72	-	-	-	18-50 years old
tolterodine tartrate	other genitourinary and anal drugs	1.16 (1.10)	-	-	-	-	-	-	(Active metabolites: DD01)
topiroxostat	gout remedy	1.26	0.97	1.17	-	-	-	-	
zolmitriptan	vasoconstrictor	1.50	1.50	-	-	-	-	-	

AUC, area under the serum concentration-time; C_{max}: maximum serum concentration; C_{ss}, steady-state blood concentration; $T_{1/2}$, elimination half-life; CL, clearance; M, men; W, women; [a] For the medicinal efficacy classification of pharmaceutical ingredients, we used the "Therapeutic category number" used in Japan. [b] The number of digits after the decimal point conforms to the numerical value stated in the package insert. [c] For drugs with approximate pharmacokinetic descriptions for male and female in the package insert, detailed numerical information was calculated with reference to the "Interview Form," which is a comprehensive information form provided by the pharmaceutical company to supplement information that is inadequate in the prescription drug's package insert. [d] No gender differences were provided in adolescent data.

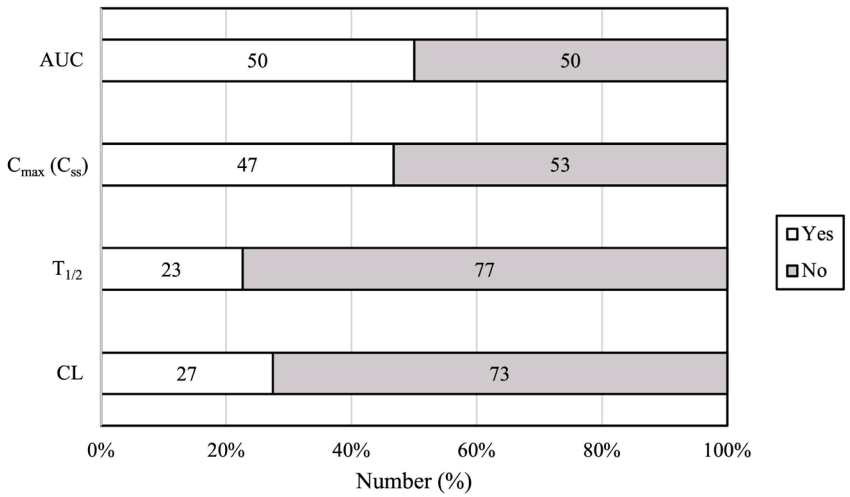

Figure 3. Number of prescription drug package inserts with information on gender differences for each pharmacokinetic parameter (*n* = 62). AUC, area under the serum concentration-time; C_{max}: maximum serum concentration; C_{ss}, steady-state blood concentration; $T_{1/2}$, elimination half-life; CL, clearance. The package inserts of 62 drugs mentioned gender differences in the "PHARMACOKINETICS" section. Of these, 31 drugs (50%) included information on gender differences in the AUC. Next were 29 drugs (47%) for C_{max} and 14 drugs (23%) for $T_{1/2}$ as well as 17 drugs (27%) that referred to CL. We counted the number of medicines for these four parameters. About half of the drugs provided AUC and C_{max} data.

The results of the present study indicated that for many drugs with information on gender differences, a higher incidence of adverse reactions was noted in women compared with men, which is consistent with the findings of many previous studies (*1,2*). This is thought to be due to one of the reasons being the existence of gender differences in the absorption, distribution, metabolism, and excretion (*3*).

The package inserts of 62 drugs mentioned gender differences in the "PHARMACOKINETICS" section. Among the pharmacokinetic data, the AUC was the most frequently reported numerical item. However, as shown in Figure 4, it is clear that this information is not sufficient and is far from being complete. Improving how these items are described is important in preventing adverse reactions caused by higher drug levels in the blood and slower drug elimination.

In the package inserts of prescription drugs, sections on gender differences information are not specified. Therefore, information on gender differences may be included in many different sections of the package inserts, making it difficult to quickly find this information. Among the drugs for which information on gender differences in pharmacokinetics was included in the package inserts, some had a "Gender" sub-item in the "Patients with Specific Backgrounds" sub-section of the "PHARMACOKINETICS" section. To further enhance and use information on gender differences, it would be useful to add a "Gender" sub-section, as well as "Elderly" and "Pediatric", under the "PRECAUTIONS CONCERNING PATIENTS WITH SPECIFIC BACKGROUNDS" section of the package insert.

The package inserts of relatively few drugs included information on gender differences. To implement pharmacotherapy considering gender differences, it is necessary to include sufficient information on gender differences in package inserts. Therefore, it will lead to further promotion of gender-specific medicine. Additionally, it might be possible to prevent adverse reactions that occur more frequently in women at the same level as in men by mandating the inclusion of information on gender in the package insert.

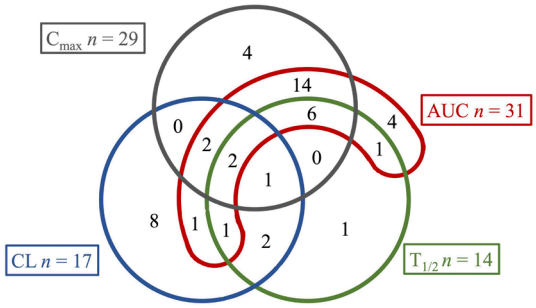

Figure 4. Venn diagram; number of duplications of information on gender differences for each pharmacokinetic parameter (*n* = 62). AUC, area under the serum concentration-time; C_{max}: maximum serum concentration; C_{ss}, steady-state blood concentration; $T_{1/2}$, elimination half-life; CL, clearance. The number of coverages of information for each of the four pharmacokinetic parameters by component was confirmed by a Venn diagram, and it was found that only two drugs included all four parameters, while 10 drugs (AUC, C_{max}, and $T_{1/2}$; 6 drugs, AUC, C_{max}, and CL; 2 drugs, C_{max}, $T_{1/2}$, and CL; 1drug, AUC, $T_{1/2}$, and CL; 1drug) included three parameters. The other 50 drugs included two or fewer pharmacokinetics parameters with information on gender differences.

Funding: This work was supported by the JST SPRING, Grant Number JPMJSP2123. The sponsor had no role in the study design, in the collection, analysis, or interpretation of data, in the writing of the report, or in the decision to submit the article for publication.

Conflict of Interest: The authors have no conflicts of interest to disclose.

References

1. Zopf Y, Rabe C, Neubert A, Gassmann KG, Rascher W, Hahn EG, Brune K, Dormann H. Women encounter ADRs more often than do men. Eur J Clin Pharmacol. 2008; 64:999-1004.
2. Yu Y, Chen J, Li D, Wang L, Wang W, Liu H. Systematic analysis of adverse event reports for sex differences in adverse drug events. Sci Rep. 2016; 6:24955.
3. Mauvais-Jarvis F, Berthold HK, Campesi I, Carrero JJ, Dakal S, Franconi F, Gouni-Berthold I, Heiman ML, Kautzky-Willer A, Klein SL, Murphy A, Regitz-Zagrosek V, Reue K, Rubin JB. Sex- and gender-based pharmacological response to drugs. Pharmacol Rev. 2021; 73:730-762.
4. U. S. Department of Health, Education and Welfare, Food and Drug Administration. General considerations for the clinical evaluation of drugs. *https://www.fda.gov/regulatory-information/search-fda-guidance-documents/general-considerations-clinical-evaluation-drugs*. (accessed October 5, 2023).
5. Public Health Service Task Force on Women's Health Issues. Women's health: Report of the Public Health Service Task Force on Women's Health Issues, volume I. Public Health Rep. 1985;100:73-106.
6. National Institutes of Health. Inclusion of women in study populations. NIH Guide for Grants and Contracts. Public Health Rep. 1986; 15:1.
7. National Institutes of Health. Inclusion of women in study populations. NIH Guide for Grants and Contracts. Public Health Rep.1986; 16:2.
8. Food and Drug Administration Drug Safety Communication. Risk of next-day impairment after use of insomnia drugs; FDA requires lower recommended doses for certain drugs containing zolpidem (Ambien, Ambien CR, Edular, and Zolpimist). *https://www.fda.gov/drugs/drug-safety-and-availability/questions-and-answers-risk-next-morning-impairment-after-use-insomnia-drugs-fda-requires-lower* (accessed October 5, 2023).
9. Food and Drug Administration Drug Safety Communication. FDA approves new label changes and dosing for zolpidem products and a recommendation to avoid driving the day after using Ambien CR. *https://www.fda.gov/drugs/drug-safety-and-availability/fda-drug-safety-communication-fda-approves-new-label-changes-and-dosing-zolpidem-products-and* (accessed October 5, 2023).
10. Director-Genera, Pharmaceutical Safety and Environmental Health Bureau, Ministry of Health, Labour and Welfare in Japan. Instructions for the Electronic Formatting of Package Inserts of Prescription Drugs. *https://www.pmda.go.jp/files/000241061.pdf* (accessed October 5, 2023). (in Japanese).
11. Takeda Pharmaceutical Company Limited. ACTOS Tablets 15/30, ACTOS OD Tablets 15/30 Interview Form. (accessed October 5, 2023). (in Japanese).
12. Lactic Acidosis International Study Group. Risk factors for lactic acidosis and severe hyperlactataemia in HIV-1-infected adults exposed to antiretroviral therapy. AIDS. 2007; 21:2455-2464.
13. Baylor MS, Johann-Liang R. Hepatotoxicity associated with nevirapine use. J Acquir Immune Defic Syndr. 2004; 35:538-539.
14. U. S. Department of Health and Human Services, Panel on Antiretroviral Guidelines for Adults and Adolescents. (2021). Guidelines for the Use of Antiretroviral Agents in Adults and Adolescents with HIV. *https://clinicalinfo.hiv.gov/sites/default/files/guidelines/documents/adult-adolescent-arv/guidelines-adult-adolescent-arv.pdf*. (accessed October 5, 2023).

Received November 29, 2023; Revised December 6, 2023; Accepted December 10, 2023.

**Address correspondence to:*
Shingo Kondo, Division of Social Pharmacy, Center for Social Pharmacy and Pharmaceutical Care Sciences, Faculty of Pharmacy, Keio University, 1-5-30 Shibakoen, Minato-ku, Tokyo 105-8512, Japan.
E-mail: kondo-sn@keio.jp

Released online in J-STAGE as advance publication December 15, 2023.

Original Article

DOI: 10.5582/ddt.2023.01080

Single intratracheal administration toxicity study on safety of vapor inhalation of electrolyzed reduced water in rats

Yuko Wada Imanaka[1,*], Yoshinao Okajima[1,2], Yutaka Oshima[3], Ken-ichi Shimokawa[1], Masahiro Okajima[1,2], Fumiyoshi Ishii[1]

[1] Department of Pharmaceutical Sciences, Meiji Pharmaceutical University, Tokyo, Japan;
[2] A. I. System products, Corp., Aichi, Japan;
[3] Chemicals Evaluation and Research Institute, Oita, Japan.

SUMMARY The effects of acute intratracheal administration of electrolyzed reduced water (ERW; alkaline electrolyzed water) were investigated in rats. In this study, no deaths or near-deaths were recorded in either group, namely those treated with ERW or purified water (maximum doses of 900 mg/kg). The main symptoms observed in the rats were decreased spontaneous movements and abnormal breath sounds, which were considered to be transient symptoms caused by intratracheal administration. In addition, low values of alkaline phosphatase, total protein and lactate dehydrogenase were found in BALF tests, but these values were considered to be of low toxicological significance, since they are usually high in the presence of lung inflammation or cellular damage. This suggests that the alkalinity of ERW partially contributes to broken peptide bonds in proteins. There were no significant increases in bronchoalveolar lavage fluid protein in either group. ERW did not cause an increase in the influx of neutrophils, eosinophils, basophils, or lymphocytes, suggesting that intratracheal administration of ERW did not cause lung inflammation. ERW did not cause abnormalities in the body or pathological changes in the lungs. Aggregates of alveolar macrophages, as a measure of inflammation, were observed in both groups. These may be transient symptoms due to intratracheal administration, not due to ERW toxicity. This study confirmed the safety of intratracheal ERW infusion and demonstrated the low risk of acute toxicity for inhalation exposure to ERW aerosol or vapor. Therefore, ERW may be an effective air purifier against viruses or bacteria.

Keywords alkaline electrolyzed water, acute toxicity, intratracheal instillation

1. Introduction

Electrolyzed reduced water (ERW) is a functional water that has a high pH, negative oxidative redox potential, and a high concentration of dissolved hydrogen and is produced near the cathode during the electrolysis of water. It possesses reactive oxygen species-free radical scavenging activity, conferred by the dissolved H_2 (*1*).

Several studies have shown that ERW has antibacterial activity against some bacteria (*2,3*) and antiviral effects against some types of viruses (*4*). It was recently reported that ERW has antiviral activity against severe acute respiratory syndrome coronavirus 2 (SARS-CoV-2), which is the etiological agent responsible for coronavirus infectious disease, emerged in 2019 (COVID-19) (*5,6*). Potent antibacterial and antiviral activities are the motivation for further development of ERW as a monotherapy or in combination with other effective agents against infection.

There is a growing consensus that improved disinfection of environmental surfaces is needed for effective infection prevention, and traditional manual disinfection techniques are often suboptimal because of various personnel issues (*7*). Therefore, automated decontamination technologies, including aerosol (*8*) and vaporized disinfectant (*9*), are gaining more attention for the reduction of bacterial surface contamination. Similarly, ERW aerosols or vapors may be increasingly applied for air purification and to prevent the spread of viral infections, including SARS-CoV-2. Although the safety of ERW for drinking has been confirmed (*10,11*), the safety of inhaling ERW as an aerosol or vapor has not been reported. In this study, we examined the toxicity of a single intratracheal dose of ERW in rats.

2. Materials and Methods

2.1. Reagents

The ERW (product name, S-100® Medical grade) was supplied by A.I. System Products Corp. (Japan). Purified water was purchased from Takasugi Pharmaceutical (Japan).

2.2 Animals

Sprague Dawley rats were obtained from Charles River Japan (Production Plant: Hino Breeding Center, Japan). In this study, twelve 7-week-old male rats weighing 256.8-269.4 g and free of viral pathogens and parasites were used. The rats were housed in ventilated stainless cages, one per cage, with 12-hr light-dark cycles. They were provided air ventilated 10-15 times/hour, irradiated solid feed MF (Oriental Yeast Co., Ltd, lot number 200819), and tap water with sodium hypochlorite (Purax, OYALOX Co. Ltd., Japan).

All animal procedures were carried out in accordance with the "Animal Experiment at Chemicals Evaluation Research Institute (CERI) Hita" prepared by this testing facility with reference to "Act on Welfare and Management and of Animals" (Act No. 105,), 1973 "Standards relating to the Care and Keeping and Reducing Pain of Laboratory Animals" (Ministry of the Environment, 2006), "Fundamental Guidelines for Proper Conduct of Animal Experiment and Related Activities in Research Institutions under the jurisdiction of the Ministry of Health, Labour and Welfare" (Ministry of Health, Labor and Welfare, 2006), "Fundamental Guidelines for Proper Conduct of Animal Experiment and Related Activities in Academic Research Institutions under the jurisdiction of the Ministry of Agriculture, Forestry, and Fisheries" (Ministry of Agriculture, Forestry and Fisheries, 2006), "Fundamental Guidelines for Proper Conduct of Animal Experiment and Related Activities in Academic Research Institutions" (Ministry of Education, Culture, Sports, Science and Technology, 2006), and "Guidelines for Proper Conduct of Animal Experiments" (Japan Academic Conference, 2006).

2.3. Time-course study design

On day 0, rats were anesthetized with isoflurane and intratracheally instilled with 0.9 mL/kg of ERW or vehicle (purified water) using a 1 mL syringe (Terumo® Syringe, Terumo, Japan) fitted with MicroSprayer® (IA-1B R, PennCentury™, USA) (Table 1). All animals were observed continuously for 10 min immediately after dosing, then again at 30 min after dosing, and then hourly for 1 to 6 h after dosing. For the first 14 days after dosing, the animals were observed once a day in the morning. Body weight was measured before dosing on day 0 and then on days 1, 3, 7, and 14 using an electronic top-loading balance (Sartorius LP2200S QUINTIX5101-1S, Sartorius AG, Germany).

All animals were humanely euthanized on day 14 under anesthesia with isoflurane followed by exsanguination. The left lung was clamped while bronchoalveolar lavage was performed on the right lung lobes, and bronchoalveolar lavage fluid (BALF) was retained for analysis. The first fraction of the bronchoalveolar lavage was obtained by inflating the right lung with 4 mL of phosphate-buffered saline (PBS), withdrawing, and repeating the process a second time with the same 4 mL of PBS. Histopathological assessment of lung inflammation and injury were performed.

2.4. Analysis of the BALF cells

The bronchoalveolar lavage cells were counted using an XT-2000i (Sysmex, Japan) multi-item automated blood cell analyzer. The BALF was centrifuged at 1,500 rpm for 10 min. The cell pellet was washed and resuspended in 1 mL of PBS on a slide glass, and then 25 or 50 μL of the resuspended cell solution was centrifuged at 1,000 rpm for 2 min. Leukocyte counts (macrophages, neutrophils, eosinophils, basophils, and lymphocytes) were examined on smears stained using the May-Grünwald-Giemsa method. From each sample, 200 cells were counted.

The supernatant obtained after centrifugation was used to examine the alkaline phosphatase (ALP), total protein, albumin, and lactate dehydrogenase (LDH) using a Hitachi Automatic Analyzer 3500 (Hitachi High-Tech, Japan). ALP activity was determined using the p-nitrophenyl phosphate method standardized by the Japan Society of Clinical Chemistry. LDH activity was quantified using the UV method standardized by the Japan Society of Clinical Chemistry. The concentration of the total protein was measured using the pyrogallol Red method, and albumin was quantified by immunonephelometry.

2.5. Pathological examination

Table 1. The composition of animal groups

group	Administration dose (mg/kg)	ERW solution concentration (w/v%)	Administration volume (mL/kg)	Number of Animals
Control group	0	0	0.9	6
Test substance group	900	100	0.9	6

After the euthanasia of rats, gross observations were made on the body surface, openings, subcutaneous, thoracic, abdominal, and pelvic cavities and their contents. The trachea, lungs, and posterior mediastinal lymph nodes were then removed from the rats. The left lung was weighed and fixed by infusion of 10% neutralized buffered formalin. Multiple thin transverse slices were made through the left lung. These slices were embedded in paraffin and stained with hematoxylin and eosin (H&E). Selected lung sections were observed using a light microscope, and their general morphologies were noted.

2.6. Statistical analyses

The data were analyzed using Microsoft EXCEL 2016. The results were expressed as the mean ± standard deviation. Groups were compared using an unpaired two-tailed Student's *t*-test or Welch's *t*-test according to the results of the *F*-test, and a *p*-value of < 0.01 or 0.05 was considered significant, respectively.

3. Results

3.1. General clinical observations

In this study, there were no deaths or near-deaths in either group. The main symptoms were decreased spontaneous movements at a rate of 100% (6/6) and 100% (6/6) and abnormal breath sounds at a rate of 50.0% (3/6) and 33.3% (2/6) in rats treated with ERW and purified water, respectively (Table 2). The abnormal breath sounds disappeared within 1 h after dosing, and the decreased spontaneous movements disappeared 1 day after dosing. From 1 to 14 days after dosing, no abnormalities were observed in either group.

Abnormal respiratory sounds and decreased spontaneous locomotion were recorded not only in the group exposed to ERW but also in the negative control group and disappeared within 1 day. Therefore, these symptoms were considered to be transient responses caused by intratracheal administration, not due to ERW toxicity.

3.2. Body weight

The average body weight in the groups treated with ERW and purified water increased by 14.2% (from 259.3 ± 3.0 to 367.7 ± 22.5) and 14.0% (from 264.2 ± 4.6 to 368.9 ± 26.1) 14 days after administration, respectively (Figure 1).

3.3. BALF cells differentials

Cell differentials were performed on BALF cells to further assess inflammation (Table 3). ERW did not cause an increase in the influx of neutrophils, eosinophils, basophils, or lymphocytes. This is consistent with the observation of BALF proteins, further indicating that intratracheal administration of ERW did not cause lung inflammation.

3.4. BALF chemical examinations

Protein mediators were assessed in BALF to evaluate the inflammation and immune response (Figure 2). There were no significant increases in BALF protein in groups exposed to 900 mg/kg of ERW, compared with the control. These observations suggest that intratracheal injection of ERW did not cause inflammation in the lungs. However, administration of ERW did cause a significant decrease in total proteins, ALP, and LDH compared with the control. This suggests that the alkalinity of ERW was partially responsible for breaking peptide bonds in proteins.

3.5. Pathological examination

Lung (left) weight was measured after the euthanasia of rats (Table 4). The average lung weights in the groups treated with ERW and purified water were 0.523 ± 0.023 and 0.530 ± 0.045, respectively. There was no significant difference in lung weights between the two groups.

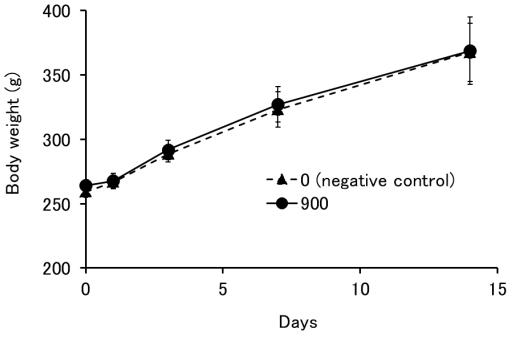

Figure 1. Single intratracheal administration toxicity study in rats. Summary of body weights. Values are shown as the mean ± S.D. *Significantly different from vehicle control at $p < 0.05$.

Table 2. Single intratracheal administration toxicity study in rats. Summary of general clinical observations

Signs	Number of cases		
	Dose (mg/kg)	0 (negative control) ($n = 6$)	900 ($n = 6$)
Deaths and near-deaths		0	0
Abnormal respiratory sound		2	3
Decreased spontaneous locomotion		6	6

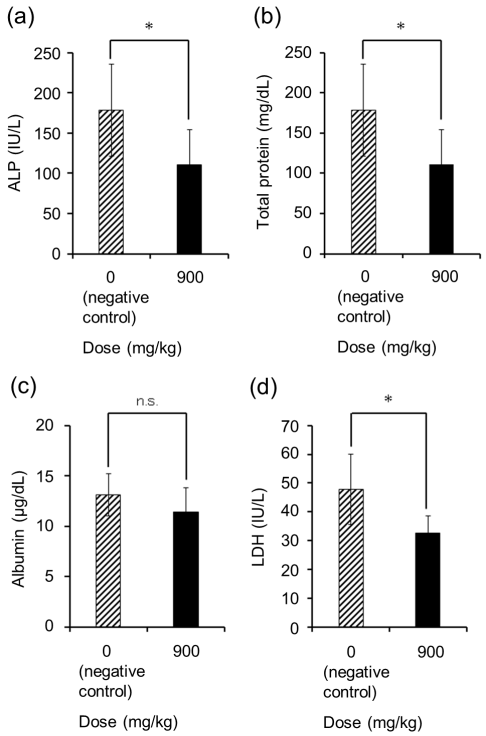

Figure 2. Single intratracheal administration toxicity study in rats. Summary of BALF chemical examinations. a): ALP (IU/L), b): Total protein (mg/dL), c): Albumin (μg/dL), d): LDH (IU/L). Values are shown as the mean ± S.D. *Significantly different from vehicle control at $p < 0.05$.

3.6. Gross observations and H&E-stained lung tissue sections

Gross observations and H&E-stained lung tissue sections were evaluated (Table 5). ERW at 900 (mg/kg) dose did not cause abnormalities on the body surface, openings, subcutaneous, thoracic, abdominal, and pelvic cavities, and pathological changes in the lung. Aggregates of alveolar macrophages, as a measure of inflammation, were observed in ERW and purified water-exposed groups. Very slight aggregates of macrophages were observed at a rate of 16.7% (1/6) and 50% (3/6) respectively, and slight aggregates were observed at a rate of 33.3% (2/6) and 16.7% (1/6) respectively in ERW-exposed and control groups. These aggregates of macrophages were inferred to be transient symptoms due to intratracheal administration, not due to ERW toxicity.

4. Discussion

In this study, the upper limit of the dose for intratracheal administration was set at 900 mg/kg, based on the draft guidelines on risk assessment methods for the indoor use of insecticides as OTC drugs and quasi-drugs issued by the Ministry of Health, Labour and Welfare in Japan (*12*). Furthermore, the reasonable dose for the upper limit of the

Table 3. Single intratracheal administration toxicity study in rats. Summary of BALF cell examinations

		BALF cell examinations		
		Dose (mg/kg)	0 [a] (negative control) ($n = 6$)	900 ($n = 6$)
Total cells	($\times 10^2$/μL)		1.27 ± 0.55	1.23 ± 0.45
Differentiation of leukocyte	Macrophages (%)		99.58 ± 0.80	99.08 ± 2.01
	Neutrophils (%)		0.08 ± 0.20	0.00 ± 0.00
	Eosinophils (%)		0.00 ± 0.00	0.08 ± 0.20
	Basophils (%)		0.00 ± 0.00	0.00 ± 0.00
	Lymphocytes (%)		0.33 ± 0.61	0.83 ± 1.81

Values are shown as the mean ± S.D. [a]In the control group, 0.9 mL/kg of purified water was administered.

Table 4. Single intratracheal administration toxicity study in rats. Summary of organ weights

	weights		
	Dose (mg/kg)	0[a] (negative control) ($n = 6$)	900 ($n = 6$)
Lung (left) (g)		0.523 ± 0.023	0.530 ± 0.045
(g/100g)		(0.140 ± 0.011)	(0.143 ± 0.012)
Final body weight (g)		367.7 ± 23.0	368.9 ± 26.1

Values are shown as the mean ± S.D. [a]In the control group, 0.9 mL/kg of purified water was administered.

Table 5. Single intratracheal administration toxicity study in rats. Macroscopic examination and histopathological examinations

			Number of cases	
		Dose (mg/kg)	0 [a] (control) ($n = 6$)	900 ($n = 6$)
Gross observations	Abnormalities		0	0
H&E-stained lung tissue sections	abnormalities		0	0
	aggregates of alveolar	very slight	3	1
	macrophages	slight	1	2

Values are shown as the mean ± S.D. [a]In the control group, 0.9 mL/kg of purified water was administered.

dose for intratracheal administration was determined as follows. The respiratory volume in rats has been reported to be 0.27 m^3/day in male Sprague Dawley rats weighing 267 g (*13*). The respiratory volume is estimated to be 0.01125 m^3/hr. Based on the limiting concentration in the acute inhalation toxicity test of 5 mg/L (5,000 mg/m^3) and the respiratory volume of the rats, and assuming that all the inhaled substance reaches the lungs, the amount is estimated to be equivalent to 5,000 mg/m^3 × 0.01125 m^3/h = 56.25 mg/h. In addition, if the exposure time of the acute inhalation toxicity test is 4 h, the maximum amount of exposure to the lungs of rats is estimated to be 56.25 mg/h × 4 h = 225 mg. In other words, if the body weight of a rat is 267 g, assuming that all particles in the air reach the lungs by respiration, the maximum dose is calculated to be approximately 843 mg/kg. Therefore, the maximum dose of 900 mg/kg is considered to be a reasonable dose above the limiting concentration of 5 mg/L in the acute inhalation toxicity study.

The ERW (product name, S-100® Medical grade) used in this study is manufactured by the high-voltage electrolysis of water containing natural salt. It contains mineral ions, namely Na^+, K^+, Ca^{2+}, Mg^{2+}, and Cl^- (*14*). It has a high pH (12.1), low surface tension (62.3 dyne/cm), and BAP (4,905 μmol/L) (*5*).

No deaths or near-deaths occurred in the animals during the dose-finding study or in the first step when ERW was administered at 900 mg/kg. Furthermore, according to the Globally Harmonized System of Classification and Labelling of Chemicals, the LC50 cut-off value for acute toxicity of ERW in rats under the conditions of this study, when converted from intratracheal administration to inhalation exposure, corresponds to ∞, and is considered to be "Not applicable to classification". This also suggests that there are no toxic effects for the intratracheal administration of ERW. Therefore, considering the potent anti-virus and anti-microbial activities, further development of ERW as an effective air purifier by spraying against virus or microbial infection is warranted.

Funding: A portion of this study was supported by Iwatani Corporation Japan.

Conflict of Interest: The electrolyzed reduced water (ERW, product name S-100® Medical grade) used in this study was manufactured by A. I. System products, Corp. Yoshinao Okajima and Masahiro Okajima are employees of A. I. System products, Corp.

References

1. Hamasaki T, Harada G, Nakamichi N, Kabayama S, Teruya K, Fugetsu B, Gong W, Sakata I, Shirahata S. Electrochemically reduced water exerts superior reactive oxygen species scavenging activity in HT1080 cells than the equivalent level of hydrogen-dissolved water. PLoS One. 2017; 12:e0171192.
2. Kim J, Lee HJ, Hong SH. Inhibition of streptococcal biofilm by hydrogen water. J Dent. 2017; 58:34-39.
3. Feliciano L, Lee J, Pascall MA. Transmission electron microscopic analysis showing structural changes to bacterial cells treated with electrolyzed water and an acidic sanitizer. J Food Sci. 2012; 77:M182-187.
4. Bui VN, Nguyen KV, Pham NT, Bui AN, Dao TD, Nguyen TT, Nguyen HT, Trinh DQ, Inui K, Uchiumi H, Ogawa H, Imai K. Potential of electrolyzed water for disinfection of foot-and-mouth disease virus. J Vet Med Sci, 2017; 79:726-729.
5. Okajima Y, Okajima M, Ikeda M, Wada Y, Shimokawa K, Ishii F. Antiviral effect of electrolyzed reduced water on SARS-CoV-2. Drug Discov Ther. 2021; 15:268-272.
6. Wurtz N, Hasni I, Bancod A, La Scola B. Confirmatory virucidal activity of ionised active water S-100® on the SARS-CoV-2 virus. Adv Virol. 2022; 2022:5995775.
7. Boyce JM. Modern technologies for improving cleaning and disinfection of environmental surfaces in hospitals. Antimicrob Resist Infect Control. 2016; 5:10.
8. Mitchell BG, Digney W, Locket P, Dancer SJ. Controlling methicillin-resistant *Staphylococcus aureus* (MRSA) in a hospital and the role of hydrogen peroxide decontamination: an interrupted time series analysis. BMJ Open. 2014; 4:e004522.
9. Rogers JV, Sabourin CLK, Choi YW, Richter WR, Rudnicki DC, Riggs KB, Rudnicki DC, Riggs KB, Taylor ML, Chang J. Decontamination assessment of *Bacillus anthracis*, *Bacillus subtilis*, and *Geobacillus stearothermophilus* spores on indoor surfaces using a hydrogen peroxide gas generator. J Appl Microbiol. 2005; 99:739-748.
10. Watanabe T, Pan I, Fukuda Y, Murasugi E, Kamata H, Uwatoko K. Influences of alkaline ionized water on milk yield, body weight of offspring, and perinatal dam in rats. J Toxicol Sci. 1998; 23:365-371.
11. Watanabe T. Effect of alkaline ionized water on reproduction in gestational and lactational rats. J Toxicol Sci. 1995; 20:135-142.
12. Risk assessment methods for the indoor use of insecticides as OTC drugs and quasi-drugs issued by the Ministry of Health, Labour and Welfare in Japan. https://www.env.go.jp/water/dojo/noyaku/hisan_risk/hyoka_tih/com06/ref04.pdf (Accessed 2023/10/5).
13. U.S. EPA. Recommendations for and Documentation of Biological Values for use in Risk Assessment. EPA. 1988. *https://cfpub.epa.gov/ncea/risk/recordisplay.cfm?deid=34855* (Accessed 2023/10/5).
14. Okajima M, Shimokawa K, Ishii F. Physicochemical properties of magnesium alminum silicate (smectone®) gels prepared useing electrolytic-reduction ion water (2): Effects of various salts on the phase diagram. Colloids Surf B Biointerfaces. 2009; 72:284-288.

Received October 7, 2023; Revised December 5, 2023; Accepted December 15, 2023.

**Address correspondence to:*
Yuko Wada Imanaka, Department of Pharmaceutical Sciences, Meiji Pharmaceutical University, 2-522-1 Noshio, Kiyose, Tokyo 204-8588, Japan.
E-mail: fishii@my-pharm.ac.jp

Released online in J-STAGE as advance publication December 22, 2023.

Original Article

DOI: 10.5582/ddt.2023.01076

Generic selection criteria for safety and patient benefit [XII]: Comparing the physicochemical and pharmaceutical properties of brand-name and generic tulobuterol tape

Ken-ichi Shimokawa[1,*], Kayo Yotsukura[1], Mitsuru Nozawa[2], Yuko Wada[3], Fumiyoshi Ishii[3]

[1] Department of Pharmaceutical Sciences, Meiji Pharmaceutical University, Tokyo, Japan;
[2] Triad Japan Co. Ltd., Kanagawa, Japan;
[3] Department of Self-medication and Health Care Sciences, Meiji Pharmaceutical University, Tokyo, Japan.

SUMMARY Physicochemical properties (drug release, peel strength, adhesion, and stiffness) of Hokunalin® Tape (Hokunalin) and 13 generic transdermal bronchodilator patches containing tulobuterol were characterized and evaluated for comparison. Drug-release studies evaluating sustained release behavior demonstrated better performance by the drug Hokunalin, than the generics MED, YP, Sawai, and Teikoku. Hokunalin yield a 16.2% release 1 hour after initiation, 30.1% at 3 hours, 50.0% at 8 hours. In comparison, the generics MED, YP, Sawai, and Teikoku showed an intermediate release behavior to that of Hokunalin, with more than 80% release after 8 hours. A 90-degree peel adhesion test for tape peel strength demonstrated that the generic MED (4.99 N), YP (3.26 N), Sawai (4.17 N), and Teikoku (4.37 N) tapes yielded significantly higher values compared to Hokunalin (2.66 N). Probe tack tests, evaluating adhesive strength, yielded significantly higher values for the generics HMT (4.89 N) and Towa (4.25 N) compared to Hokunalin (3.66 N). Furthermore, for the stiffness-softness test, a significantly higher value was obtained for each generic yielded compared to Hokunalin (3.7-degree). These factors are important components of product qualities that affect treatment efficacy, including "ease of application" and other usability factors.

Keywords Transdermal therapeutic drug, brand-name drug, generic drug, tulobuterol tape

1. Introduction

Tulobuterol Tape is a β_2 stimulant used to relieve dyspnea-like symptoms due to airway obstructive disorders, such as bronchial asthma. It is designed as an extended-release formulation with an expected sustained effect. As only once-daily application is required, it has a high level of compliance and is used by many patients, especially the elderly, with many generic versions available. However, prescription substitution from generic drugs to brand-name drugs can lead to poorer compliance and health outcomes due to differences in feel or insufficient efficacy (*1*). Common performance variations reported between brand-name and generic drugs include differences in peeling and adhesive strength (*2-5*) due to tape formulation additives. For tulobuterol tape formulations, the effect of these formulation variants are not yet systematically evaluated among brand-name and generic drugs. Furthermore, Hokunalin® Tape has a sustained drug release mechanism, formulated using the Crystal Reservoir System (*6,7*). As the generic drugs cannot employ this patented formulation design, variations in drug release properties are a strong possibility, potentially impacting on therapeutic outcomes. Furthermore, in patients with increased skin permeability due to factors including atopic dermatitis, long-term steroid administration, and aging, drug release rates may be affected, altering transfer across the tape-skin-blood interface (*8-11*). Due to these variations in drug-transfer properties resulting from different patient skin conditions, side effects may occur, such as tremors and palpitations, associated with rapidly rising blood drug levels immediately after administration, and then, due to early drug depletion, a shortened tape drug-delivery lifetime may insufficiently suppress asthma attacks.

Therefore, this study compares the brand-name and available generic drugs in terms of both physicochemical properties and drug-release properties, providing information to best identify treatments options for patient-focused care.

2. Materials and Methods

2.1. Materials

This study evaluated the brand name Hokunalin® Tape 2 mg (Mylan EPD G.K., Tokyo, Japan), a tulobuterol-containing tape formulation (2 mg of tulobuterol in one (3.2 cm × 3.2 cm) sheet), and 13 generic 2 mg tulobuterol tapes, including "EMEC" (Nipro Pharma Corp., Osaka, Japan), "HMT" (Hisamitsu Pharmaceutical Co., Ltd., Tokyo, Japan), "MED" (Medisa Shinyaku Inc., Tokyo, Japan), "NP" (Nipro Corp., Osaka, Japan), "QQ" (Kyukyu Pharmaceutical Co., Ltd., Tokyo, Japan), "YP" (Yutoku Pharmaceutical Industries, Ltd., Saga, Japan), "Ohara" (Ohara Pharmaceutical Industries, Ltd., Shiga, Japan), "Sawai" (Sawai Pharmaceutical Co., Ltd., Osaka, Japan), "Takata" (Takata Pharmaceutical Co., Ltd., Saitama, Japan), "Teikoku" (Teikoku Seiyaku Co., Ltd., Kagawa, Japan), "Towa" (Towa Pharmaceutical Co., Ltd., Osaka, Japan), "Nichi-Iko" (Nichi-Iko Pharmaceutical Co., Ltd., Toyama, Japan), and "Pfizer" (Pfizer Japan Inc., Tokyo, Japan). The 14 tape products used in this study are listed in Table 1.

2.2. Measurement of drug release

The paddle over disk method of release testing for preparations applied to the skin, listed in the 18th edition of the Japanese Pharmacopoeia, was used (*12*). The formulation was placed with double-sided tape on a D2414 disc (Toyama Sangyo Co., Ltd., Osaka, Japan) made of stainless steel (SUS316) mesh with a 125 μm aperture, with the adhesive side up, 32 mm × 32 mm, and eluted in a dissolution tester (Varian VK 7010, Tokyo, Japan) filled with 500 mL of water at a temperature of 32°C. The eluent temperature was 32°C. The formulation was then taped to the disc using a double-sided adhesive tape; Agilent Technologies International Japan Ltd. Solutions were collected at 1, 3, 8, and 24 hours after the start of elution and quantified by HPLC using a YMC-Pack ODS-A analytical column (125 mm × 4.0 mm I.D., YMC Corp., Kyoto, Japan), a PU-4180 pump (Japan Spectroscopic Company, Tokyo, Japan) and absorbance measured at 215 nm using a UV-4075 UV-visible detector (Japan Spectroscopic Company). The mobile phase used was acetonitrile and 20 mM potassium dihydrogen phosphate in a 1:3 ratio. The mobile phase flow rate was 1.0 mL/min, column temperature set 30°C using a column oven CO-4061 (Japan Spectroscopic Company), and sample solutions of 10 μL were injected. ChromNAV (LC-Met II/ADC, Japan Spectroscopic Company) was used for data processing.

2.3. Measurement of peeling force

The 90-degree peel adhesion test was performed according to the 90-degree peel adhesion test method listed in the 18th edition of the Japanese Pharmacopoeia (*13*). That is, a formulation was cut to 28 mm × 32 mm was applied to a stainless-test plate P90-200N (Imada Co., Ltd., Aichi, Japan), and a 2 kg roller passed back and forth at a speed of 5 mm/sec. The 4 mm long side was clipped and peeled off at a speed of 2 mm/sec angle 90-degree using a digital force gauge MX-2-500N (Imada Co., Ltd.) fixed on a vertical motorized test stand M-2-500N (Imada Co., Ltd.). After the start of the measurement, the measured values of 50% of the length pulled off the test plate were averaged to obtain the value (N/cm) for the 90-degree peel adhesion test.

2.4. Measurement of adhesive strength

Probe tack testing was performed according to the Probe tack test method listed in the 18th edition of the Japanese Pharmacopoeia (*14*). That is, a digital force gauge ZTS-20N (Imada Co., Ltd.) was used with the formulation cut to 15 mm × 15 mm and attached to a weight ring MED-IS-20N (Imada Co., Ltd.) and fixed to a vertical motorized test stand MX-2-500N (Imada Co., Ltd.). The maximum force required to move the weight ring at a speed of 5 mm/sec and to pull off the probe and sample after bonding them at 1 N/cm^2 for 1 second was

Table 1. Tape products used in this study

Product name	Abbreviated name	Class	Company name	Lot number
Hokunalin® tape 2 mg	Hokunalin	brand-name	Mylan EPD G.K.	86718YQ1, 9711YQ1
Tulobuterol tape 2 "EMEC"	EMEC	generic	Nipro Pharma Corp.	AS02C
Tulobuterol tape 2 mg "HMT"	HMT	generic	Hisamitsu Pharmaceutical Co., Inc.	U503T, U710T
Tulobuterol tape 2 mg "MED"	MED	generic	Medisa Shinyaku Inc.	17901
Tulobuterol tape 2 mg "NP"	NP	generic	Nipro Corp.	17R321
Tulobuterol tape 2 mg "QQ"	QQ	generic	Kyukyu Pharmaceutical Co., Ltd.	7T11T
Tulobuterol tape 2 mg "YP"	YP	generic	Yutoku Pharmaceutical Ind. Co., Ltd.	8C010
Tulobuterol tape 2 "Ohara"	Ohara	generic	Ohara Pharmaceutical Industries, Ltd.	7Y14
Tulobuterol tape 2 mg "Sawai"	Sawai	generic	Sawai Pharmaceutical Co., Ltd.	18206
Tulobuterol tape 2 mg "Takata"	Takata	generic	Takata Pharmaceutical Co., Ltd.	TZ01
Tulobuterol tape 2 mg "Teikoku"	Teikoku	generic	Teikoku Seiyaku Co., Ltd.	18302
Tulobuterol Tape 2 mg "Towa"	Towa	generic	Towa Pharmaceutical Co., Ltd.	A0048
Tulobuterol tape 2 mg "Nichi-Iko"	Nichi-Iko	generic	Nichi-Iko Pharmaceutical Co., Ltd.	7T13N
Tulobuterol tape 2 mg "Pfizer"	Pfizer	generic	Pfizer Japan Inc.	180217

measured.

2.5. Measurement of stiffness

The angle of flexure was measured visually at 2.5-degree intervals when one half of a 32 mm × 32 mm formulation was affixed to a test stand and a 100 mg weight was attached to the other end (*15*).

2.6. Statistical analysis

Statistical significance was evaluated using *Dunnett's* multiple comparison test method, with a risk rate of 5% or less considered significant (*16*). In graphs, products significantly different from the original drug (Hokunalin® tape) at a risk rate of 1% or less are marked with asterisks (**).

3. Results

3.1. Measurement of drug release

Drug release results are shown in Figure 1 and Table 2. Hokunalin yield a 16.2% release 1 hour after initiation, 30.1% at 3 hours, 50.0% at 8 hours, 65.1% at 12 hours, and 93.5% at 24 hours. In comparison, the generics EMEC, NP, QQ, Ohara, Takata, and Nichi-Iko released over 90% after 1 hour, while HMT, Towa, and Pfizer reached almost 90% release after 3 hours. MED, YP, Sawai, and Teikoku showed an intermediate release behavior to that of Hokunalin, with more than 80% release after 8 hours.

3.2. Measurement of peeling force

The peel force measurements immediately after crimping are shown in Figure 2 and Table 2. Significantly higher values were obtained for generics MED (4.89 N), YP (3.26 N), Sawai (4.17 N) and Teikoku (4.37 N) compared to Hokunalin (2.66 N). However, the other generics (EMEC, HMT, NP, QQ, Ohara, Takata, Towa, Nichi-Iko, and Pfizer) showed significantly lower values.

Figure 3 and Table 2 shows the peel-off force measurements immediately after application (applying), peeling off, and then reapplying. The comparison of affixation, removal, and reapplication showed a

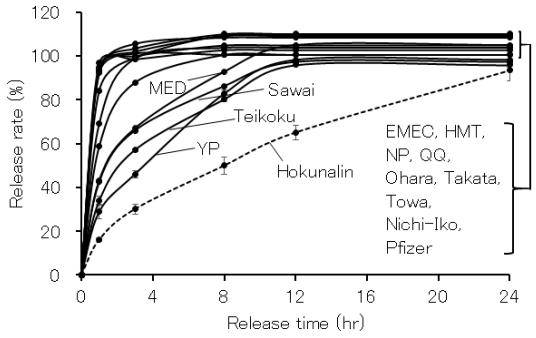

Figure 1. Comparison of drug release curves (*n* = 6). Dotted line: brand-name drug, solid line: generic drugs.

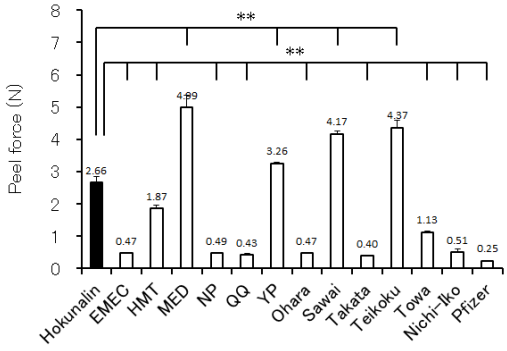

Figure 2. Comparison of peel force by the 90-degree test. (*n* = 6, *vs.* Hokunaline, $**p < 0.01$, *Dunnett's*-test), Black bar: brand-name drug, white bar: generic drugs.

Table 2. Summary of test measurements

Products	Release rate (%) (after 3 h/ 8 h/ 12 h)	Peel force (N)	Peel - re-peel force (N)	Adhesive force (N)	Bending resistance (degree)
Hokunalin	**30.1 / 50.0 / 65.1**	2.66	-0.35	3.66	**3.67**
EMEC	105.7 / - / -	0.47	0.05	1.93	44.17
HMT	87.9 / - / -	1.87	-0.10	**4.89**	59.58
MED	66.9 / 92.8 / -	**4.99**	**-0.79**	3.74	34.58
NP	103.5 / - / -	0.49	0.04	2.11	58.33
QQ	99.9 / - / -	0.43	0.00	1.98	25.42
YP	45.9 / 82.7 / 98.2	3.26	**0.78**	3.79	9.58
Ohara	101.3 / - / -	0.47	0.01	0.83	22.50
Sawai	65.9 / 86.1 / 97.2	**4.17**	**-0.55**	3.41	32.92
Takata	101.7 / - / -	0.40	0.07	1.95	56.25
Teikoku	57.1 / 80.3 / 95.9	**4.37**	**-0.58**	3.31	38.33
Towa	98.9 / - / -	1.13	0.05	**4.25**	**5.83**
Nichi-Iko	98.5 / - / -	0.51	0.01	1.87	22.92
Pfizer	99.1 / - /	0.25	0.02	1.59	26.25

-: Indicates a release rate (%) of 100% or more. Peel- re-peel force: Amount of change in peel and re-peel force.

significant increase in force required for YP, whereas significantly lower forces for Hokunalin and the generics MED, Sawai, and Teikoku. The remaining generics yielded smaller changes in the required peel-off force.

3.3. Measurement of adhesive strength

Adhesion measurements for the probe tack test are shown in Figure 4 and Table 2. The generic drugs HMT (4.89 N) and Towa (4.25 N) yielded significantly higher adhesive strength than Hokunalin (3.66 N). On the other hand, EMEC (1.93 N), NP (2.11 N), QQ (1.98 N), Ohara (0.83 N), Takata (1.95 N), Nichi-Iko (1.87 N), and Pfizer (1.59 N) all yielded significantly lower adhesive values.

3.4. Measurement of stiffness

Rigidity measurements are shown in Figure 5 and Table 2. All generics, except Towa (5.8-degree), yielded significantly higher values compared to Hokunalin (3.7-degree). Particularly, HMT (59.6-degree), NP (58.3-degree), and Takata (56.3-degree) gave rigid softness values greater than 50-degree, indicating they are very soft products.

4. Discussion

In drug release assays, Hokunalin exhibited a slower, more sustained release compared to other tape formulations (Figure 1 and Table 2). The active ingredient release rate for Hokunalin was 30% at 3 hours and 50% at 8 hours, while the generics YP and Teikoku gave release rates of 46% and 57%, respectively, at 3 hours, with both over 80% at 8 hours. The release rate for YP was about 1.5 times greater than that of Hokunalin after 3 hours, and about 2 times greater than that of Teikoku, demonstrating that Hokunalin has better sustained-release characteristics. One reason for this may be the use of the patented "Crystal Reservoir System" (*6*) mechanism, which gradually releases the drug from the tape to the skin, yielding an effective release over 24 hours. Lacking this technique, developing products with similar sustained-release characteristics may be difficult.

Tulobuterol pastes can reduce side effect risks and provide improved efficacy for symptoms like asthma attacks at the latter period of individual treatment times before reapplication, due to better sustained-release properties. On the other hand, patients' skin permeability may also affect drug formulation release rates (*8-11*). Therefore, caution is required in selecting generic drugs for patients with weak skin barrier functions, such as children and patients with skin diseases that compromise skin-barrier integrity.

Next, comparing tape peel strengths showed that the generics MED (4.99 N), YP (3.26 N), Sawai (4.17 N), and Teikoku (4.37 N) were significantly higher than that of Hokunalin (2.66 N) (Figure 2 and Table 2). The peel-off force for MED, Sawai and Teikoku was more than 4 N, indicating that a strong force is required to peel off the tape. A high peeling force implies the tape is difficult to peel off and is expected to be more invasive to the skin, causing pain during the peeling process and an associated exfoliation of dead skin cells. Peeling difficulty and skin

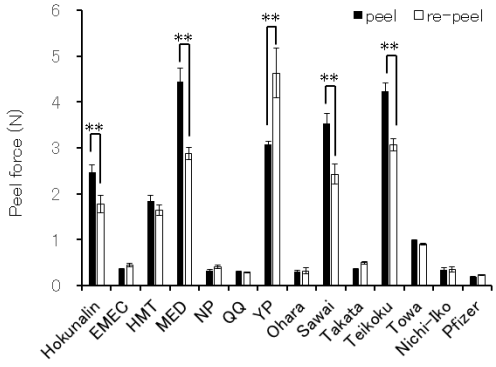

Figure 3. Comparison of re-peel force by the 90-degree test. (*n* = 6, ***p* < 0.01, Paired *t*-test), Black bar: peel force, white bar: re-peel force.

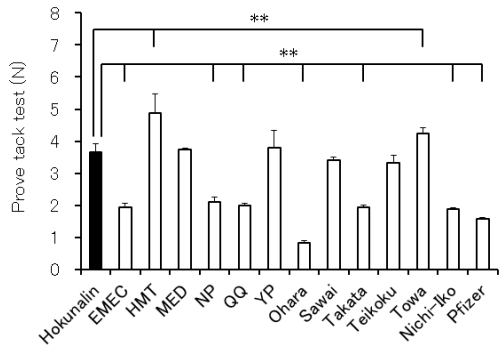

Figure 4. Comparison of adhesive force by the probe tack test. (*n* = 6, *vs.* Hokunaline, ***p* < 0.01, *Dunnett's*-test), Black bar: brand-name drug, white bar: generic drugs.

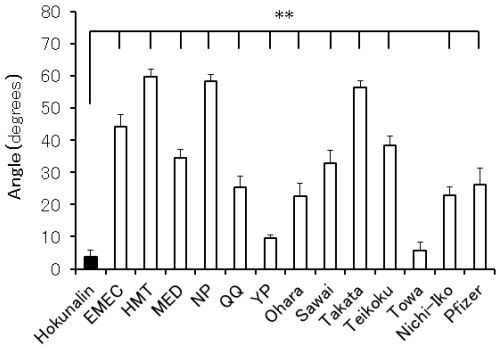

Figure 5. Comparison of bending resistance. (*n* = 6, *vs.* Hokunaline, ***p* < 0.01, *Dunnett's*-test), Black bar: brand-name drug, white bar: generic drugs.

irritation are considered likely problems that patients may experience when using these products. These results assist in appropriate formulation selection according to patients' skin condition.

On the other hand, generics EMEC (0.47 N), HMT (1.87 N), NP (0.49 N), QQ (0.43 N), Ohara (0.47 N), Takata (0.40 N), Towa (1.13 N), Nichi-Iko (0.51 N), and Pfizer (0.25 N) yielded significantly lower peel strength values. Products with a peel strength of less than 1 N indicate easy removal, which may be a positive depending on the patient's skin condition. As these products are applied daily for the prevention of bronchial asthma to either the chest, back, or upper arm, *etc.*, a weaker peel-off force may reduce skin irritation. However, keratin damage during tape removal is not the only source of skin irritation. It can also be caused by "steaming" due to prolonged application, "blistering" by strongly pulling the skin upon application, and "chemical irritation" caused by additives. These irritating factors require minimization to improve patient comfort.

Though it may be considered relatively rare to peel off and reapply the tape, there are cases where tape is wrinkled during application and is reapplied after being peeled off from the skin. Thus, reapplication (reattachment) tests were conducted for each tape formulation (Figure 3 and Table 2). For Hokunalin, and the generics MED, Sawai, and Teikoku, peeling and immediate reapplication on tape adhesive strength led to significantly lower peel-off forces. In this test, the peel force was measured by tape application to a stainless-steel plate, peeled off once, reapplied, and peeled off once more. Usually, tape application to skin involves keratin and other skin substances adhering to the tape adhesive side after removal, strongly decreasing adhesive strength upon reapplication. This test is complicated to perform, so the simplification of application to a stainless plate was used rather than skin, and simply compared the magnitude of change in peeling strength upon reapplication. The four tapes with high peel force values, Hokunalin, MED, Sawai, and Teikoku, all underwent significant decreases in peel strength upon reapplication (Figure 3 and Table 2). On the other hand, YP yielded a significantly higher peel strength after reapplication compared to the first application. This is attributed to part of the tape adhesive surface detaching and contaminating the stainless test plate after the first peeling. This then exposes a new adhesive surface tape adhesive side, which then adheres more strongly to the stainless-steel surface with the deposited adhesive.

Next, the probe tack test measured tape adhesiveness, with the results shown in Figure 4 and Table 2. The probe tack test indicated that the generic drugs HMT (4.89 N) and Towa (4.25 N) were significantly higher than Hokunalin (3.65 N). On the other hand, EMEC (1.93 N), NP (2.11 N), QQ (1.98 N), Ohara (0.83 N), Takata (1.95 N), Nichi-Iko (1.87 N), and Pfizer (1.59 N) all showed significantly lower values. Particularly, Ohara yielded the lowest adhesive stickiness, at less than 1 N. As adhesiveness is generally an ease-of-application indicator, the high adhesive strength of HMT and Towa suggested they are easy-to-apply products.

Next, the tape stiffness measurement results are shown in Figure 5 and Table 2. This shows that all generics, except Towa, were significantly stiffer than Hokunalin. Products with low rigidity and high softness values can flexibly conform to skin movements, which is desirable. However, low rigidity and high softness may also increase difficulties in applying the tape, as the adhesive surface may fold and adhere to itself. Therefore, the appropriate formulation varies depending on user circumstances, physical capability, and skin condition. Thus, the results of these analyses provide a basis to select the appropriate formulation for patient-focused care.

A summary of measured values for each test is shown in Table 2. The highest performing formulations, in terms of active ingredient sustained release, are Hokunalin and the generic products YP and Teikoku. MED, Sawai, and Teikoku yielded high peel-off force values, indicating the possibility of skin damage. No correlation was observed between peeling force and adhesive strength. Furthermore, given the softness of products other than Hokunalin and Towa, they may be difficult to apply, especially when applied by the elderly and people with poor manual dexterity.

Given the varying characteristics among the tapes, pharmacists must select the best product for the patient, accounting for the patient's background (*e.g.*, to include effects of increased skin permeability, *etc.*), patient's dexterity, and the patient's comfort in using the product.

Funding: None.

Conflict of Interest: The authors have no conflicts of interest to disclose.

References

1. Izumi T, Hori S, Sato H, Miki A, Sawada Y. Questionnaire survey on change of asthmatic response, adverse events and product usability due to switch between tulobuterol tapes. Yakugaku Zasshi. 2012; 132:617-627. (in Japanese)
2. Wada Y, Takaoka Y, Nozawa M, Goto M, Shimokawa K, Ishii F. Generic selection criteria for safety and patient benefit [VI]: Comparing the physicochemical and pharmaceutical properties of brand-name, generic, and OTC felbinac tapes. Drug Discov Ther. 2016; 10:300-306.
3. Nozawa M, Goto M, Wada Y, Yotsukura K, Gannichida A, Ishii F, Shimokawa K. Generic selection criteria for safety and patient benefit [VIII]: Comparing the physicochemical and pharmaceutical properties of brand-name and generic diclofenac sodium tapes. Drug Discov Ther. 2019; 13:150-156.
4. Nozawa M, Goto M, Wada Y, Ishii F, Shimokawa K. Generic selection criteria for safety and patient benefit

[X]: Watervapor permeability and peel force properties of brand-name and generic ketoprofen tapes. Drug Discov Ther. 2021; 15:87-92.
5. Nozawa M, Gannichida A, Wada Y, Kumazawa M, Ishii F, Shimokawa K. Generic selection criteria for safety and patient benefit [XI]: Usability scores of brand-name and generic tapes containing sodium diclofenac by questionnaire survey. Drug Discov Ther. 2022; 16:210-216.
6. Hokunalin® tape home page. *http://hokunalin.jp/patient/introduction/structure.html* (accessed September 24, 2023).
7. Yamazaki M. Development of transdermal drug delivery system of tulobuterol for asthma treatment based on chronotherapy. Membrane. 2003; 28:255-262. (in Japanese)
8. Tojo K, Hikima T. Bioequivalence of marketed transdermal delivery systems for tulobuterol. Biol Pharm Bull. 2007; 30:1576-1579.
9. Nakamura A, Mori D, Tojo K. Evaluation of the predicted time-concentration profile of serum tulobuterol in human after transdermal application. Chem Pharm Bull. 2012; 60:300-305.
10. Watanabe T, Satoh H, Hori S, Miki A, Ohtani H, Sawada Y. Model analysis of tulobuterol patch formulations to explain the influence of drug release rate and transdermal transfer rate on the plasma concentration profile. Yakugaku Zasshi. 2011; 131:1483-1492. (in Japanese)
11. Naruto I, Kitano A, Nishikata M, Matsuyama K. Comparative study of brand-name and generic tulobuterol transdermal preparations, Jpn J Med Pharm Sci. 2006; 56:727-734. (in Japanese)
12. The Japanese Pharmacopoeia, Eighteenth Edition (JP18), General tests, 6.13 Release Test for Preparations for Cutaneous Application, 1. Paddle over disk method, pp. 177-178.
13. The Japanese Pharmacopoeia, Eighteenth Edition (JP18), General tests, 6.12 Methods of adhesion testing, 3.1.2.2. 90-degree peel test, pp. 175-176.
14. The Japanese Pharmacopoeia, Eighteenth Edition (JP18), General tests, 6.12 Methods of adhesion testing, 3.4. Probe tack testing, p. 177.
15. Japanese Industrial Standards, JIS L 1913:2010 General Nonwoven Testing Method, 6.7 Rigid-softness cantilever method. *https://jis.eomec.com/jisl19132010/3#gsc.tab=0* (in Japanese) (accessed September 24, 2023).
16. Yanai H. 4 Steps Excel Statistics (3rd Edition), OMS Publishing, Saitama Japan 2015. (in Japanese)

Received September 24, 2023; Revised November 22, 2023; Accepted November 23, 2023.

**Address correspondence to:*
Ken-ichi Shimokawa, Department of Pharmaceutical Sciences, Meiji Pharmaceutical University, 2-522-1, Noshio, Kiyose, Tokyo 204-8588, Japan.
E-mail: kshimoka@my-pharm.ac.jp

Released online in J-STAGE as advance publication December 3, 2023.

Original Article

DOI: 10.5582/ddt.2023.01047

Quercetin antagonized advanced glycated end products induced apoptosis and functional inhibition of fibroblasts from the prolapsed uterosacral ligament

Yizhen Sima[1,2,3,4,§], Junwei Li[1,§], Leimei Xu[1,§], Chengzhen Xiao[1], Lisha Li[2,3,4], Ling Wang[2,3,4,*], Yisong Chen[1,*]

[1] Department of Gynecology, Obstetrics and Gynecology Hospital of Fudan University, Shanghai, China;
[2] Laboratory for Reproductive Immunology, Obstetrics and Gynecology Hospital of Fudan University, Shanghai, China;
[3] The Academy of Integrative Medicine of Fudan University, Shanghai, China;
[4] Shanghai Key Laboratory of Female Reproductive Endocrine-related Diseases, Shanghai, China.

SUMMARY The altered behaviors and functions of pelvic floor fibroblasts are pathophysiological changes of pelvic organ prolapse (POP). Our previous study showed that advanced glycated end products (AGEs) accumulated in the pelvic tissues of POP and induced fibroblast apoptosis. The study was designed to investigate whether quercetin antagonize AGEs-induced apoptosis and functional inhibition of fibroblasts. The uptake of 5-ethynyl-2'-deoxyuridine (EdU) was evaluated for cell proliferation. Flow cytometric analysis was applied for cell apoptosis. Intracellular reactive oxygen species (ROS) content was determined by the fluorescence of dichlorofluorescein (DCF). The contractility of fibroblasts was measured by collagen gel contraction assay. The expressions of extracellular matrix (ECM) related genes and the expression of miR-4429 and caspase-3 were quantified by qPCR. The expressions of phosphatase and tensin homolog (PTEN), phosphoinositide 3-kinase (PI3K), serine-threonine kinase (Akt), and phosphorylated Akt (p-Akt) were analyzed by Western Blot. The down-regulation of miR-4429 was achieved by cell transfection. Quercetin antagonized AGEs-induced apoptosis, proliferation inhibition, and ROS increase in fibroblasts. Quercetin did not alleviate AGEs-induced contractile impairment of fibroblasts. Quercetin reduced the gene expressions of lysyl oxidase like protein 1 (LOXL1) and matrix metallopeptidase 1 (MMP1), and increased the gene expressions of lysyl oxidase (LOX) and fibrillin 2 (FBN2) in fibroblasts. Quercetin reversed AGEs-induced upregulation of PTEN and downregulation of PI3K, P-Akt, and miR-4429 in fibroblasts. The inhibitory effect of quercetin on AGEs-induced fibroblast apoptosis was inhibited by downregulating the expression of miR-4429. In conclusion, quercetin antagonized AGEs-induced apoptosis and functional inhibition of fibroblasts from the prolapsed uterosacral ligament. And inhibiting AGEs-induced down-regulation of miR-4429/PTEN/PI3K/Akt pathway was the mechanism underlying the antagonistic effect of quercetin on AGEs-induced apoptosis.

Keywords pelvic organ prolapse, quercetin, fibroblasts, advanced glycation end products

1. Introduction

Pelvic organ prolapse (POP), caused by damages or weakness of the pelvic supportive tissues, is a common degenerative disease in women. The incidence of symptomatic POP was 9.6% in Chinese women over the age of 20 (*1*). Given the high prevalence, the pathophysiology of POP has not been understood. The abnormal contents and structures of collagen and elastic fibers in pelvic floor connective tissues lead to the decrease of mechanical strength for pelvic organs. Pelvic supportive tissues include the levator ani muscle complex and connective-tissue attachments of the pelvic organs (*2*). Fibroblasts are responsible for the regulation of extracellular matrix (ECM) that determines the mechanical properties of pelvic connective tissues. The previous studies reported functional differences among cell proliferation, contractility, adhesion, oxidative stress, and ECM metabolism between fibroblasts from the prolapsed and normal tissues (*3-7*). Therefore, investigation on fibroblasts is important to reveal the reasons behind the impaired supportive structures in

POP.

Advanced glycation end products (AGEs) refer to a heterogeneous group of glycation adducts of proteins by glucose or other saccharides. AGEs could induce a series of cell inflammation and oxidative stress and have been extensively investigated in diabetes mellitus (*8,9*). In addition, AGEs affected the metabolism of collagens by accelerating collagen degeneration, resulting in tissue strength impaired, skin aging (*10*), and bone remodeling (*11*). In 1996, Jackson *et al.* first reported that the level of advanced glycation cross-links elevated in prolapsed vaginal-epithelial tissue (*12*). Our previous report indicated that AGEs content increased in the vaginal wall of the POP patients in contrasted with the non-POP patients (*13*). Then, several studies also found an elevated level of AGEs in the muscularis propria of vaginal wall among POP patients (*14,15*), but the mechanisms of AGEs participating in the development of POP were not studied. Similar to the pathogenesis in diabetes complications, we previously reported that AGEs reduced the type I collagen by increasing the expression of matrix metalloproteinase-1 (MMP-1) in human vaginal fibroblasts through the receptor for AGEs on cell membrane (*16*). In our recent study, we reported that AGEs induced the expression of phosphatase and tensin homolog (PTEN) *via* reducing the expression of miR-4429, thus suppressing the phosphoinositide 3-kinase (PI3K)/ serine-threonine kinase (Akt) pathway and induced fibroblast apoptosis (*17*).

Quercetin, as a widely studied natural flavonoid, was reported as an effective antioxidant, which improved renal function in diabetic nephropathy rats by inhibiting intracellular reactive oxygen species (ROS) (*18*) and ameliorated myocardial injury caused by oxidative stress (*19*). Oxidative stress is one of the factors leading to cellular senescence, and the role of quercetin in delaying cellular senescence has been studied. Quercetin delayed the senescence of skin fibroblasts by inhibiting the increase of intracellular H_2O_2 and iron death caused by UV irradiation (*20*). Quercetin selectively eliminated senescent cells, and its use in combination with dasatinib was known as Senolytics therapy (*21*). In the mouse model of idiopathic pulmonary fibrosis, quercetin induced the apoptosis of senescent fibroblasts to inhibit fibrosis (*22*). Aging is a risk factor for POP. In addition, senescence and oxidative stress of pelvic floor fibroblasts resulted in the apoptosis and dysregulation of ECM metabolism (*23,24*). Therefore, it is worth exploring whether quercetin achieve the therapeutic effect for POP by inhibiting the apoptosis of pelvic floor fibroblasts and maintaining ECM homeostasis. What's more, quercetin inhibits AGEs formation *via* chelating metal ions and trapping methylglyoxal (*25*). Previous studies reported that quercetin suppressed AGEs-induced cell apoptosis in human skin fibroblasts (*26*) and reversed dietary AGEs-induced cognitive dysfunction in aged mice (*27*).

The present study aimed to investigate whether quercetin antagonizes the apoptosis and functional inhibition of pelvic floor fibroblasts induced by AGEs, and further explore the mechanism of quercetin in antagonizing the apoptosis of fibroblasts. We isolated fibroblasts from the human uterosacral ligament in POP and non-POP patients and evaluated the influences of AGEs and quercetin on cell proliferation, apoptosis, ROS, contractility, and ECM production. We found that quercetin antagonized AGE-induced apoptosis and functional inhibition of fibroblasts. In addition, quercetin reduced the apoptosis of fibroblasts by inhibiting the AGEs-induced downregulation of the miR-4429/PTEN/PI3K/Akt pathway.

2. Materials and Methods

2.1. Ethics statement

Human protocols in current study were authorized by the local Ethics Committee of the Obstetrics and Gynecology Hospital of Fudan University (Shanghai, China). The number is 2021-234. The study included a total of 20 subjects who underwent a hysterectomy at the same hospital from January to October 2021. All subjects in the study had signed informed consent before the operations. The sample in the study was a piece of the uterosacral ligament with a size of 0.5 cm^2 which was cut from the removed uterus during operations.

2.2. Patients

There were 20 patients included in the POP and non-POP groups according to the inclusion and exclusion criteria, 10 patients in each group. Inclusion criteria of the POP group are including ≥ 45 years old, POP-Q (pelvic organ prolapsed quantification) ≥ stage III (*28,29*), and received hysterectomy. Inclusion criteria of the non-POP group are including ≥ 45 years old, without any pelvic organ prolapsed manifestation, received a hysterectomy at the same hospital due to other benign gynecological diseases (uterine fibroids, cervical precancerous lesions, endometrial lesions, postmenopausal ovarian benign tumors). Patients who had pelvic surgeries, pelvic inflammation, malignant diseases, severe systemic diseases, and with a history of hormone replacement therapy were ruled out. The clinical data files were collected from all the included patients and the information about age, body mass index, parity, and menopause rate were reported in our previous study (*17*).

2.3. Isolation and culture of the primary cells

Human uterosacral ligament fibroblasts were obtained from patients who underwent a hysterectomy. A piece of fresh tissue with a size of 0.5 cm^2 was collected after the removal of the uterus during the operation. The fresh

tissue specimens were washed with phosphate-buffered saline (PBS) containing 1% penicillin, streptomycin, and amphotericin B (Genom, Hangzhou, Zhejiang, China) and cut into 1 mm^3 pieces. Then the tissue pieces were put into the type I collagenase (Sigma-Aldrich, St. Louis, MO, USA) solution and shook up for 1 hour at 37°C. The digested mixture was centrifuged to collect the cell pellet. The cell pellet was resuspended in 1 mL of DMEM medium containing 20% fetal bovine serum (FBS) (Gibco, Grand Island, NY, USA) and 1% triple antibiotic (Genom) and transferred to six-well plates. The culture plates were placed in a cell incubator and the culture medium was changed when some adherent cells could be observed. From then on, the primary cells were cultured at 37°C in a 5% CO_2 atmosphere, and renewed the medium every 2-3 days. Identification of the primary fibroblasts was performed and the results were reported in the previous study (*17*). Fibroblasts were passaged at 80% confluency and the cells with passages 3-5 were used in the current study.

2.4. Cell apoptosis assay

Cell apoptosis assays were conducted by flow cytometric analysis using a fluorescein isothiocyanate (FITC) Annexin V/propidium iodide (PI) kit (BD Bioscience, San Jose, CA, USA) according to the manufacturer's instructions. Cultured fibroblasts were collected and washed by staining buffer (BD Bioscience) for 2 times. The cell suspension was centrifuged at 800× *g* for 5 min. Then FITC and PI were successively added into the 300 μL staining buffer to make cells stained by the fluorescence for 15 min and 10 min in dark at room temperature. All prepared cell samples were assayed by a flow cytometry (Becton Dickinson, Franklin Lakes, NJ, USA). The viable cells and apoptotic cells were distinguished by the detection of fluorescence signals. All data generated by flow cytometry were processed by the FlowJo version X.0.7. Number of positive cells was determined in comparison to the unstained cells as controls.

2.5. Cell proliferation assay

Proliferative capacity was assessed by the incorporation of a thymidine analog 5-ethynyl-2'-deoxyuridine (EdU) using an EdU cell proliferation kit (Beyotime, Shanghai, China). The cultured fibroblasts were incubated on 6-well plates and labeled with 10 μM EdU for 6 hours after BSA or AGE-BSA treatment. After discarding the culture solution, fibroblasts were incubated in 4% paraformaldehyde for 20 min at ambient temperature. Then fibroblasts were incubated with 0.3% Triton X-100 for 10 min at ambient temperature. Click additive solution was prepared by blending the click reaction buffer, CuSO4, 488 Azide according to the instructions. And then click additive solution was added into cell culture dishes, incubating for 30 min in dark. Then the Hoechst 33342 was added to cell culture dishes, incubating for 30 min in dark. Fluorescent images were captured using a fluorescence microscope (Leica, Wetzlar, Germany). EdU positive cell rate was calculated by Image J software (1.40g, Wayne Rasband National Institutes of Health, USA). The cell proliferation rates were calculated as the ratio of EdU positive nuclei number to total nuclei number.

2.6. Contractility assay

The contractile activity of fibroblasts was determined by cell-mediated collagen gel contraction assay according to the method previously reported (*30*). 1.0 mg/mL type I rat tail collagen solution (BD Biosciences) was prepared by adding 1 M NaOH, to adjust the final pH value to 7.2. The adherent cells were digested and resuspended in PBS to obtain the final cell concentration. The appropriate number of fibroblasts was then transferred to the neutralized collagen solution. Then the mixture was incubated on ice for 5 min and was pipetted into 12-well culture dishes. The gel coagula were then gently detached from the bottom of the well after being incubated for 1 h at 37°C. A DMEM solution with 50 μg/mL BSA, 50 μg/mL AGE-BSA, or 20 μM quercetin (Sigma) was added to each well. Then cells were static cultured and the gels were observed periodically. Maximum effects on gel contraction were obtained within 72 hours of culture. A chemiluminescence imager was used to take pictures and record gel shrinkage at 0, 24, 48, and 72 hours after the culture. The area of each gel was measured using Image J, and the area proportion of each gel compared to its initial area was calculated. The percentage of gel area to the initial gel area was calculated. The area proportion was inversely proportional to the cell-mediated collagen contractile capacity.

2.7. Intracellular ROS quantification

The intracellular ROS levels were determined by measuring the fluorescent dichlorofluorescein (DCF) using a ROS assay kit (Beyotime). Fluorescent DCF was transformed from the cell-permeable 2', 7' dichlorofluorescein diacetate (DCFH-DA) under oxidation by intracellular ROS. Before loading DCFH-DA, cells were treated with 50 μg/mL BSA, 50 μg/mL AGE-BSA, or 20 μM quercetin for 24 hours. Then, the culture medium was replaced by DMEM with 10 μM DCFH-DA, and cells were incubated at 37°C for 30 min. The culture media were removed and cells were washed using DMEM. Then DCF fluorescence distribution was detected by fluorescence microscope or analysis by flow cytometry after cell collection at the wavelength of 488 nm/535 nm.

2.8. Cell transfection

Fibroblasts were cultured in a 6-well plate with complete medium without antibiotics. Once achieving 40-50% confluence, the complete medium was replaced by 1.5 mL/well preheated serum-free DMEM medium. Then, miR-4429 inhibitor or negative control (NC) was diluted by Opti-MEM (Gibco) (15 μL miR-4429 inhibitor or inhibitor NC in 250 μL Opti-MEM) and blended with diluted Lipofectamine 2000 (Thermo Fisher Scientific, Waltham, MA, USA) (5 μL Lipofectamine 2000 in 250 μL Opti-MEM). The mixture was thoroughly mixed and stood for 20 minutes at ambient temperature, and then it was carefully added to the culture medium, 500 μL/well. The 6-well plates were static cultured for 6 hours. Then the culture medium was replaced by the completed culture medium and the cells were continued to culture for 24-48 hours before they were used in the subsequent experiments. The sequences of miR-4429 inhibitor and inhibitor-NC were listed in Table 1.

Table 1. Primer sequences

Name	Sequence (5' to 3')
COL1 forward	GTGCGATGACGTGATCTGTGA
COL1 reverse	CGGTGGTTTCTTGGTCGGT
COL3 forward	GGTAGTCTCACAGCCTTGCG
COL3 reverse	GAGGATGGTTGCACGAAACAC
COL5 forward	TCCGAAGGGGCCAGAATCA
COL5 reverse	GAGCAGTTTCCCACGCTTGA
MMP1 forward	GGGGCTTTGATGTACCCTAGC
MMP1 reverse	TGTCACACGCTTTTGGGGTTT
MMP3 forward	ATGAACAATGGACAAAGGATACAACAG
MMP3 reverse	CATCTTGAGACAGGCGGAACC
TIMP1 forward	CTTCTGCAATTCCGACCTCGT
TIMP1 reverse	ACGCTGGTATAAGGTGGTCTG
Elastin forward	CCTCCCTTCTGCTTCCTCTC
Elastin reverse	CGACTGTTCTTTCGCTGCTG
LOX forward	GGCGAAGGGTGAGGAGTAAG
LOX reverse	TGGGAGACCTAAACGTCAGC
LOXL1 forward	TATGTCCAGAGAGCCCACCT
LOXL1 reverse	TAGCACCCGCACATCGTAGT
LOXL2 forward	ATGTCACCTGCGAGAATGGG
LOXL2 reverse	TGCTCTGGCTTGTACGCTTT
FBN2 forward	CTCTTCTTCTGGGGGCGACTT
FBN2 reverse	CGCTCCGAAGACGGATATTGG
FBLN5 forward	TCTGGAAAGGGCAGCAACTT
FBLN5 reverse	CTTGTCTATCAGCCGATGCG
CASP3 forward	CCAAAGATCATACATGGAAGCG
CASP3 reverse	CTGAATGTTTCCCTGAGGTTTG
PTEN forward	TTTTGAAGACCATAACCCAC
PTEN reverse	TATCATTACACCAGTTCGTC
GAPDH forward	GGAGCGAGATCCCTCCAAAAT
GAPDH reverse	GGCTGTTGTCATACTTCTCATGG
miR-4429 inhibitor	CGCCUCUCAGCCCAGCUUUU
inhibitor NC	UCUACUCUUUCUAGGAGGUUGUGA

COL, collagen; MMP, matrix metalloproteinase; TIMP, tissue inhibitor of matrix metalloproteinase; LOX, lysyl oxidase; LOXL, lysyl oxidase like protein; FBN, fibrilin; FBLN, fibulin; CASP, caspase; PTEN, phosphatase and tensin homolog; GAPDH, glyceraldehyde-3-phosphate dehydrogenase; NC, negative control.

2.9. Western blotting

The cultured fibroblasts were treated by lysis buffer (Beyotime). Total proteins were extracted by centrifugation and were separated under electrophoresis. Separate proteins were transferred to polyvinylidene fluoride membranes. The blocking solution was 5% bovine serum albumin (Sigma) or nonfat-dried milk/TBST. Then, membranes were successively incubated with the primary and secondary antibodies under optimal conditions. The antibodies in the present study included anti-PI3K antibody, anti-pan-Akt antibody, anti-phosphorylated Akt (S473) antibody (Cell Signaling Technology, Danvers, MA, USA), anti-PTEN antibody, and anti-GAPDH antibody (Abcam, Cambridge, MA, USA). After being washed completely, the membrane was covered by an appropriate amount of chemiluminescence reagent (Merck Millipore, Billerica, MA, USA) to carry out the enhanced chemiluminescence. Relative intensities of the images were measured by Image J (1.40 g, USA).

2.10. Quantitative polymerase chain reaction (qPCR)

Total RNA was extracted by an RNA purification kit (EZBioscience, Roseville,CA, USA) from the fibroblasts which were cultured under different indicated treatments. The concentration of RNA was determined by NanoDrop Spectrophotometer (Thermo Fisher Scientific). Then RNA was converted into cDNA by reverse transcription. After the qPCR system was prepared using SYBR Green qPCR master mix (Takara, Tokyo, Japan), the mixture was thoroughly mixed and pipetted into a 384-well plate. The expressions of target genes at the mRNA level were detected by the QuantStudio Flex Real-Time PCR System (Thermo Fisher Scientific). The valid cycle threshold values were collected from each group's data. The expression of GAPDH was considered as the internal reference, and the relative gene expression was calculated by the $2^{(-\Delta\Delta CT)}$ method. All of the primer sequences in the present study were shown in Table 1.

2.11. Statistical analysis

Student's *t*-test was conducted to calculate the statistic difference between two groups when the data obey normal distribution with equal standard deviations. When the data did not obey normal distribution, Mann-Whitney test was applied for the contrast between two groups. The significant differences between 3 or more groups were identified by ANOVA, and Tukey test was applied to determine the significant differences in pairs. Differences were regarded as statistically significant when $p < 0.05$. All the tests were calculated by the GraphPad Prism software (Version 9).

3. Results

3.1. Quercetin inhibited AGEs-induced fibroblast apoptosis

The apoptotic rate in fibroblasts exposed to AGE-BSA was significantly higher than that in fibroblasts exposed to BSA. This AGEs-induced fibroblast apoptosis was inhibited by quercetin with concentrations of 20 μM, 40 μM, 80 μM, and 160 μM for 24 hours (Figures 1A and 1B). Similarly, the gene expression of caspase-3 was upregulated by AGE-BSA, and this upregulation was reversed by quercetin with concentrations of 20 μM, 40 μM, and 80 μM for 24 hours (Figure 1C). To evaluate the inhibitory effects of quercetin with different exposure duration in AGEs-induced fibroblast apoptosis, the fibroblasts treated with AGE-BSA were subsequently treated with 20 μM quercetin for 12, 24, 36, and 48 hours. The AGEs-induced cell apoptosis was inhibited by quercetin in 12, 24, 36, and 48 hours groups (Figures 1D and 1E). Therefore, the optimum condition of quercetin as an antagonist to AGEs in fibroblast apoptosis was 20 μM for 24 hours, which was applied in the following experiments.

3.2. Quercetin antagonized the inhibiting effect of AGEs on cell proliferation

To determine the influence of AGEs on cell proliferation, we assessed the level of EdU in fibroblasts exposed to 50 μg/mL AGE-BSA or BSA (Figure 2A). The proliferation rates were calculated and illustrated (Figure 2B). As shown in Figures 2A and 2B, the proliferation rate was apparently reduced in the AGE-BSA treated groups compared with the BSA treated group both in fibroblasts from POP tissues or fibroblasts from non-POP tissues. And there was no significant difference between the fibroblasts from POP and non-POP groups exposed to BSA only. Notably, the AGEs-inhibited proliferation rate in fibroblasts of the POP group was reversed by quercetin (Figures 2C and 2D).

3.3. Quercetin inhibited AGEs-induced intracellular ROS increase in fibroblasts

To measure the effect of AGEs on the inner cellular ROS of fibroblasts, we detected the DCF positive cells using a flow cytometer and fluorescence microscope. The positive cell rates were increased both in POP and non-POP groups when treated by AGE-BSA compared to cell samples treated by BSA (Figures 3A-3C). And there was no significant difference in positive cell rates between fibroblasts from the POP and non-POP groups. Noticeably, AGEs-induced intracellular ROS increase was inhibited by quercetin, for the positive cell rate inhibition was alleviated by quercetin in fibroblasts from the POP group (Figures 3D-3F).

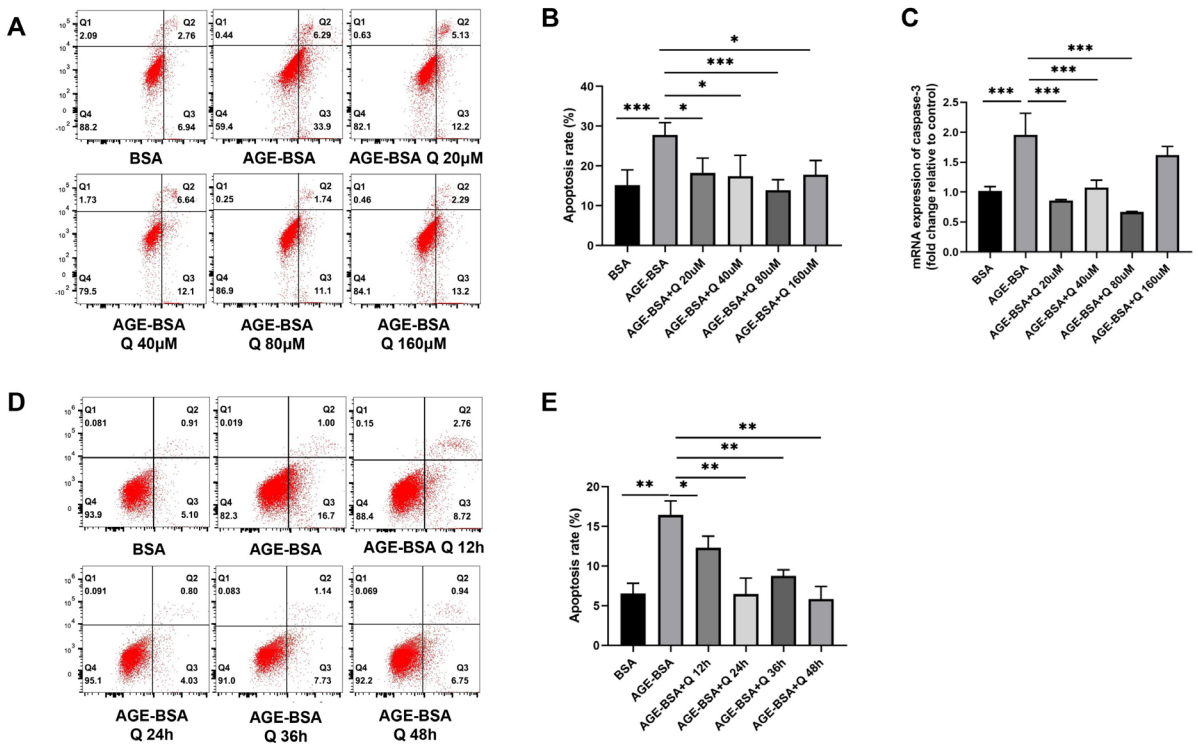

Figure 1. Quercetin inhibited AGEs-induced fibroblast apoptosis. (A) Flow cytometry analysis of cell apoptosis in fibroblasts treated by BSA, BSA-AGE, and quercetin with different concentrations. **(B)** The apoptosis rates of fibroblasts treated by BSA, BSA-AGE, and quercetin with different concentrations. **(C)** The mRNA expression of caspase-3 in fibroblasts treated by BSA, BSA-AGE, and quercetin. **(D)** Flow cytometry analysis of cell apoptosis in fibroblasts treated by BSA, BSA-AGE, and quercetin with different durations. **(E)** The apoptosis rates of fibroblasts treated by BSA, BSA-AGE, and quercetin with different durations. Error bars represent mean± SD of 3 independent experiments, *$p < 0.05$, **$p < 0.01$, ***$p < 0.005$. AGE: advanced glycation end products; BSA: bovine serum albumin; Q: quercetin; SD: standard deviation.

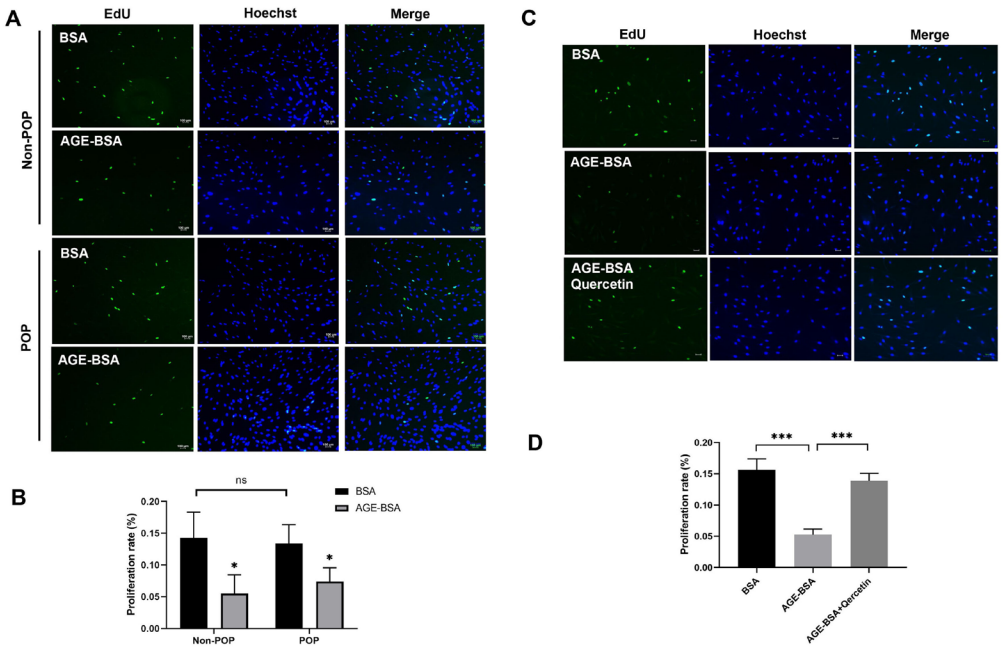

Figure 2. Quercetin alleviated the inhibitory effect of AGEs on cell proliferation. (A) The level of EdU in fibroblasts treated with AGE-BSA or BSA. **(B)** The cell proliferation rates in fibroblasts treated with AGE-BSA or BSA. **(C)** The level of EdU in fibroblasts treated with BSA, AGE-BSA, and quercetin. **(D)** The cell proliferation rates in fibroblasts treated with BSA, AGE-BSA, and quercetin. Error bars represent mean± SD of 3 independent experiments, *$p < 0.05$, ***$p < 0.005$. Scar bar: 100μm. AGE: advanced glycation end products; BSA: bovine serum albumin; POP: pelvic organ prolapse; EdU: 5-ethynyl-2'-deoxyuridine; SD: standard deviation.

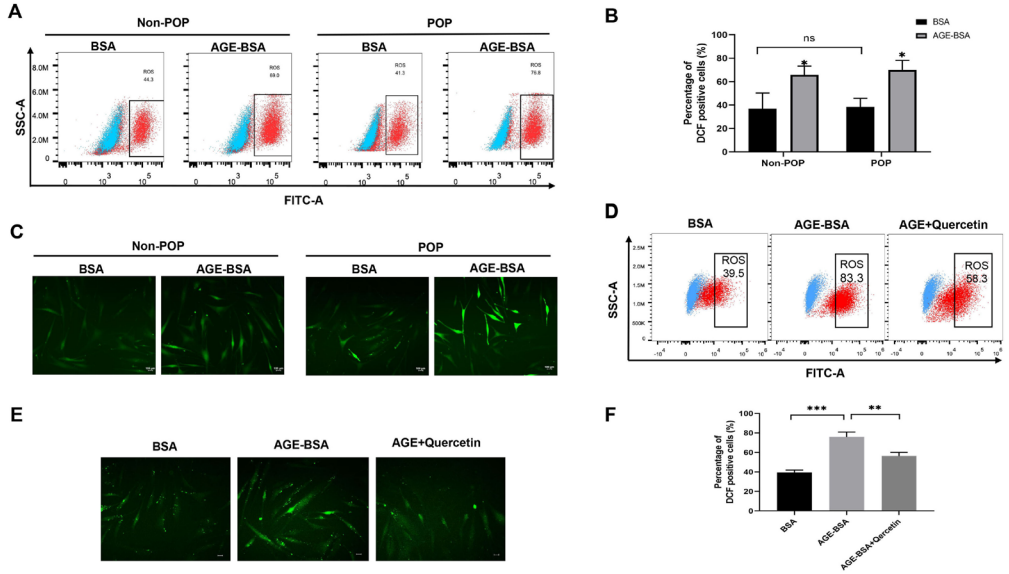

Figure 3. Quercetin inhibited AGEs-induced intracellular ROS increase in fibroblasts. (A) Flow cytometry analysis of DCF-positive cells in fibroblasts treated with AGE-BSA or BSA. **(B)** Percentage of DCF-positive cells in fibroblasts treated with AGE-BSA or BSA. **(C)** The level of DFC in fibroblasts treated with AGE-BSA or BSA. **(D)** Flow cytometry analysis of DCF-positive cells in fibroblasts treated with BSA, AGE-BSA, and quercetin. **(E)** The level of DFC in fibroblasts treated with BSA, AGE-BSA, and quercetin. **(F)** Percentage of DCF-positive cells in fibroblasts treated with BSA, AGE-BSA, and quercetin. Error bars represent mean± SD of 3 independent experiments, *$p < 0.05$, **$p < 0.01$, ***$p < 0.005$. Scar bar: 100μm. AGE: advanced glycation end products; BSA: bovine serum albumin; POP: pelvic organ prolapse; FITC-A: fluorescein isothiocyanate-area; SSC-A: side scatter-area; ROS: reactive oxygen species; DCF: dichlorofluorescein; ns: no significance; SD: standard deviation.

3.4. Quercetin did not improve the contractile impairment of fibroblasts induced by AGEs

We assessed whether AGEs and quercetin affect the contractility of fibroblasts by evaluating the cell-induced gel contraction of type I collagen. Results showed that cell contractility was impaired in fibroblasts from the POP group compared with the non-POP group (Figures 4A and 4B). In addition, treatment with AGE-BSA was found to significantly block the contractile activity of fibroblasts compared to BSA-treated cells in the non-POP group (Figures 4A and 4B). In the POP group,

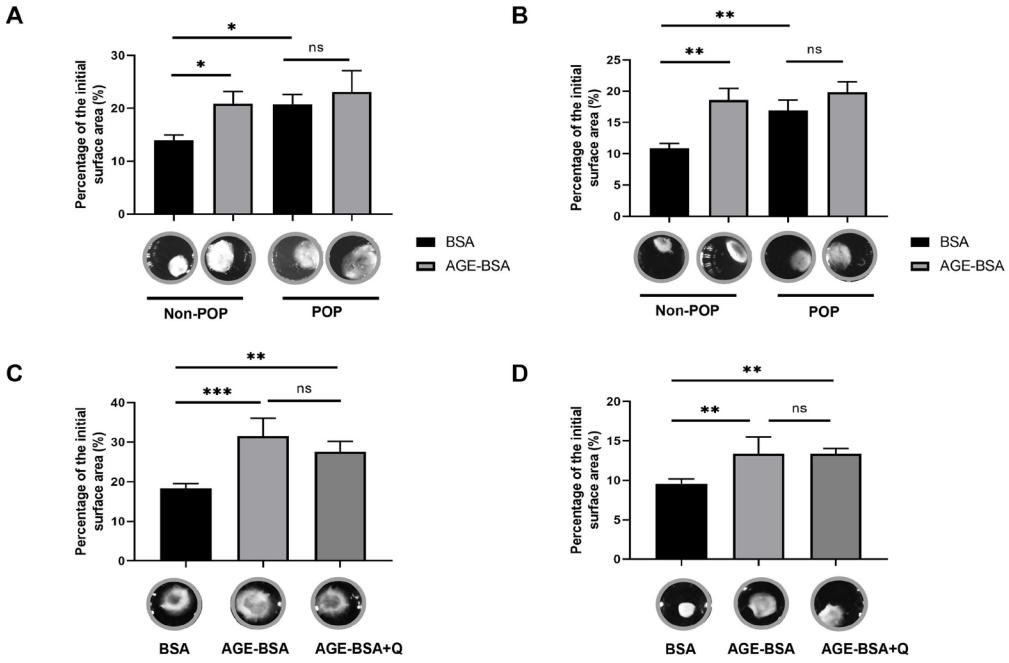

Figure 4. Quercetin did not improve the contractile impairment of fibroblasts induced by AGEs. (A) Percentage of the initial surface area in fibroblasts treated with AGE-BSA or BSA for 48 hours. **(B)** Percentage of the initial surface area in fibroblasts treated with AGE-BSA or BSA for 72 hours. **(C)** Percentage of the initial surface area in fibroblasts treated with BSA, AGE-BSA, and quercetin for 48 hours. **(D)** Percentage of the initial surface area in fibroblasts treated with BSA, AGE-BSA, and quercetin for 72 hours. Error bars represent mean± SD of 3 independent experiments; $*p < 0.05$, $**p < 0.01$, $***p < 0.005$. AGE: advanced glycation end products; BSA: bovine serum albumin; Q: quercetin; POP: pelvic organ prolapse; ns: no significance; SD: standard deviation.

although there was a trend that fibroblasts treated by AGE-BSA exhibited impaired contractility, there was no statistical difference between fibroblasts treated by AGE-BSA and BSA. Therefore, fibroblasts from the POP group were used for assessing the effects of quercetin on cell contractility. Results showed that the AGEs-induced cell contractility impairment was not influenced by quercetin in fibroblasts from the non-POP group (Figures 4C and 4D).

3.5. Quercetin partially reversed AGEs-induced imbalance of ECM gene expression in fibroblasts

To investigate whether quercetin antagonizes AGEs-induced disordered ECM production of fibroblasts, the expression of collagen and elastin-related genes in fibroblasts exposed to quercetin and AGE-BSA or BSA were assessed by qPCR. There was no statistical difference between collagen-related genes in fibroblasts from the POP and non-POP groups (Figures 5A-5F). AGE-BSA downregulated the expressions of COL1 (collagen type 1) both in the POP and non-POP groups (Figure 5A). AGE-BSA downregulated TIMP1 (tissue inhibitor of matrix metalloproteinase 1) expression and upregulated MMP1 expression of fibroblasts in the POP group (Figures 5D and 5F). Quercetin reversed AGEs-induced upregulation of MMP1, but not influenced the expressions of AGEs-downregulated COL1 and TIMP1 in fibroblasts from the POP group (Figures 5G-5I). For elastin-related genes, results showed that the expressions of LOX, LOXL2, FBN2, and FBLN5 decreased, and the expression of LOXL1 increased in fibroblasts from the POP group compared with the non-POP group (Figures 6A-6F). AGE-BSA upregulated the expressions of elastin and FBLN5 in fibroblasts from both the POP and non-POP groups. Quercetin increased the expressions of LOX, and FBN2, and decreased the expression of LOXL1 in fibroblasts from the POP group, suggesting that quercetin reduced the expression differences of LOX, FBN2, and LOXL1 between the POP and non-POP group (Figures 6G-6L). However, the disorders of elastin and FBLN5 expression induced by AGEs were not reversed by quercetin.

3.6. Quercetin inhibited AGEs induced apoptosis of fibroblasts *via* miR-4429 /PTEN/PI3K/Akt

Next, we assessed the influences of quercetin on the expressions of PTEN, PI3K, phosphorylated Akt (p-Akt), and miR-4429 in AGEs-treated fibroblasts. Results showed that AGEs suppressed the expressions of PI3K and p-Akt but increased the expression of PTEN. Quercetin with a concentration of 20 μM effectively antagonized the influences of AGEs on the expressions of PI3K, p-Akt, and PTEN in fibroblasts (Figure 7A). AGEs also significantly downregulated the expression of miR-4429, and the decreased expression of miR-4429 was reversed by 20 μM quercetin (Figure 7B).

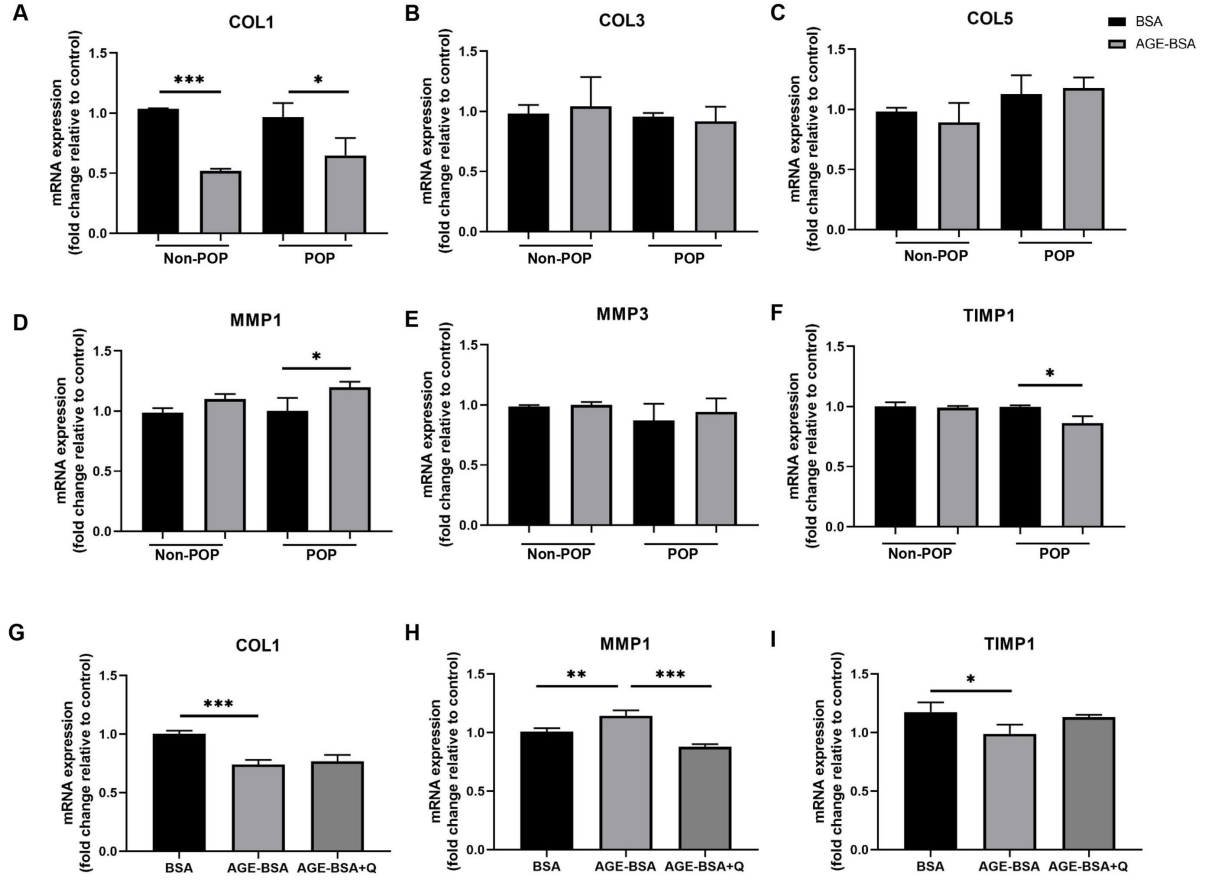

Figure 5. Effects of quercetin on AGEs-induced imbalance of collagen-related gene expression in fibroblasts. (A-F) The mRNA expression of COL1, COL3, COL5, MMP1, MMP3, and TIMP1 in fibroblasts treated with BSA or AGE-BSA. **(G-I)** The mRNA expression of COL1, MMP1, and TIMP1 in fibroblasts treated with BSA, AGE-BSA, and quercetin. Error bars represent mean± SD of 3 independent experiments; *$p<0.05$, **$p<0.01$, ***$p<0.005$. COL: collagen; MMP, matrix metalloproteinase; TIMP, tissue inhibitor of matrix metalloproteinase; AGE: advanced glycation end products; BSA: bovine serum albumin; Q: quercetin; POP: pelvic organ prolapse; SD: standard deviation.

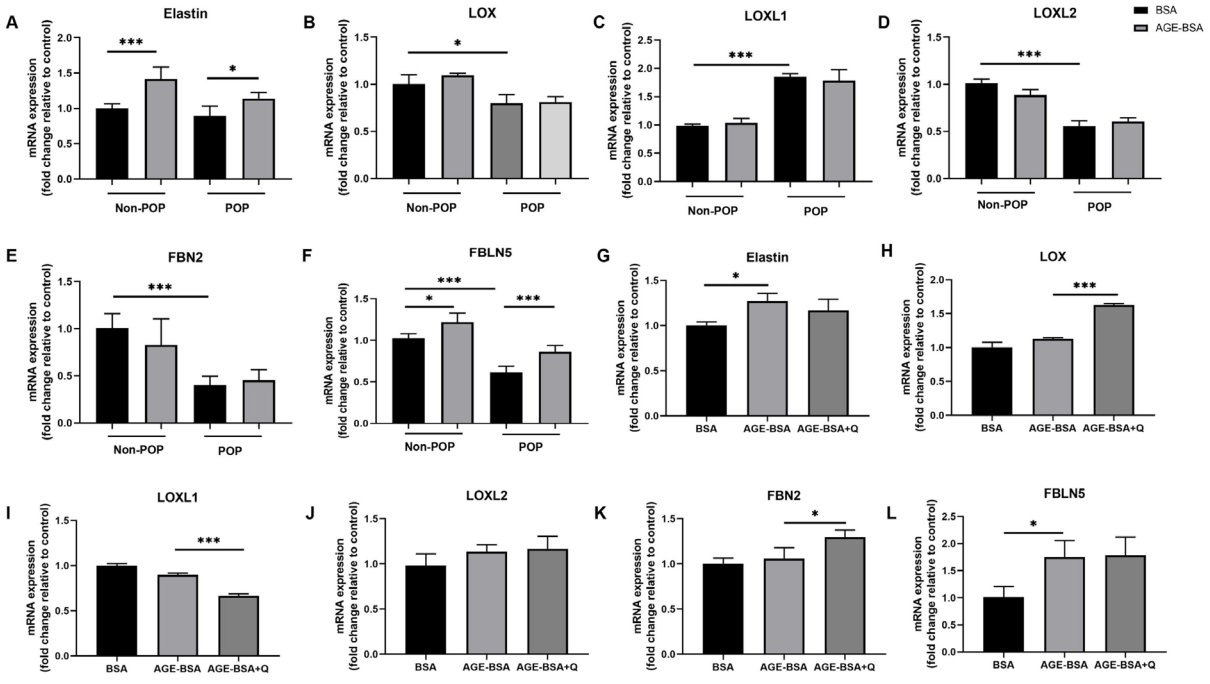

Figure 6. Effects of quercetin on AGEs-induced imbalance of elastin-related gene expression in fibroblasts. (A-F) The mRNA expression of elastin, LOX, LOXL1, LOXL2, FBN2, and FBLN5 in fibroblasts treated with BSA or AGE-BSA. **(G-L)** The mRNA expression of elastin, LOX, LOXL1, LOXL2, FBN2, and FBLN5 in fibroblasts treated with BSA, AGE-BSA, and quercetin. Error bars represent mean± SD of 3 independent experiments; *$p<0.05$, ***$p<0.005$. LOX, lysyl oxidase; LOXL, lysyl oxidase like protein; FBN, fibrilin; FBLN, fibulin; AGE: advanced glycation end products; BSA: bovine serum albumin; Q: quercetin; POP: pelvic organ prolapse; SD: standard deviation.

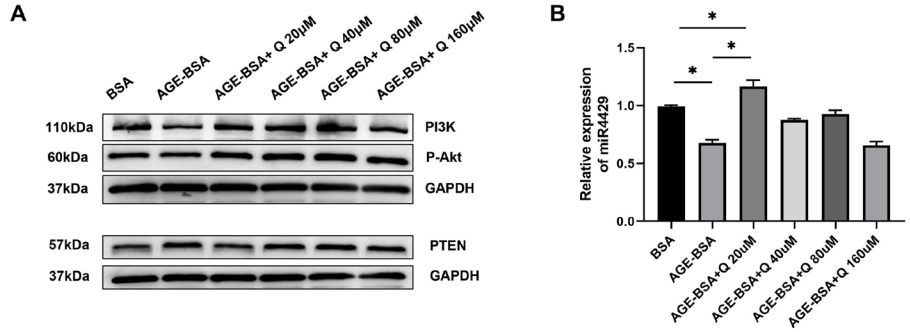

Figure 7. Quercetin antagonized AGEs-induced abnormal expressions of PTEN, PI3K, Akt, and miR-4429 in fibroblasts. (A) Western blot analysis of PI3K, P-Akt, and PTEN in fibroblasts treated with BSA, AGE-BSA, and quercetin with different concentrations. **(B)** The expression of miR-4429 in fibroblasts treated with BSA, AGE-BSA, and quercetin with different concentrations. Error bars represent mean± SD of 3 independent experiments; *$p<0.05$. PI3K: phosphoinositide 3-kinase; P-Akt: phosphorylated Akt; PTEN: phosphatase and tensin homolog; GAPDH: glyceraldehyde-3-phosphate dehydrogenase; BSA: bovine serum albumin; AGE: advanced glycation end products; Q: quercetin; SD: standard deviation.

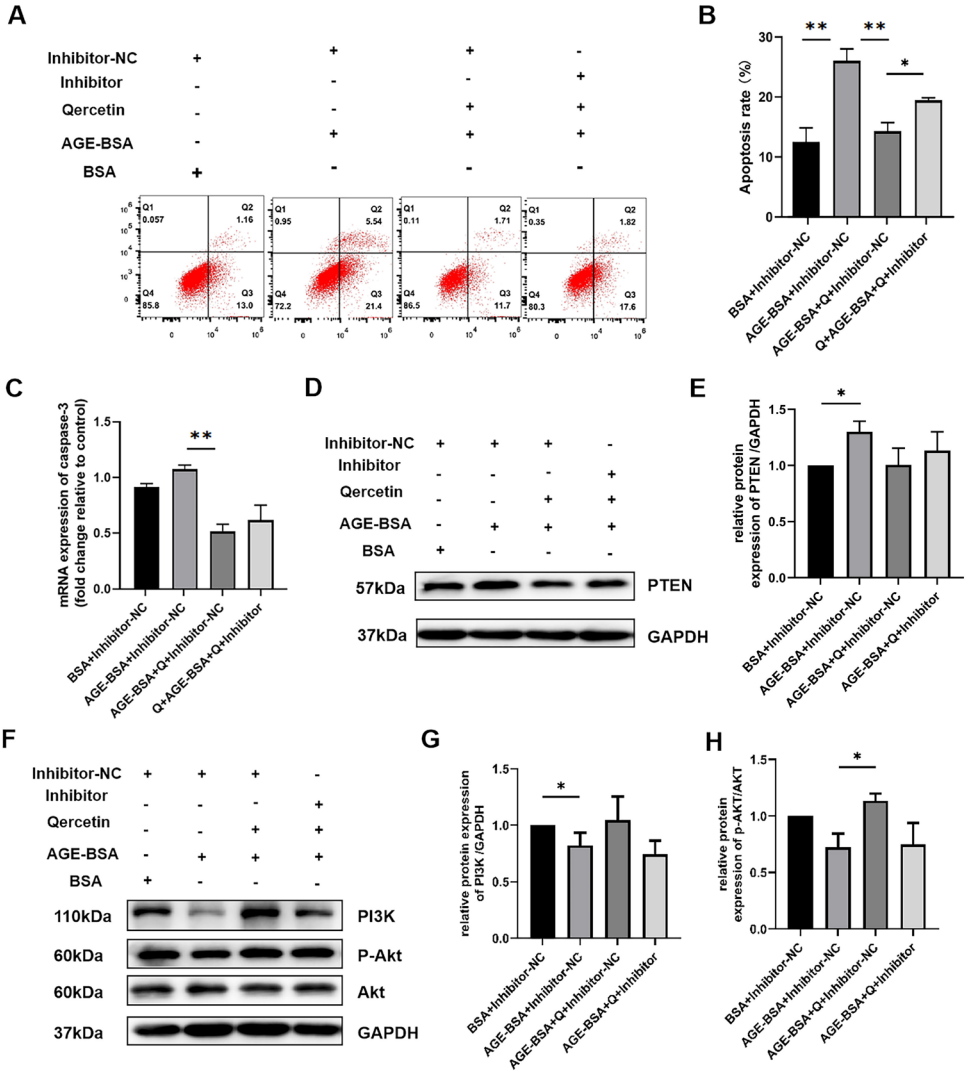

Figure 8. Quercetin inhibited AGEs induced apoptosis of fibroblasts *via* miR-4429 /PTEN/PI3K/Akt. (A) Flow cytometry analysis of cell apoptosis in fibroblasts transfected with miR-4429 inhibitor or inhibitor-NC, treated with BSA, BSA-AGE, or quercetin. **(B)** The apoptosis rates of fibroblasts transfected with miR-4429 inhibitor or inhibitor-NC, treated with BSA, BSA-AGE, or quercetin. **(C)** The mRNA expression of caspase-3 in fibroblasts transfected with miR-4429 inhibitor or inhibitor-NC, treated with BSA, BSA-AGE, or quercetin. **(D)** The protein expression of PTEN in fibroblasts transfected with miR-4429 inhibitor or inhibitor-NC, treated with BSA, BSA-AGE, or quercetin. **(E)** The relative protein expression of PTEN. **(F)** The protein expression of PI3K, Akt, and P-Akt in fibroblasts transfected with miR-4429 inhibitor or inhibitor-NC, treated with BSA, BSA-AGE, or quercetin. **(G)** The relative protein expression of PI3K. **(H)** The relative protein expression ratio of P-Akt/Akt. Error bars represent mean± SD of 3 independent experiments, *$p < 0.05$, **$p < 0.01$. AGE: advanced glycation end products; BSA: bovine serum albumin; Q: quercetin; PTEN: phosphatase and tensin homolog; PI3K: phosphoinositide 3-kinase; Akt: protein kinase B; P-Akt: phosphorylated Akt; GAPDH: glyceraldehyde-3-phosphate dehydrogenase; NC: negative control; SD: standard deviation.

Furthermore, transfection with miR-4429 inhibitor downregulated the expression of miR-4429 in fibroblasts from the POP group, and then the effects of different cell treatment conditions on fibroblast apoptosis were detected. As shown in Figures 8A and 8B, AGE-BSA significantly increased the cell apoptosis rate. Quercetin effectively reversed the increase of cell apoptosis rate and caspase-3 expression induced by AGE-BSA (Figures 8A-8C). However, this antagonistic effect on AGEs of quercetin was weakened by inhibiting the expression of miR-4429 (Figures 8A and 8B). In addition, AGE-BSA upregulated the protein expression of PTEN, which were reversed by quercetin (Figures 8D and 8E). While downregulating the expression of miR-4429, quercetin did not inhibit the protein expression of PTEN. Similarly, quercetin elevated the protein expressions of PI3K and p-Akt that were downregulated under the exposure to AGEs in fibroblasts. And the antagonistic effect of quercetin was diminished by reducing the expression of miR-4429 (Figures 8F-8H).

4. Discussion

The effect of AGEs on fibroblasts has been reported mainly in diabetes mellitus and its complications. AGEs inhibited the proliferation of tendon fibroblasts, leading to tendon pain and degenerative changes (*31*). AGEs induced inflammation and overexpression of fibrotic genes, resulting in diabetic fibrosis (*32*). AGEs accumulation in skin resulted in collagen structural damages and fibroblast apoptosis, collagen degradation in diabetes non-healing wounds (*33*). However, the effects of AGEs on the behavior and function of pelvic floor fibroblasts are rarely studied. This study comprehensively explored the effects of AGEs on the behavior and function of pelvic floor fibroblasts and found that quercetin could antagonize the inhibitory effects of AGEs on the behavior and function of pelvic floor fibroblasts in terms of cell proliferation, apoptosis, oxidative stress, and ECM metabolism.

Firstly, the proliferation rates of fibroblasts were detected and there was no significant difference in proliferation ability between the POP and non-POP groups, which was consistent with a previous report (*34*). We found that quercetin antagonized the decrease in the proliferation rate of fibroblasts induced by AGEs. Studies on the influences of quercetin on fibroblasts suggest that quercetin may be applied in the treatment of rheumatoid arthritis and fibrotic diseases due to its anti-inflammatory and anti-fibrotic effects (*22,35*). In addition, quercetin delayed the senescence of human dermal fibroblasts induced by UV irradiation (*36*). However, the effect of quercetin on pelvic floor fibroblasts is rarely studied. And in the present study, we hypothesized that quercetin could antagonize AGEs-induced apoptosis and functional inhibition of fibroblasts from the prolapsed uterosacral ligament.

In this study, we found that AGEs increased the ROS levels in fibroblasts, while quercetin effectively alleviated this oxidative stress status. Oxidative stress was reported as a negative factor in the pathogenesis of POP, and the previous results showed that oxidative stress status existed in prolapsed tissues (*37,38*). Increased production and decreased elimination of intracellular ROS leads to oxidative stress, an imbalance between intracellular oxidants and antioxidants (*39*). The antioxidant effect of quercetin has been widely reported and quercetin prevented myocardial fibrosis and diabetic nephropathy by inhibiting ROS production (*18,40*).

The contractility of fibroblasts is crucial for regulating connective tissue remodeling during normal and pathological wound healing (*41*). Meyer *et al*. preliminarily demonstrated that myofibroblasts of vaginal wall tissue derived from POP had impaired contractile ability by cell-mediated collagen gel contractility assay, and their contractile ability decreased with age (*42*). Ruiz-Zapata *et al.* reported that the fibroblasts derived from the POP tissues exhibited delayed contractility compared with the normal fibroblasts (*6*). In our study, the contractility of fibroblasts from the POP group was inferior to that in the non-POP group, and AGEs treatment significantly damaged cell contractility in fibroblasts of the non-POP group. However, quercetin did not antagonize AGEs-induced contractility decrease in fibroblasts, suggesting quercetin did not influence the contractile-related molecules in fibroblasts.

Dysfunctions of fibroblasts lead to dysregulated metabolism of collagen, elastin, and other ECM-related genes, resulting in the damaged mechanical strength of pelvic connective tissues and contributing to the development of POP (*43*). The extracellular matrix proteins have been detected in human tissues such as the vaginal wall and the uterosacral ligament, and there were significant differences between the prolapsed and normal tissues, indicating that ECM alterations are correlated with POP (*44,45*). Considering that the formation and remodeling of ECM are regulated by fibroblasts, the related gene expressions of fibroblasts were quantified in this study.

The ECM of pelvic connective tissue is mainly consisted of the most abundant type I and III collagen that provide the primary tensile resistance to connective tissue. In the pathological alterations of POP, collagen was reported with a decreased content in POP. MMP1, as a kind of degrading enzyme of collagen was increased in POP, and reversely, TIMP1 as the inhibitor of MMP was decreased in POP (*46*). In this study, the collagen expression of the POP group was not significantly different from the non-POP group, which was different from the previous reports. The reason for the result may be that the fibroblasts were detached from the *in-vivo* environment with high AGEs concentration or the sample size in the experiment was too small. AGEs downregulated the expression of COL1 and TIMP1

but increased the expression of MMP1 in the POP group. This result coincides with our previous report (*16*), suggesting that AGEs decreased the expression of COL1 by increasing the degradation of COL1. The previous studies revealed that quercetin downregulated the expression of MMP2 and MMP9 to prevent fibrosis and contributed to wound healing (*47,48*). Our results suggested that quercetin antagonized AGEs-induced upregulation of MMP1 in fibroblasts.

Elastin is another important fibrous structural protein and constitutes the elastic fiber of ECM, allowing the pelvic floor connective tissue with high extensibility and passive retraction. The molecules including LOX, LOXL, FBLN, and FBNs are correlated with the composition of elastic fibers and the synthesis of elastin (*49*). Animal studies demonstrated that the knockout of *LOXL1*, *FBLN3*, and *FBLN5* resulted in rectal or vaginal prolapse in mice (*50*). However, few studies have focused on the influence of AGEs or quercetin on elastin metabolism in pelvic floor fibroblasts. Our results showed that the gene expressions of LOX, LOXL2, FBN2, and FBLN5 were reduced in fibroblasts from the POP group compared with the non-POP group, which was in line with the previous reports that the *FBLN5* knockout mice exhibited organ prolapse (*50*). AGEs treatment promoted the expressions of Elastin and FBLN5 in fibroblasts, while AGEs did not influence the expression of LOX, LOXL1, LOXL2, and FBN2. Quercetin promoted the expressions of LOX and FBN2, while inhibiting the expression of LOXL1, which means quercetin reduced the expression differences of *LOX*, *FBN2*, and *LOXL1* genes between the POP group and non-POP group. But quercetin had no significant effect on the expressions of Elastin and FBLN5 in POP fibroblasts induced by AGEs.

Confirming the antagonistic effects of quercetin on AGEs, we tried to understand the molecular process of the antagonism of quercetin on AGEs-induced fibroblast apoptosis. Our previous study indicated that AGEs induced fibroblast apoptosis by increasing the expression of PTEN (*17*). The expression of PTEN was post-transcriptionally regulated by miR-4429, and then the upregulation of PTEN did antagonize the PI3K/Akt pathway, which consequently increased cell apoptosis. In the current study, quercetin significantly antagonized the influences of AGEs on fibroblasts, including the upregulation of cell apoptosis and PTEN expression, and the downregulation of miR-4429, PI3K, and phosphorylated Akt expression. Furthermore, the antagonistic effects of quercetin on AGEs were neutralized by inhibiting the expression of miR-4429.

The limitation of our study is the lack of *in vivo* experiments to verify the effects and mechanism of quercetin in the treatment of POP. Humans are strictly biped, and the direction in which the pelvic organs are subjected to gravity differs from that of model animals commonly used in laboratories. Besides, vaginal delivery in humans causes more serious damage to pelvic floor structures than in other species. Therefore, we plan to test and select the most appropriate animal model to explore whether quercetin improves the functional damage of AGEs to fibroblasts *in vivo*, and further verify the molecular mechanism at the cellular level found in the present study.

In summary, quercetin antagonized AGE-induced apoptosis, proliferation inhibition, and ROS increase in fibroblasts, but not AGEs-induced contractile impairment in fibroblasts. Quercetin partially improved the expression disorder of ECM-related genes in fibroblasts induced by AGEs. Furthermore, quercetin reduced fibroblasts apoptosis in POP through reversing AGEs-induced downregulation of miR-4429, upregulation of PTEN, and downregulation of PI3K/Akt.

Acknowledgements

We gratefully acknowledge the assistance of Jing Zhou in preparing the manuscript.

Funding: This study was supported by Science and Technology Commission of Shanghai Municipality (grant no. 20Y11907300 and 21Y11906700 to YS Chen), the Scientific and Technological Innovation Action Plan of the Shanghai Natural Science Fund (grant no. 20ZR1409100 to L Wang), a project of the Chinese Association of Integration of Traditional and Western Medicine special foundation for Obstetrics and Gynecology-PuZheng Pharmaceutical Foundation (grant no. FCK-PZ-08 to L Wang), a project for hospital management of the Shanghai Hospital Association (grant no. X2021046 to L Wang), and a clinical trial project of the Special Foundation for Healthcare Research of the Shanghai Municipal Health Commission (grant no. 202150042 to L Wang).

Conflict of Interest: The authors have no conflicts of interest to disclose.

References

1. Pang H, Zhang L, Han S, Li Z, Gong J, Liu Q, Liu X, Wang J, Xia Z, Lang J, Xu T, Zhu L. A nationwide population-based survey on the prevalence and risk factors of symptomatic pelvic organ prolapse in adult women in China - a pelvic organ prolapse quantification system-based study. BJOG. 2021; 128:1313-1323.
2. Jelovsek JE, Maher C, Barber MD. Pelvic organ prolapse. Lancet. 2007; 369:1027-1038.
3. Lu Y, Chen HY, Wang XQ, Wang JX. Correlations between Mitofusin 2 expression in fibroblasts and pelvic organ prolapse: an *in vitro* study. Chin Med J (Engl). 2017; 130:2951-2959.
4. Li Y, Hong L, Liu C, Min J, Hong S, Hu M, Zhao Y, Yang Q, Tang J, He S. Effect of puerarin on collagen metabolism of fibroblasts in pelvic tissue of women with pelvic organ prolapse. Mol Med Rep. 2018; 17:2705-2711.
5. Kufaishi H, Alarab M, Drutz H, Lye S, Shynlova O.

Comparative characterization of vaginal cells derived from premenopausal women with and without severe pelvic organ prolapse. Reprod Sci. 2016; 23:931-943.
6. Ruiz-Zapata AM, Kerkhof MH, Zandieh-Doulabi B, Brölmann HA, Smit TH, Helder MN. Functional characteristics of vaginal fibroblastic cells from premenopausal women with pelvic organ prolapse. Mol Hum Reprod. 2014; 20:1135-1143.
7. Feng J, Li Y, Jin X, Gong R, Xia Z. ATF3 regulates oxidative stress and extracellular matrix degradation *via* p38/Nrf2 signaling pathway in pelvic organ prolapse. Tissue Cell. 2021; 73:101660.
8. Jing C, Zhang G, Liu Z, Xu Q, Li C, Cheng G, Shi R. Peroxidasin promotes diabetic vascular endothelial dysfunction induced by advanced glycation end products *via* NOX2/HOCl/Akt/eNOS pathway. Redox Biol. 2021; 45:102031.
9. Zhou Q, Cheng KW, Gong J, Li ETS, Wang M. Apigenin and its methylglyoxal-adduct inhibit advanced glycation end products-induced oxidative stress and inflammation in endothelial cells. Biochem Pharmacol. 2019; 166:231-241.
10. Gkogkolou P, Böhm M. Advanced glycation end products: Key players in skin aging? Dermatoendocrinol. 2012; 4:259-270.
11. Willett TL, Pasquale J, Grynpas MD. Collagen modifications in postmenopausal osteoporosis: advanced glycation endproducts may affect bone volume, structure and quality. Curr Osteoporos Rep. 2014; 12:329-337.
12. Jackson SR, Avery NC, Tarlton JF, Eckford SD, Abrams P, Bailey AJ. Changes in metabolism of collagen in genitourinary prolapse. Lancet. 1996; 347:1658-1661.
13. Chen Y, Huang J, Hu C, Hua K. Relationship of advanced glycation end products and their receptor to pelvic organ prolapse. Int J Clin Exp Pathol. 2015; 8:2288-2299.
14. Sferra R, Pompili S, D'Alfonso A, Sabetta G, Gaudio E, Carta G, Festuccia C, Colapietro A, Vetuschi A. Neurovascular alterations of muscularis propria in the human anterior vaginal wall in pelvic organ prolapse. J Anat. 2019; 235:281-288.
15. Vetuschi A, Pompili S, Gallone A, D'Alfonso A, Carbone MG, Carta G, Festuccia C, Gaudio E, Colapietro A, Sferra R. Immunolocalization of advanced glycation end products, mitogen activated protein kinases, and transforming growth factor-β/smads in pelvic organ prolapse. J Histochem Cytochem. 2018; 66:673-686.
16. Chen YS, Wang XJ, Feng W, Hua KQ. Advanced glycation end products decrease collagen I levels in fibroblasts from the vaginal wall of patients with POP *via* the RAGE, MAPK and NF-κB pathways. Int J Mol Med. 2017; 40:987-998.
17. Sima Y, Li L, Xiao C, Xu L, Wang L, Chen Y. Advanced glycation end products (AGEs) downregulate the miR-4429/PTEN axis to promote apoptosis of fibroblasts in pelvic organ prolapse. Ann Transl Med. 2022; 10:821.
18. Ding T, Wang S, Zhang X, Zai W, Fan J, Chen W, Bian Q, Luan J, Shen Y, Zhang Y, Ju D, Mei X. Kidney protection effects of dihydroquercetin on diabetic nephropathy through suppressing ROS and NLRP3 inflammasome. Phytomedicine. 2018; 41:45-53.
19. Ferenczyova K, Kalocayova B, Bartekova M. Potential implications of quercetin and its derivatives in cardioprotection. Int J Mol Sci. 2020; 21:1585.
20. Smith MJ, Fowler M, Naftalin RJ, Siow RCM. UVA irradiation increases ferrous iron release from human skin fibroblast and endothelial cell ferritin: Consequences for cell senescence and aging. Free Radic Biol Med. 2020; 155:49-57.
21. Li C, Shen Y, Huang L, Liu C, Wang J. Senolytic therapy ameliorates renal fibrosis postacute kidney injury by alleviating renal senescence. FASEB J. 2021; 35:e21229.
22. Hohmann MS, Habiel DM, Coelho AL, Verri WA, Jr., Hogaboam CM. Quercetin enhances ligand-induced apoptosis in senescent idiopathic pulmonary fibrosis fibroblasts and reduces lung fibrosis *in vivo*. Am J Respir Cell Mol Biol. 2019; 60:28-40.
23. Huang L, Zhao Z, Wen J, Ling W, Miao Y, Wu J. Cellular senescence: A pathogenic mechanism of pelvic organ prolapse (Review). Mol Med Rep. 2020; 22:2155-2162.
24. Marcu RD, Mischianu DLD, Iorga L, Diaconu CC, Surcel M, Munteanu AN, Constantin C, Isvoranu G, Bratu OG. Oxidative stress: A possible trigger for pelvic organ prolapse. J Immunol Res. 2020; 2020:3791934.
25. Bhuiyan MN, Mitsuhashi S, Sigetomi K, Ubukata M. Quercetin inhibits advanced glycation end product formation *via* chelating metal ions, trapping methylglyoxal, and trapping reactive oxygen species. Biosci Biotechnol Biochem. 2017; 81:882-890.
26. Shimoda H, Nakamura S, Morioka M, Tanaka J, Matsuda H, Yoshikawa M. Effect of cinnamoyl and flavonol glucosides derived from cherry blossom flowers on the production of advanced glycation end products (AGEs) and AGE-induced fibroblast apoptosis. Phytother Res. 2011; 25:1328-1335.
27. Yang S, Wang G, Ma ZF, Qin LQ, Zhai YJ, Yu ZL, Xue M, Zhang YH, Wan Z. Dietary advanced glycation end products-induced cognitive impairment in aged ICR mice: protective role of quercetin. Mol Nutr Food Res. 2020; 64:e1901019.
28. Madhu C, Swift S, Moloney-Geany S, Drake MJ. How to use the pelvic organ prolapse quantification (POP-Q) system? Neurourol Urodyn. 2018; 37:S39-s43.
29. Bump RC, Mattiasson A, Bø K, Brubaker LP, DeLancey JO, Klarskov P, Shull BL, Smith AR. The standardization of terminology of female pelvic organ prolapse and pelvic floor dysfunction. Am J Obstet Gynecol. 1996; 175:10-17.
30. Renthal NE, Chen CC, Williams KC, Gerard RD, Prange-Kiel J, Mendelson CR. miR-200 family and targets, ZEB1 and ZEB2, modulate uterine quiescence and contractility during pregnancy and labor. Proc Natl Acad Sci U S A. 2010; 107:20828-20833.
31. Patel SH, Yue F, Saw SK, Foguth R, Cannon JR, Shannahan JH, Kuang S, Sabbaghi A, Carroll CC. Advanced glycation end-products suppress mitochondrial function and proliferative capacity of achilles tendon-derived fibroblasts. Sci Rep. 2019; 9:12614.
32. Tuleta I, Frangogiannis NG. Diabetic fibrosis. Biochim Biophys Acta Mol Basis Dis. 2021; 1867:166044.
33. Qing C. The molecular biology in wound healing & non-healing wound. Chin J Traumatol. 2017; 20:189-193.
34. Sun B, Zhou L, Wen Y, Wang C, Baer TM, Pera RR, Chen B. Proliferative behavior of vaginal fibroblasts from women with pelvic organ prolapse. Eur J Obstet Gynecol Reprod Biol. 2014; 183:1-4.
35. Sun HT, Li JP, Qian WQ, Yin MF, Yin H, Huang GC. Quercetin suppresses inflammatory cytokine production in rheumatoid arthritis fibroblast-like synoviocytes. Exp Ther Med. 2021; 22:1260.
36. Zou Z, Long X, Zhao Q, *et al*. A single-cell transcriptomic

atlas of human skin aging. Dev Cell. 2021; 56:383-397. e388.
37. Kim EJ, Chung N, Park SH, Lee KH, Kim SW, Kim JY, Bai SW, Jeon MJ. Involvement of oxidative stress and mitochondrial apoptosis in the pathogenesis of pelvic organ prolapse. J Urol. 2013; 189:588-594.
38. Liu C, Yang Q, Fang G, Li BS, Wu DB, Guo WJ, Hong SS, Hong L. Collagen metabolic disorder induced by oxidative stress in human uterosacral ligament-derived fibroblasts: A possible pathophysiological mechanism in pelvic organ prolapse. Mol Med Rep. 2016; 13:2999-3008.
39. Valko M, Leibfritz D, Moncol J, Cronin MT, Mazur M, Telser J. Free radicals and antioxidants in normal physiological functions and human disease. Int J Biochem Cell Biol. 2007; 39:44-84.
40. Min Z, Yangchun L, Yuquan W, Changying Z. Quercetin inhibition of myocardial fibrosis through regulating MAPK signaling pathway *via* ROS. Pak J Pharm Sci. 2019; 32:1355-1359.
41. Tomasek JJ, Gabbiani G, Hinz B, Chaponnier C, Brown RA. Myofibroblasts and mechano-regulation of connective tissue remodelling. Nat Rev Mol Cell Biol. 2002; 3:349-363.
42. Meyer S, Achtari C, Hohlfeld P, Juillerat-Jeanneret L. The contractile properties of vaginal myofibroblasts: is the myofibroblasts contraction force test a valuable indication of future prolapse development? Int Urogynecol J Pelvic Floor Dysfunct. 2008; 19:1399-1403.
43. Zhu Y, Li L, Xie T, Guo T, Zhu L, Sun Z. Mechanical stress influences the morphology and function of human uterosacral ligament fibroblasts and activates the p38 MAPK pathway. Int Urogynecol J. 2022; 33:2203-2212.
44. Zhu YP, Xie T, Guo T, Sun ZJ, Zhu L, Lang JH. Evaluation of extracellular matrix protein expression and apoptosis in the uterosacral ligaments of patients with or without pelvic organ prolapse. Int Urogynecol J. 2021; 32:2273-2281.
45. Eser A, Unlubilgin E, Hizli F, Acar M, Kamalak Z, Kosus A, Kosus N, Hizli D, Gunduz E. Is there a relationship between pelvic organ prolapse and tissue fibrillin-1 levels? Int Neurourol J. 2015; 19:164-170.
46. Hu Y, Wu R, Li H, Gu Y, Wei W. Expression and significance of metalloproteinase and collagen in vaginal wall tissues of patients with pelvic organ prolapse. Ann Clin Lab Sci. 2017; 47:698-705.
47. Yoon JS, Chae MK, Jang SY, Lee SY, Lee EJ. Antifibrotic effects of quercetin in primary orbital fibroblasts and orbital fat tissue cultures of Graves' orbitopathy. Invest Ophthalmol Vis Sci. 2012; 53:5921-5929.
48. Kant V, Jangir BL, Sharma M, Kumar V, Joshi VG. Topical application of quercetin improves wound repair and regeneration in diabetic rats. Immunopharmacol Immunotoxicol. 2021; 43:536-553.
49. Theocharis AD, Skandalis SS, Gialeli C, Karamanos NK. Extracellular matrix structure. Adv Drug Deliv Rev. 2016; 97:4-27.
50. Allen-Brady K, Bortolini MAT, Damaser MS. Mouse knockout models for pelvic organ prolapse: a systematic review. Int Urogynecol J. 2022; 33:1765-1788.

Received July 11, 2023; Revised November 15, 2023; Accepted November 26, 2023.

[§]These authors contributed equally to this work.

*Address correspondence to:
Yisong Chen, Department of Gynecology, Obstetrics and Gynecology Hospital of Fudan University, 419 Fangxie Road, Shanghai, China.
E-mail: cys373900207@163.com

Ling Wang, Laboratory for Reproductive Immunology, Obstetrics and Gynecology Hospital of Fudan University, 419 Fangxie Road, Shanghai, China.
E-mail: Dr.wangling@fudan.edu.cn

Released online in J-STAGE as advance publication December 3, 2023.

Brief Report

DOI: 10.5582/ddt.2023.01074

Development of a simple high-performance liquid chromatography-ultraviolet detection method for olaparib in patients with ovarian cancer

Takeo Yasu[1,2,5,*], Ryosuke Nishijima[1], Risa Ikuta[3,5], Mikio Shirota[2,5], Haruko Iwase[4,5]

[1] Department of Medicinal Therapy Research, Pharmaceutical Education and Research Center, Meiji Pharmaceutical University, Tokyo, Japan;
[2] Department of Pharmacy, Tokyo Metropolitan Bokutoh Hospital, Tokyo, Japan;
[3] Department of Clinical Laboratory, Tokyo Metropolitan Bokutoh Hospital, Tokyo, Japan;
[4] Department of Obstetrics and Gynecology, Tokyo Metropolitan Bokutoh Hospital, Tokyo, Japan;
[5] Bokutoh Hospital-Meiji Pharmaceutical University Joint Research Center, Tokyo, Japan.

SUMMARY Olaparib is a small-molecule inhibitor of poly(ADP)-ribose polymerase (PARP) used as maintenance therapy for recurrent ovarian cancer and newly diagnosed advanced ovarian cancer after initial chemotherapy. An exposure-toxicity correlation has been reported between the probability of anemia, a common adverse event associated with olaparib, and the steady-state minimum plasma concentration (Cmin) as well as the predicted maximum plasma concentration (Cmax). On the other hand, olaparib exhibits high interpatient variability with regard to the area under the concentration-time curve, Cmax, and Cmin. Therefore, we developed a simple and sensitive assay based on high-performance liquid chromatography with ultraviolet light (HPLC-UV) for the therapeutic drug monitoring of olaparib. The analysis was performed on an octadecylsilyl column with a mobile phase consisting of 0.5% KH_2PO_4 (pH 4.5) and acetonitrile (71:29, v/v), at a flow rate of 0.8 mL/min. Olaparib and an internal standard (imatinib) were well separated from the co-extracted material, with retention times of 13.6 and 11.5 min, respectively. The calibration curve for olaparib showed linearity over the concentration range of 0.10-10.0 μg/mL ($r^2 = 0.9998$). The intra- and inter-day validation coefficients ranged from 1.79 to 4.13% and 1.37 to 3.55%, respectively. Measurement accuracy ranged from − 6.07 to 3.26%, with a recovery rate of more than 91.06%. The developed method was then applied to evaluate the plasma olaparib concentrations in patients with ovarian cancer. Our findings demonstrate that HPLC-UV is an economical, simple, and sensitive method for clinical application and holds promise for the effective drug monitoring of olaparib during ovarian cancer treatment.

Keywords olaparib, PARP inhibitor, HPLC-UV, therapeutic drug monitoring, ovarian cancer

1. Introduction

Ovarian cancer has a poor prognosis, as approximately 70% of the patients with newly diagnosed advanced disease who undergo surgery and platinum-based chemotherapy relapse within the next three years (*1*). Olaparib is an oral, small-molecule inhibitor of poly(ADP)-ribose polymerase (PARP) used as maintenance therapy in patients with platinum-sensitive ovarian cancer who are being treated for relapse as well as after response to initial chemotherapy in patients with advanced ovarian cancer harboring mutations in the breast cancer susceptibility (*BRCA1/2*) genes. Olaparib is the new standard of care for ovarian cancer, leading to prolonged progression-free survival, and is administered orally as a 300 mg tablet twice daily.

In the SOLO-1 trial, which evaluated the efficacy of olaparib maintenance therapy after platinum- and taxane-based chemotherapy regimens, olaparib maintenance therapy reduced the risk of disease progression or death by 70% compared to the placebo (hazard ratio for disease progression or death, 0.30; 95% confidence interval, 0.23-0.41) (*2*). The excellent results of the SOLO-1 trial were limited to patients who could receive 300 mg olaparib twice daily for 2 years as a maintenance therapy. However, discontinuation due to adverse events was reported in 12% of patients in the SOLO-1 trial, with a dose reduction rate of 28% and a

discontinuation rate of 52%. The most common adverse events that led to discontinuation were anemia and nausea. Moreover, an exposure-toxicity relationship has been demonstrated between the probability of anemia and the minimum steady-state concentration as well as the predicted Cmax of olaparib (*3*).

A trough concentration of 2.5 μg/mL has been reported as the threshold for olaparib dose adjustment (*4*). However, it is unclear whether olaparib exposure is associated with efficacy (*5*). To date, the effective therapeutic range of olaparib has not been determined, with high interpatient variabilities of 50%, 39%, and 87% in the area under the concentration-time curve (AUC), maximum plasma concentration (Cmax), and minimum plasma concentration (Cmin), respectively, as determined using a population pharmacokinetic model (*3*). Many factors are thought to significantly affect olaparib exposure, with food shown to delay olaparib absorption, resulting in a significant decrease in Cmax, while the impact on AUC is only marginal (*6*). Furthermore, olaparib is primarily metabolized *via* cytochrome P450 (CYP) 3A, and thus, the concurrent administration of potent CYP3A inhibitors or inducers affects olaparib concentrations (*7*). High olaparib concentrations are associated with impaired renal function, necessitating the careful consideration of blood olaparib levels (*8*). Thus, the therapeutic drug monitoring (TDM) of olaparib in patients receiving the drug is essential.

To date, olaparib concentrations in the human plasma have only been determined using liquid chromatography-tandem mass spectrometry (LC-MS/MS) (*9-14*). LC-MS/MS is expensive; thus, it is available only at a limited number of facilities. Meanwhile, high-performance liquid chromatography-ultraviolet (HPLC-UV) instruments remain popular, owing to their low initial cost and high utility in general hospitals. In light of this, we developed a simple HPLC-UV method to determine olaparib concentrations in patients with ovarian cancer, suitable for routine TDM in clinical practice.

2. Materials and Methods

2.1. Standards and reagents

Olaparib and imatinib were acquired from Toronto Research Chemicals Inc. (Ontario, Canada). The mobile phases comprised HPLC-grade acetonitrile, methanol, water (Kanto Chemical Co., Inc., Tokyo, Japan), and KH_2PO_4 (Wako, Osaka, Japan).

2.2. Chromatographic conditions

The HPLC system consisted of a pump (PU-4180; Jasco, Tokyo, Japan), UV detector (UV-4075; Jasco, Tokyo, Japan), and autosampler (AS-4550; Jasco, Tokyo, Japan). Analysis was performed using an octadecylsilyl column (Capcell Pak C18 MG II; 250 mm × 4.6 mm; i.d., 5 μm; Osaka Soda, Tokyo, Japan). The detection wavelength was 218 nm. The mobile phase consisted of 0.5% KH_2PO_4 (pH 4.5) and acetonitrile (71:29, v/v), which was eluted at a flow rate of 0.8 mL/min. The injection volume for HPLC analysis was 30 μL.

2.3. Calibration curve and quality control samples

Stock solutions of 1 mg/mL olaparib and imatinib were prepared in methanol. For the calibration curve, fresh blank plasma was spiked with the olaparib stock solution to obtain final concentrations of 0.1, 0.5, 1.0, 2.5, 5.0, and 10.0 μg/mL. The olaparib stock solution was diluted in methanol to obtain working solutions of 0.5, 2.5, 5, 12.5, 25.0, and 50.0 μg/mL. Imatinib was diluted in methanol to obtain a working solution of 10 μg/mL. Subsequently, the prepared stock and working solutions were stored at −60°C in the dark until use.

2.4. Sample preparation

Plasma (50 μL) was pipetted into a 2.0 mL microtube. Thereafter, 10 μL of the olaparib working solution was vortexed with 50 μL of the plasma in a 2.0 mL microtube for 10 s. Subsequently, 60 μL of olaparib-spiked plasma, 10 μL of the internal standard (IS; 10 μg/mL imatinib), and 330 μL of methanol chilled to −60°C were added. The mixture was then vortexed for 1 min and centrifuged at 15,000 ×*g* for 10 min at 4°C. Finally, the resulting supernatant was transferred to an HPLC autosampler vial, and 30 μL was injected into the HPLC system.

2.5. Method validation

Method validation was based on the Guidelines for the Validation of Methods for the Quantitative Analysis of Biological Samples by the US Food and Drug Administration (FDA) (*15*). The calibration concentrations of olaparib ranged from 0.1 to 10.0 μg/mL; the recovery and accuracy of the assay were determined at these concentrations. Assay precision was evaluated by analyzing five sets of control samples on the same day (intra-day) and five different days (inter-day) at concentrations of 0.1, 0.5, 1.0, 2.5, 5.0, and 10.0 μg/mL.

The stability of olaparib in plasma samples was assessed at three different concentrations (0.1, 1.0, and 10.0 μg/mL). To establish benchtop stability, five samples (n = 5) stored at 25°C for 6 h were evaluated. Processed sample stability was evaluated by storing five samples (n = 5) at 4°C for 24 h. To determine long-term stability, five samples (n = 5) were stored at −60°C for one month and three months and then assessed. Finally,

freeze-thaw stability was determined by subjecting five samples (n = 5) to three cycles of freezing at −60°C and thawing.

2.6. Clinical application

Blood samples were collected after obtaining written informed consent from patients receiving olaparib. Plasma samples were obtained by centrifuging the blood samples at 3,000× g for 5.5 min. Plasma and serum were stored at − 80°C until analysis. This study was approved by the institutional review board of Tokyo Metropolitan Bokutoh Hospital (#04–127) and conducted in accordance with the Declaration of Helsinki. Concomitant medications used in the five patients receiving olaparib were magnesium oxide, rosuvastatin calcium, loxoprofen sodium hydrate, pemafibrate, teprenone, montelukast sodium, dextromethorphan hydrobromide hydrate, ambroxol hydrobromide, tenofovir alafenamide fumarate, candesartan cilexetil, calcium sennoside A and B, anastrozole, duloxetine hydrochloride, lorazepam, metoclopramide hydrochloride, trazodone hydrochloride, zolpidem tartrate, and daikenchueto, which did not interfere with the assay.

3. Results and Discussion

In the present study, we introduce a simple and sensitive HPLC-UV method for quantifying plasma olaparib concentrations in clinical settings. Figure 1A presents the chromatogram of the blank plasma sample. Figures 1B and 1C show the representative chromatograms of plasma samples containing 0.10 μg/mL and 1.0 μg/mL of olaparib, respectively. The background of the treated blank plasma sample was clean at the olaparib and IS imatinib peak positions, with no interference from spurious peaks. Olaparib and the IS were well separated from the co-extracted materials under the chromatographic conditions, with retention times of 13.6 and 11.5 min, respectively. The six-point olaparib standard calibration curve exhibited linearity across the concentration range of 0.10-10.0 μg/mL (r^2 = 0.9998). The limits of detection and quantification for olaparib were 0.025 μg/mL and 0.10 μg/mL, respectively. The recovery rate of olaparib exceeded 91.06%. Considering this concentration range, the intra- and inter-day CVs ranged at 1.79-4.13% and 1.37-3.55%, respectively (Table 1). The assay accuracy ranged at − 6.07-3.26%.

The plasma stability of olaparib was also assessed under various conditions (Table 2). No significant olaparib degradation was observed, and final concentrations were maintained within 93.0-111.8% of the theoretical values. No interference from olaparib or the IS was observed for the endogenous substances in the blank plasma. The precision and accuracy of the intra- and inter-assay variability and stability under diverse conditions were in accordance with the guidelines outlined by the FDA (*15*). To the best of our knowledge, this is the first study to combine a liquid-liquid extraction pretreatment method with isocratic gradient elution and UV detection to achieve effective olaparib TDM.

Previously reported methods for measuring olaparib levels in human plasma samples were exclusively LC-MS/MS-based (*9-14*). However, owing to the high cost of the equipment required, it is difficult to adopt these methods in resource-limited areas. The advantage of the HPLC-UV method presented herein is that it can be

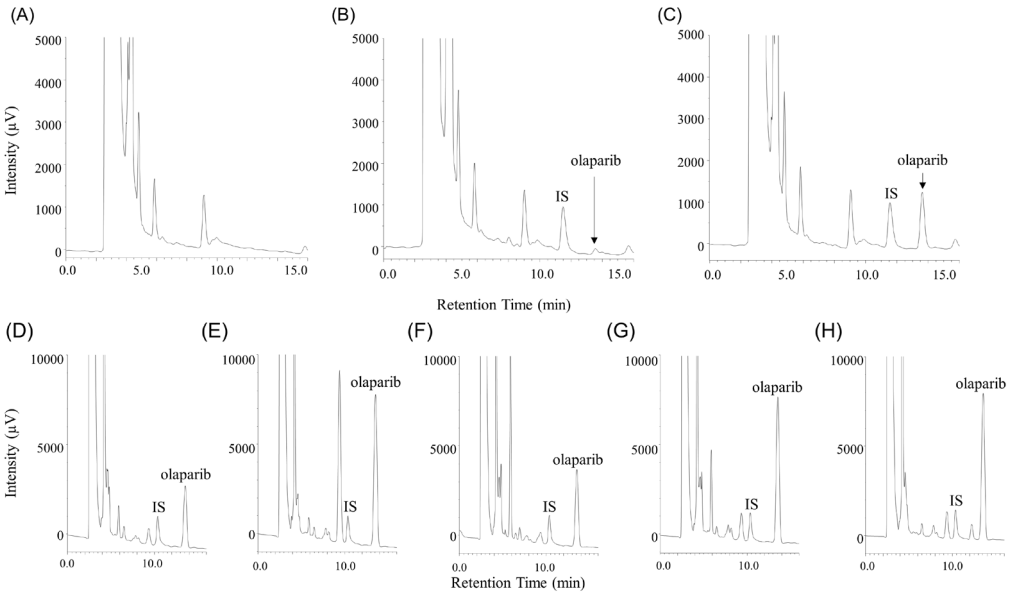

Figure 1. Chromatograms of the (A) blank plasma sample, (B) plasma sample containing 0.1 μg/mL olaparib, (C) plasma sample containing 1.0 μg/mL olaparib, and (D, E, F, G, H) those of the five patients included in this study.

Table 1. Intra-day and inter-day accuracy and precision of olaparib concentrations

Olaparib added (μg/mL)	Intra-day (n = 5)			Intra-day (n = 5)			Recovery (%)
	Mean ± SD (μg/mL)	CV (%)	Accuracy (%)	Mean ± SD (μg/mL)	CV (%)	Accuracy (%)	
0.1	0.09 ± 0.00	2.51	-6.07	0.10 ± 0.00	3.49	-1.07	100.64
0.5	0.49 ± 0.01	1.79	-2.06	0.50 ± 0.02	3.55	0.42	96.54
1.0	0.98 ± 0.03	3.36	-1.68	1.01 ± 0.01	1.37	0.71	94.54
2.5	2.53 ± 0.06	2.55	1.05	2.50 ± 0.08	2.99	0.13	94.92
5.0	5.16 ± 0.13	2.42	3.26	5.03 ± 0.10	2.05	0.51	91.06
10.0	10.13 ± 0.42	4.13	1.27	10.07 ± 0.29	2.83	0.67	92.78

CV, coefficient of variation; SD, standard deviation.

Table 2. Stability analyses under various conditions (n = 5)

Olaparib added (μg/mL)	Stability condition (%)				
	Benchtop mean ± SD	Processed sample mean ± SD	1 month mean ± SD	Long-term 3 months mean ± SD	Freeze-and-thaw mean ± SD
0.1	106.8 ± 1.2	111.8 ± 0.7	97.5 ± 1.6	97.4 ± 3.0	93.0 ± 3.3
1.0	99.6 ± 1.6	99.1 ± 1.8	100.0 ± 0.8	93.5 ± 1.3	98.1 ± 2.6
10.0	105.0 ± 0.7	100.4 ± 2.4	100.7 ± 1.3	94.5 ± 0.1	99.7 ± 0.6

SD, standard deviation.

easily transferred from one system to another. This is the most important feature when applying an existing method from the literature to the laboratory. In the past, a method for measuring olaparib levels in human plasma *via* HPLC using fluorescence detection has been reported (*16*). However, our method was the first to measure olaparib levels in human plasma using HPLC-UV. Our HPLC-UV-based method for determining olaparib plasma concentrations was established based on less-demanding techniques: liquid-liquid extraction and isocratic elution. The accessible equipment and simpler operation reduce laboratory and labor costs, making this method particularly suitable for resource-poor countries and regions.

The concomitant medications used by the five patients receiving olaparib in the current study included magnesium oxide, rosuvastatin calcium, loxoprofen sodium hydrate, pemafibrate, teprenone, montelukast sodium, dextromethorphan hydrobromide hydrate, ambroxol hydrobromide, tenofovir alafenamide fumarate, candesartan cilexetil, calcium sennoside, anastrozole, duloxetine hydrochloride, lorazepam, metoclopramide hydrochloride trazodone hydrochloride, zolpidem tartrate, and daikenchueto. No interference from these concomitant medications was noted in the chromatograms of olaparib and the IS (Figures 1D, 1E, 1F, 1G and 1H). Thus, our method achieved good olaparib extraction and avoided disturbance by plasma constituents and concomitant medications. Admittedly, this HPLC-UV method cannot achieve the same level of sensitivity as mass spectrometry-based methods. Nevertheless, the plasma olaparib concentrations of patients receiving maintenance therapy were all within the detection range of this method, highlighting its clinical applicability. It should be noted, however, that we evaluated only five patients. Therefore, we plan to validate the accuracy of our method in a larger cohort of patients.

Table 3. Plasma concentrations of olaparib in patients with ovarian cancer

Patient number	Daily dose	Plasma concentration	Timing of blood sampling after olaparib administration
1	300 mg twice daily	2.47 μg/mL	6 h
2	300 mg twice daily	6.38 μg/mL	3 h
3	200 mg twice daily	3.11 μg/mL	2 h
4	300 mg twice daily	5.98 μg/mL	3 h
5	300 mg twice daily	5.90 μg/mL	3 h

Olaparib plasma concentrations were evaluated in samples collected from five female patients diagnosed with ovarian cancer and undergoing maintenance therapy with olaparib. The mean olaparib plasma concentration was 4.77 μg/mL (range, 2.47-6.38 μg/mL) (Table 3). Olaparib reached a steady state after approximately 3-4 days and the Cmax was reached within 1-3 h after oral administration. As the Cmax had high inter-individual variability, determining the minimum concentration before a subsequent dose of the drug may be of great clinical value. We believe that monitoring trough concentrations is clinically appropriate when performing TDM of olaparib. However, this study aimed to determine whether our assay could accurately measure olaparib levels in patient samples. Therefore, we collected blood samples from patients during their outpatient visits, which allowed us to collect samples 2-6 h after olaparib administration. Patients 2, 3, 4, and 5 had samples collected 2 and 3 h after administration, and these samples were recorded as the Cmax. The mean Cmax for olaparib 300 mg

twice daily was previously reported to be 7.6 μg/mL in patients with ovarian cancer, breast cancer, and other types of solid tumors (*16*). In our study, patients 2, 4, and 5, who received olaparib 300 mg twice daily, had a lower mean Cmax, 6.09 μg/mL. One possible reason for this lower Cmax in our case was that, in previous reports (*17*), the Cmax was measured in solid tumors other than ovarian cancer. Currently, the indications of olaparib have been extended to breast, pancreatic, and prostate cancer (*18*). In the future, we hope that the assay presented herein may be used to determine the Cmax and Cmin in patients with each of these cancer types, which would facilitate the assessment of differences between tumors. In the present study, Patient 2 experienced nausea and headache, which led to the temporary discontinuation of olaparib. After resuming therapy, the Cmax determined on day 34 was 6.38 μg/mL, with an estimated trough concentration of approximately 3.0 μg/mL, greater than the threshold for dose adjustment of 2.5 μg/mL (*4*).

In conclusion, we developed a cost-effective, simple, and sensitive HPLC-UV method for measuring plasma olaparib concentrations in the clinical setting. Successful application of this assay to patient blood samples demonstrated its reliability. Further studies using this assay are required to clarify the relationship between the blood levels of olaparib and its clinical efficacy and safety.

Acknowledgements

This research was funded by the Japan Society for the Promotion of Science (JSPS) KAKENHI [grant number JP20K16095].

Funding: None.

Conflict of Interest: The authors have no conflicts of interest to disclose.

References

1. Ledermann JA, Raja FA, Fotopoulou C, Gonzalez-Martin A, Colombo N, Sessa C; ESMO Guidelines Working Group. Newly diagnosed and relapsed epithelial ovarian carcinoma: ESMO Clinical Practice Guidelines for diagnosis, treatment and follow-up. Ann Oncol. 2013; 24 Suppl 6:vi24-32.
2. Moore K, Colombo N, Scambia G, *et al*. Maintenance olaparib in patients with newly diagnosed advanced ovarian cancer. N Engl J Med. 2018; 379:2495-2505.
3. US Food and Drug Administration (FDA). Center for drug evaluation and research-clinical pharmacology and biopharmaceutics review(s), Olaparib. 2014. *https://www.accessdata.fda.gov/drugsatfda_docs/nda/2014/206162Orig1s000ClinPharmR.pdf* (accessed August 1, 2023).
4. Velev M, Puszkiel A, Blanchet B, *et al*. Association between olaparib exposure and early toxicity in BRCA-mutated ovarian cancer patients: Results from a retrospective multicenter study. Pharmaceuticals (Basel). 2021; 14:804.
5. Mohmaed Ali MI, Bruin MAC, Dezentjé VO, Beijnen JH, Steeghs N, Huitema ADR. Exposure-response analyses of olaparib in real-life patients with ovarian cancer. Pharm Res. 2023; 40:1239-1247.
6. Plummer R, Swaisland H, Leunen K, van Herpen CM, Jerusalem G, De Grève J, Lolkema MP, Soetekouw P, Mau-Sørensen M, Nielsen D, Spicer J, Fielding A, So K, Bannister W, Molife LR. Olaparib tablet formulation: effect of food on the pharmacokinetics after oral dosing in patients with advanced solid tumours. Cancer Chemother Pharmacol. 2015; 76:723-729.
7. Pilla Reddy V, Bui K, Scarfe G, Zhou D, Learoyd M. Physiologically based pharmacokinetic modeling for olaparib dosing recommendations: Bridging formulations, drug interactions, and patient populations. Clin Pharmacol Ther. 2019; 105:229-241.
8. Rolfo C, de Vos-Geelen J, Isambert N, *et al*. Pharmacokinetics and safety of olaparib in patients with advanced solid tumours and renal impairment. Clin Pharmacokinet. 2019; 58:1165-1174.
9. Nijenhuis CM, Lucas L, Rosing H, Schellens JHM, Beijnen JH. Development and validation of a high-performance liquid chromatography-tandem mass spectrometry assay quantifying olaparib in human plasma. J Chromatogr B Analyt Technol Biomed Life Sci. 2013; 940:121-125.
10. Jolibois J, Schmitt A, Royer B. A simple and fast LC-MS/MS method for the routine measurement of cabozantinib, olaparib, palbociclib, pazopanib, sorafenib, sunitinib and its main active metabolite in human plasma. J Chromatogr B Analyt Technol Biomed Life Sci. 2019; 1132:121844.
11. Bruin MAC, de Vries N, Lucas L, Rosing H, Huitema ADR, Beijnen JH. Development and validation of an integrated LC-MS/MS assay for therapeutic drug monitoring of five PARP-inhibitors. J Chromatogr B Analyt Technol Biomed Life Sci. 2020; 1138:121925.
12. Morosi L, Matteo C, Ceruti T, Giordano S, Ponzo M, Frapolli R, Zucchetti M, Davoli E, D'Incalci M, Ubezio P. Quantitative determination of niraparib and olaparib tumor distribution by mass spectrometry imaging. Int J Biol Sci. 2020; 16:1363-1375.
13. Krens SD, van der Meulen E, Jansman FGA, Burger DM, van Erp NP. Quantification of cobimetinib, cabozantinib, dabrafenib, niraparib, olaparib, vemurafenib, regorafenib and its metabolite regorafenib M2 in human plasma by UPLC-MS/MS. Biomed Chromatogr. 2020; 34:e4758.
14. Canil G, Orleni M, Posocco B, Gagno S, Bignucolo A, Montico M, Roncato R, Corsetti S, Bartoletti M, Toffoli G. LC-MS/MS method for the quantification of PARP inhibitors olaparib, rucaparib and niraparib in human plasma and dried blood spot: Development, validation and clinical validation for therapeutic drug monitoring. Pharmaceutics. 2023; 15:1524.
15. US DHHS, FDA, CDER, CVM. Guidance for Industry: Bioanalytical method validation. US Department of Health and Human Services, Food and Drug Administration, Center for Drug Evaluation and Research and Center for Veterinary Medicine, Rockville, MD, 2018.
16. Darwish IA, Khalil NY. Development and comparative evaluation of two different label-free and sensitive

fluorescence platforms for analysis of olaparib: A recently FDA-approved drug for the treatment of ovarian and breast cancer. Molecules. 2023; 28:6524.
17. Zhou D, Li J, Learoyd M, Bui K, Berges A, Milenkova T, Al-Huniti N, Tomkinson H, Xu H. Efficacy and safety exposure-response analyses of olaparib capsule and tablet formulations in oncology patients. Clin Pharmacol Ther. 2019; 105:1492-1500.
18. US Food and Drug Administration (FDA). LYNPARZA (olaparib) tablets, for oral use. Prescribing information. *https://www.accessdata.fda.gov/drugsatfda_docs/label/2020/208558s014lbl.pdf* (accessed August 1, 2023).

Received September 20, 2023; Revised November 24, 2023; Accepted November 26, 2023.

**Address correspondence to:*
Takeo Yasu, Department of Medicinal Therapy Research, Pharmaceutical Education and Research Center, Meiji Pharmaceutical University; 2-522-1, Noshio, Kiyose, Tokyo 204-8588, Japan.
E-mail: yasutakeo-tky@umin.ac.jp

Released online in J-STAGE as advance publication December 3, 2023.

Brief Report

DOI: 10.5582/ddt.2023.01083

Evaluation of D-amino acid oxidase activity in rat kidney using a D-kynurenine derivative, 6-methylthio-D-kynurenine: An *in vivo* microdialysis study

Takeshi Fukushima*, Ayano Kansaku, Maho Umino, Tatsuya Sakamoto, Mayu Onozato

Department of Analytical Chemistry, Faculty of Pharmaceutical Sciences, Toho University, Chiba, Japan.

SUMMARY D-Amino acid oxidase (DAO), a D-amino acid metabolizing enzyme, is reportedly associated with the psychiatric disease schizophrenia, suggesting a role for DAO inhibitors in its treatment. We have previously reported that DAO catalyzes the conversion of nonfluorescent 6-methylthio-D-kynurenine (MeS-D-KYN) to fluorescent 5-methylthiokynurenic acid (MeS-KYNA) *in vitro*. The present study aimed to determine the potential of MeS-D-KYN in evaluating DAO activity *in vivo* using renal microdialysis technique in rats. Male Sprague-Dawley rats were subjected to linear microdialysis probe implantation in the left kidney. Continuous perfusion of MeS-D-KYN was maintained, and DAO activity in the kidney cortex was evaluated by measuring the MeS-KYNA content in the microdialysate. The microdialysate was collected every 30 min and analyzed by high-performance liquid chromatography with fluorescence detection, monitored at 450 nm with an excitation wavelength of 364 nm. A significant production of MeS-KYNA was observed during, but not before, infusion of MeS-D-KYN, indicating that this compound is not endogenous. MeS-KYNA production was suppressed by the co-infusion of DAO inhibitor, 5-chlorobenzo[*d*]isoxazol-3-ol (CBIO), suggesting that MeS-D-KYN was converted to MeS-KYNA by renal DAO. Moreover, oral administration of CBIO effectively suppressed DAO activity in a dose-dependent manner. DAO converted MeS-D-KYN to MeS-KYNA *in vivo*, suggesting the potential of this compound in evaluating DAO activity. The use of the renal microdialysis technique developed in this study facilitates the monitoring of DAO activity in live experimental animals.

Keywords 6-methylthio-D-kynurenine, microdialysis, D-amino acid oxidase, rat kidney

1. Introduction

D-Amino acid oxidase (DAO; EC.1.4.3.3), an enzyme that metabolizes endogenous D-amino acids, especially D-serine, has been reported to be associated with schizophrenia (*1-3*). DAO activity was reportedly increased in the postmortem cortex of patients with schizophrenia (*3*), suggesting that identification of a DAO activity inhibitor might lead to the development of novel therapeutics for schizophrenia (*4*).

The general, conventional assay for the evaluation of DAO activity requires a two-step reaction system consisting of an enzyme reaction with DAO, followed by a color development reaction of co-produced H_2O_2 with peroxidase (POD) and some colorants. However, the inhibitory activity cannot be assessed if a test compound can inhibit POD or is self-oxidized by POD. As POD and chromophore or fluorogenic substances are used in the conventional DAO assay, this technique has some inherent disadvantages in the screening of DAO inhibitors.

Recently, we designed and developed 6-methylthio-D-kynurenine (MeS-D-KYN) as a fluorescence probe for evaluating DAO activity (*5*). MeS-D-KYN is a non-fluorescent compound that is converted to a fluorescent compound, 5-methylthiokynurenic acid (MeS-KYNA), by DAO (Scheme 1). We observed blue fluorescence of MeS-KYNA after an *in vitro* reaction between DAO and MeS-D-KYN (*5*). In addition, DAO activity was fluorometrically detected by fluorescence microscopy in cultured LLC-PK1 cells incubated with MeS-D-KYN (*5*). However, there are few reports on the occurrence of DAO activity in mammalian tissues *in vivo* under alive condition. Therefore, we investigated DAO activity *in vivo* using the microdialysis (MD) technique (*6–8*), which has been widely used in research on metabolic enzymes (*7*). This technique involves a dialysis membrane that is embedded in the tissue of an experimental animal.

The embedded membrane is permeable to small molecules, such as endogenous compounds or drugs, enabling the monitoring of alterations in the levels of drugs or endogenous compounds in the tissues of live experimental animals, by analyzing the molecules that pass through the dialysis membrane.

Thus, the present study aimed to determine the potential of MeS-D-KYN in evaluating DAO activity *in vivo* using the MD technique in rats (Scheme 2). As relatively high DAO activity has been reported in the rat kidney (*9*), it was selected as the target organ in the present study.

2. Material and Methods

2.1. Chemicals

HPLC-grade methanol (MeOH), acetonitrile (CH_3CN), and formic acid were purchased from FUJIFILM Wako Pure Chemical Corporation (Osaka, Japan). 5-Chlorobenzo[*d*]isoxazol-3-ol (CBIO) was purchased from AstaTech, Inc. (Bristol, PA, USA). Sterilized Ringer's solution was purchased from Otsuka Pharmaceutical Factory, Inc. (Tokushima, Japan). Ketamine hydrochloride was purchased from FUJIFILM Wako Pure Chemical Corporation. Reduced L-glutathione and xylazine hydrochloride were obtained from Sigma-Aldrich Co. LLC (St. Louis, MO, USA). MeS-D-KYN and MeS-KYNA were synthesized in our laboratory according to a previous report (*5*).

2.2. Animal experiments

Animal experiments were approved by the Animal Care Committee of the Toho University (No. 21-55-369). Male Sprague-Dawley rats (7-8 weeks old) were purchased from Charles River Japan Inc. (Kanagawa, Japan) and housed in a temperature- and humidity-controlled room for at least one week before commencing the experiment. Renal MD operation was performed as previously described (*10*). Briefly, under anesthesia with an intra-muscular injection of ketamine/xylazine (90/10 mg/kg/mL in saline), the rat was laid supine on a heating pad (Bio Research Center Co., Ltd., Tokyo, Japan). The left kidney was exposed and a linear MD probe (10 mm membrane; BAS*i,* West Lafayette, IN, USA) was implanted inside it, with the dialysis membrane of the probe completely embedded in the kidney. The probe position was fixed using a hemostatic matrix, Integran® (Nippon Zoki Pharmaceutical Co., Ltd., Osaka, Japan) and surgical glue, aronarufa® (Daiichi-Sankyo Co., Ltd., Tokyo, Japan). One end of the linear probe was connected to a 1 mL gastight syringe, and Ringer's solution with 2.0 mM sodium phosphate at pH 7.0 and 5.0 mM glutathione was perfused *via* the syringe. The perfusion was performed at a rate of 1.0 µL/min using a syringe pump, 11 plus (Harvard apparatus, Holliston, MA, USA), 0-1.5 h and 3.5-6.5 h after initiating the renal MD experiment. Ringer's solution with 5.0 µM MeS-D-KYN was infused 1.5-3.5 h after starting the experiment (n = 4). For CBIO-infusion experiment, Ringer's solution with 10, 100, 500, and 2,500 µM CBIO was used as the perfusate 0-6.5 h after starting the experiment (n = 4 per concentration). For the oral CBIO administration experiment, 5.0 and 25 mg/kg CBIO was orally administered 1.5 h after starting the experiment (n = 4 per concentration). MD samples or

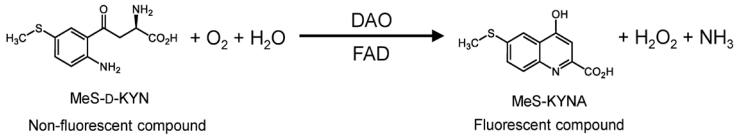

Scheme 1. The fluorescent compound MeS-KYNA is enzymatically produced from the non-fluorescent compound MeS-D-KYN by the action of DAO in the presence of FAD.

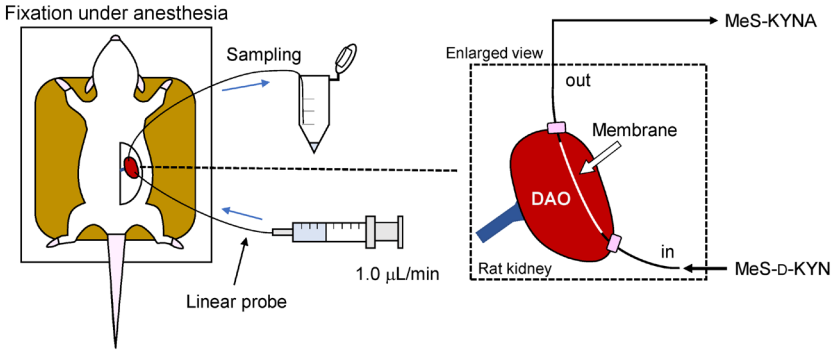

Scheme 2. Illustration of rat renal microdialysis experiment in the present study.

dialysates (approximately 30 µL) were collected every 0.5 h under ice-cold conditions. The first three samples, collected over a period of 1.5 h, were used as baseline samples.

2.3. HPLC

HPLC was conducted using an AS-4050*i* autosampler, PU-4180 intelligent pump, CO-2065 *plus* column oven (Jasco Corporation, Tokyo, Japan), and L-2485 fluorescence detector (Hitachi High-technologies, Tokyo, Japan). Inert Sustain®C18 (4.6 × 250 mm, 5.0 µm; GL Sciences Inc., Tokyo, Japan) separation column set at 40°C in the column oven was used. Mobile phases A and B were 0.05% HCO_2H in H_2O and 0.05% HCO_2H in CH_3OH, respectively, and were eluted following a gradient time-program: 0-5 min, B% = 3; 5-30 min, B% = 3-100; 30-45 min, B% = 100; and 45-60 min for initializing for next analysis. The fluorescence detection wavelength was set at 450 nm with an excitation wavelength of 364 nm. The obtained chromatograms were analyzed using ChromNavi® software (Jasco).

2.4. Statistical analysis

Data are expressed as mean ± standard error (S.E.). For comparison between the two groups, the Mann-Whitney *U*-test was used. For comparison among the three groups, a one-way analysis of variance (ANOVA) followed by the Bonferroni test was used. A p-value < 0.05 was considered statistically significant.

3. Results and Discussion

The present study evaluated the *in vivo* DAO activity through a renal MD experiment in rats. The dialysates were evaluated before (0-1.5 h), during (1.5-3.5 h), and without (3.5-6.5 h) MeS-D-KYN. The samples collected every 30 min were immediately analyzed using a reversed-phase HPLC with fluorescence detection.

A peak of standard MeS-KYNA was fluorometrically detected at approximately 22 min (Figure 1a). MeS-KYNA was barely observed in the samples before infusion of MeS-D-KYN (Figure 1b), indicating that MeS-KYNA is not an endogenous compound in rat kidneys. After infusion of 5.0 µM MeS-D-KYN, the MeS-KYNA peak was gradually observed (Figure 1c). Upon stopping the infusion of MeS-D-KYN, the MeS-KYNA peak disappeared (Figure 1d).

In addition, we previously performed MD with D-KYN infusion at 1.0 µL/min in the rat prefrontal cortex for the evaluation of DAO activity *in vivo* (*11*). In this case, the metabolite KYNA, an endogenous compound, was produced by the action of DAO. Therefore, to detect endogenous KYNA, a column-switching HPLC-fluorescence detection system (*12*), which employed a post-column reaction device with flowing 200 mM zinc ion (Zn^{2+}), was used; owing to the weak fluorescence of KYNA, Zn^{2+} addition is necessary for the formation of KYNA-Zn^{2+} fluorescence complex (*13*). This complex is usually detected by HPLC, where Zn^{2+} is added to the mobile phase, to determine the KYNA content (*14,15*). In contrast to these previous studies, in the present study, the conventional HPLC-fluorescence detection method could detect MeS-KYNA owing to the intense MeS-KYNA fluorescence that was observed without Zn^{2+} addition. The fluorescence of MeS-KYNA was approximately 200 times more intense than that of KYNA (*5*). As shown in Figure 2a, the fluorescent peak area of MeS-KYNA in the MD samples was observed at 1.0-1.5 h after starting the infusion of 2.5 or 5.0 µM MeS-D-KYN. Based on these data, the area under the curve (AUC) values for 2.5 and 5.0 µM MeS-D-KYN infusion were calculated and compared. The AUC for the 2.5 µM infusion was approximately half of that for the 5.0 µM infusion (Figure 2b), suggesting a concentration-dependent production of MeS-KYNA from MeS-D-KYN. These results clearly indicate that MeS-KYNA was produced from MeS-D-KYN in the rat kidneys. Briefly, MeS-D-KYN dissolved in Ringer's solution penetrated the rat renal cells through the MD membrane where it was oxidatively deaminated to MeS-KYNA by DAO (Scheme 2).

In addition, to clarify the involvement of renal DAO in the production of MeS-KYNA from MeS-D-KYN, a commercial inhibitor of DAO, CBIO, was continually co-infused with MeS-D-KYN 0-6.5 h after starting the MD experiment. As shown in Figure 3a,

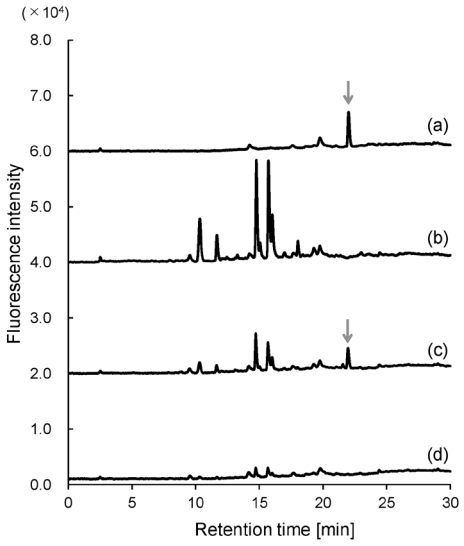

Figure 1. Chromatograms of standard MeS-KYNA and renal MD samples. (**a**) Standard MeS-KYNA and (b-d) renal MD samples on ODS column; (**b**) Before infusion of MeS-D-KYN (0-0.5 h); (**c**) During infusion of MeS-D-KYN (2.0-2.5 h), and (**d**) During infusion without MeS-D-KYN (4.0-4.5 h). The arrow indicates the peak of MeS-KYNA.

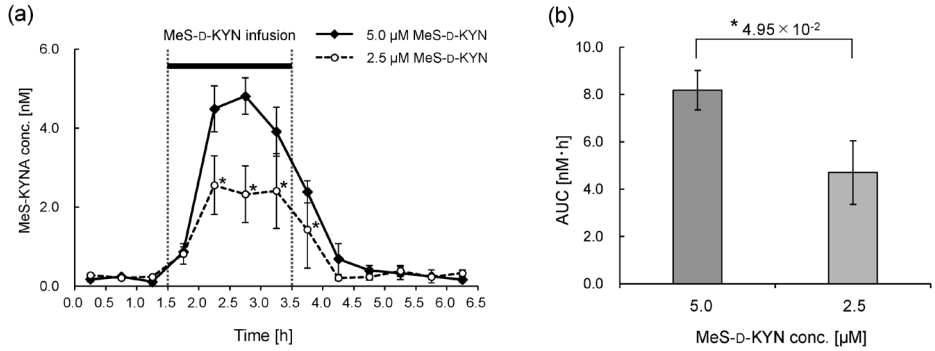

Figure 2. Changes in MeS-KYNA concentration in rat renal MD samples during infusion of 2.5 and 5.0 μM MeS-D-KYN (*n* = 4). (**a**) Time-course changes in MeS-KYNA concentration in rat renal MD samples. Open and closed circles with dotted and solid lines indicate the profiles during the infusion of 2.5 and 5.0 μM MeS-D-KYN, respectively (*n* = 4). (**b**) Area under the curves (AUCs) for MeS-KYNA during infusion of 2.5 and 5.0 μM MeS-D-KYN (*n* = 4). *$p < 0.05$.

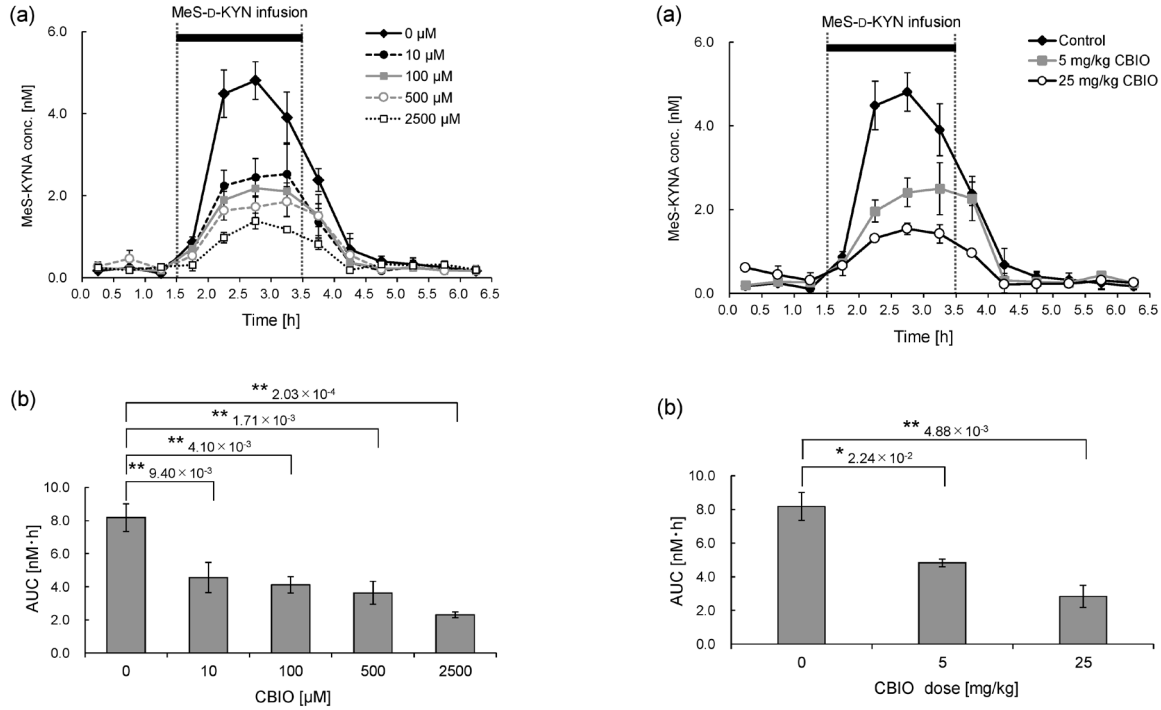

Figure 3. Changes in MeS-KYNA concentration in rat renal MD samples during infusion of 5.0 μM MeS-D-KYN in the presence of 0, 10, 100, 500, and 2,500 μM CBIO in Ringer's solution (*n* = 4). (**a**) Time-course changes in MeS-KYNA concentration in rat renal MD samples during infusion of 5.0 μM MeS-D-KYN and co-infusion of 0, 10, 100, 500, and 2,500 μM DAO inhibitor, CBIO (*n* = 4). (**b**) Area under the curves (AUCs) for MeS-KYNA during infusion of 5.0 μM MeS-D-KYN in the presence of 0, 10, 100, 500, and 2,500 μM CBIO in Ringer's solution (*n* = 4). **$p < 0.01$.

Figure 4. Changes in MeS-KYNA concentrations in rat renal MD samples during the infusion of 5.0 μM MeS-D-KYN after oral administration of CBIO at a dose of 0, 5, and 25 mg/kg (*n* = 4). (**a**) Time-course changes in MeS-KYNA concentrations in rat renal MD samples during the infusion of 5.0 μM MeS-D-KYN. Closed circles, closed squares, and open circles indicate the profiles after oral administration of DAO inhibitor CBIO at a dose of 0, 5, and 25 mg/kg (*n* = 4). (b) Area under the curves (AUCs) for MeS-KYNA during infusion of 5.0 μM MeS-D-KYN after oral administration of CBIO at a dose of 0, 5, and 25 mg/kg (*n* = 4). *$p < 0.05$, **$p < 0.01$.

CBIO remarkably suppressed the production of MeS-KYNA from MeS-D-KYN in a concentration-dependent manner. CBIO, at a concentration > 10 μM, suppressed the production of MeS-KYNA by approximately 50%. As CBIO is a small molecule, it may have penetrated the MD membrane to reach rat renal cells to directly inhibit renal DAO activity. After 2,500 μM CBIO co-infusion, MeS-KYNA levels decreased by approximately 20% compared to those in the non-infused group (Figure 3b). Taken together, these results indicate that MeS-D-KYN was oxidatively metabolized mainly by DAO, but enzymes other than DAO may also be involved in the oxidation of MeS-D-KYN.

We also investigated the influence of CBIO on renal

DAO activity by orally administering the compound to rats. At oral doses of 5.0 and 25 mg/kg, the AUCs for MeS-KYNA production were significantly decreased to approximately 60% and 35% compared to those of control (0 mg/kg), respectively. Thus, oral CBIO administration reduced the production of MeS-KYNA in a dose-dependent manner (Figures 4a and 4b). In this case, although CBIO reached the rat kidneys *via* the circulatory system, passing through the intestine and liver, it clearly inhibited DAO. Oral CBIO administration at 30 mg/kg was reported to be pharmacologically active in *in vivo* mouse behavior experiments, as the co-administration of D-serine (30 mg/kg) increases extracellular D-serine levels to attenuate pre-pulse inhibition deficits induced by dizocilpine (*16*). Although a dose of CBIO, 30 mg/kg, may be required for *in vivo* behavior experiments, such pre-pulse inhibition, the present study demonstrated that 5.0 mg/kg CBIO could suppress DAO activity in rat kidneys.

Currently, DAO is one of the target enzymes for developing novel drugs to overcome schizophrenia (*17,18*). The MD technique described in the present study using MeS-D-KYN can be used for evaluating drug candidates to inhibit DAO activity *in vivo* following oral administration.

4. Conclusion

The present study demonstrated the DAO-mediated production of MeS-KYNA from MeS-D-KYN *in vivo* using renal MD experiments in rats. This method, wherein MD is coupled with continuous MeS-D-KYN infusion, will be useful for evaluating *in vivo* DAO activity in tissues of live experimental animals.

Acknowledgements

We thank Editage (www.editage.jp) for English language editing. We would like to thank Mr. H. Sugasawa for his technical assistance in this study.

Funding: None.

Conflict of Interest: The authors have no conflicts of interest to disclose.

Ethical approval: Animal experiments were approved by the Animal Care Committee of the Toho University (No. 21-55-369).

References

1. Kawazoe T, Park HK, Iwana S, Tsuge H, Fukui K. Human D-amino acid oxidase: an update and review. Chem Rec. 2007; 7:305-315.
2. Boks MPM, Rietkerk T, van de Beek MH, Sommer IE, de Koning TJ, Kahn RS. Reviewing the role of the genes G72 and DAAO in glutamate neurotransmission in schizophrenia. Eur Neuropsychopharmacol. 2007; 17:567-572.
3. Madeira C, Freitas ME, Vargas-Lopes C, Wolosker H, Panizzutti R. Increased brain D-amino acid oxidase (DAAO) activity in schizophrenia. Schizophr Res. 2008; 101:76-83.
4. Seetharam JC, Maiti R, Mishra A, Mishra BR. Efficacy and safety of add-on sodium benzoate, a D-amino acid oxidase inhibitor, in treatment of schizophrenia: A systematic review and meta-analysis. Asian J Psychiatr. 2022; 68:102947.
5. Sakamoto T, Odera K, Onozato M, Sugasawa H, Takahashi R, Fujimaki Y, Fukushima T. Direct fluorescence evaluation of D-amino acid oxidase activity using a synthetic D-kynurenine derivative. Anal Chem. 2022; 94:14530-14536.
6. Davies MI. A review of microdialysis sampling for pharmacokinetic applications. Anal Chim Acta. 1999; 379:227-249.
7. Hansen DK, Davies MI, Lunte SM, Lunte CE. Pharmacokinetic and metabolism studies using microdialysis sampling. J Pharm Sci. 1999; 88:14-27.
8. Nandi P, Lunte SM. Recent trends in microdialysis sampling integrated with conventional and microanalytical systems for monitoring biological events: a review. Anal Chim Acta. 2009; 651:1-14.
9. Daniello A, Donofrio G, Pischetola M, Daniello G, Vetere A, Petrucelli L, Fisher GH. Biological role of D-amino-acid oxidase and D-aspartate oxidase - effects of D-amino acids. J Biol Chem. 1993; 268:26941-26949.
10. Kajiro T, Nakajima Y, Fukushima T, Imai K. A method to evaluate the renin-angiotensin system in rat renal cortex using a microdialysis technique combined with HPLC fluorescence detection. Anal Chem. 2002; 74:4519-4525.
11. Ogaya T, Song Z, Ishii K, Fukushima T. Changes in extracellular kynurenic acid concentrations in rat prefrontal cortex after D-kynurenine infusion: an *in vivo* microdialysis study. Neurochem Res. 2010; 35:559-563.
12. Mitsuhashi S, Fukushima T, Kawai J, Tomiya M, Santa T, Imai K, Toyo'oka T. Improved method for the determination of kynurenic acid in rat plasma by column-switching HPLC with post-column fluorescence detection. Anal Chim Acta. 2006; 562:36-43.
13. Iinuma F, Tabara M, Yashiro K, Watanabe M. Fluorometric-determination of kynurenic acid in urine with zinc (II) acetate. Bunseki Kagaku. 1985; 34:483-486.
14. Zhao J, Gao P, Zhu D. Optimization of Zn^{2+}-containing mobile phase for simultaneous determination of kynurenine, kynurenic acid and tryptophan in human plasma by high performance liquid chromatography. J Chromatogr B Analyt Technol Biomed Life Sci. 2010; 878:603-608.
15. Erhardt S, Blennow K, Nordin C, Skogh E, Lindstrom L, Engberg G. Kynurenic acid levels are elevated in the cerebrospinal fluid of patients with schizophrenia. Neurosci Lett. 2001; 313:96-98.
16. Hashimoto K, Fujita Y, Horio M, Kunitachi S, Iyo M, Ferraris D, Tsukamoto T. Co-administration of a D-amino acid oxidase inhibitor potentiates the efficacy of D-serine in attenuating prepulse inhibition deficits after administration of dizocilpine. Biol Psychiatry 2009; 65:1103-1106.
17. Luptak M, Michalickova D, Fisar Z, Kitzlerova E,

Hroudova J. Novel approaches in schizophrenia-from risk factors and hypotheses to novel drug targets. World J Psychiatry. 2021; 11:277-296.
18. Krogmann A, Peters L, von Hardenberg L, Bodeker K, Noles VB, Correill CU. Keeping up with the therapeutic advances in schizophrenia: a review of novel and emerging pharmacological entities. CNS Spectr. 2019; 24: 41-68.

Received October 14, 2023; Revised November 20, 2023; Accepted November 22, 2023.

*Address correspondence to:
Takeshi Fukushima, Department of Analytical Chemistry, Faculty of Pharmaceutical Sciences, Toho University, 2-2-1 Miyama, Funabashi-shi, Chiba 274-8510, Japan.
E-mail: t-fukushima@phar.toho-u.ac.jp

Released online in J-STAGE as advance publication December 3, 2023.

Correspondence

DOI: 10.5582/ddt.2023.01215

Development of amyloid beta-directed antibodies against Alzheimer's disease: Twists and turns

Daoran Lu, Fangzhou Dou, Jianjun Gao*

Department of Pharmacology, School of Pharmacy, Qingdao University, Qingdao, Shandong, China.

SUMMARY Alzheimer's disease (AD) is a severe and progressive neurodegenerative disease, and the treatment options that are currently available are limited. The amyloid cascade hypothesis has had a significant influence in explaining the pathology underlying AD. Inhibiting the production and aggregation of amyloid-beta (Aβ) and promoting its clearance have been important strategies in the development of anti-AD drugs over the past two decades. Specifically, Aβ directed antibodies have been highly anticipated, but drug development has been fraught with obstacles and challenges. Antibodies targeting the C-terminal or central region of Aβ, such as ponezumab, solanezumab, and crenezumab, primarily bind to Aβ monomers, yet no significant clearance of brain plaques or slowing of disease progression has been observed in clinical trials. Antibodies targeting the N-terminal region of Aβ, including aducanumab, lecanemab, and donanemab, primarily bind to aggregated forms of Aβ, and have shown efficacy in clearing brain plaques and slowing early-stage AD progression in clinical trials. However, clinical trials of gantenerumab, which targets conformational epitopes in the N-terminal and central sequences of Aβ and which selectively binds to aggregated forms, have failed, raising some new questions about the Aβ hypothesis. Advances in research on the pathological mechanisms of AD and advances in early diagnostic techniques may shift the time window for drug intervention and offer a potential pathway for developing effective drugs to delay the onset and progression of AD in the future.

Keywords Aβ hypothesis, AD, aducanumab, lecanemab, donanemab, gantenerumab

Alzheimer's disease (AD) is a severe neurodegenerative disease characterized by progressive memory loss, cognitive impairment, and neuropsychiatric symptoms (*1*). The incidence of AD is closely related to age (*1,2*). With the extension of the human lifespan and further aging of the population, the prevalence of AD is increasing (*3,4*). According to statistics from the World Health Organization, the number of dementia patients worldwide is expected to increase from 55 million in 2019 to 139 million in 2050, with AD patients accounting for approximately 60-70% of cases (*5*). This poses significant challenges to healthcare systems and global societal development.

The etiology and pathogenesis of AD remain elusive. The currently proposed hypotheses mainly include the Aβ cascade hypothesis, the tau hypothesis, the cholinergic hypothesis, and the excitotoxicity hypothesis (*1,6*). The drugs currently used to treat AD are mainly acetylcholinesterase inhibitors and N-methyl-*D*-aspartate (NMDA) receptor antagonists, which were developed based on the cholinergic hypothesis and the excitotoxicity hypothesis, respectively. These medications aim to ameliorate symptoms such as memory and cognitive impairments in AD patients, but they do not halt or reverse the progression of the disease, exhibiting limited clinical efficacy. The amyloid cascade hypothesis holds significant influence in explaining the pathogenesis of AD, suggesting that abnormal accumulation of Aβ in the brain leads to hyperphosphorylation of tau within neurons, thereby promoting the formation of neurofibrillary tangles, synaptic loss, and neuronal death, and ultimately resulting in cognitive impairment and other associated symptoms (*7*). Based on this hypothesis, inhibiting Aβ production and aggregation while promoting Aβ clearance has been a crucial strategy in the development of anti-AD drugs over the past two decades (*7,8*). Antibody-based therapeutics targeting Aβ in particular have held great promise, but drug development in this field has been fraught with challenges and setbacks (Table 1).

Aβ, derived from the amyloid precursor protein (APP) through cleavage by β-secretase 1 (BACE1)

Table 1. Research on and development of Aβ-directed antibodies against AD

Antibody	Epitope	Isotype	Targeted Aβ form	Study cohort in clinical trial	Outcome	*Ref.*
Ponezumab (Pfizer)	C-terminal sequence of Aβ (residues 33-40)	IgG_2	Primarily monomers	Mild-to-moderate AD (a phase 2 study), treatment for 18 months.	No effects on cognitive/functional outcomes; No dose response regarding cerebrospinal fluid biomarkers.	(*16,17*)
Solanezumab (Eli Lilly)	Central region of Aβ (residues 16-26)	IgG_1	Primarily monomers	(i) Mild to moderate AD (EXPEDITION 1 and EXPEDITION 2 studies), treatment for 80 weeks; (ii) Mild AD (EXPEDITION 3 study), treatment for 76 weeks; (iii) Asymptomatic or mildly symptomatic elderly individuals with biomarker evidence of brain amyloid deposition (A4 study), treatment for 3 years.	Increased levels of total $Aβ_{40}$ and $Aβ_{42}$ in plasma and CSF but no clearance of brain amyloid plaque; No significant cognitive and functional improvement compared to placebo.	(*19-21*)
Crenezumab (Roche)	Central regions of Aβ (residues 13-24)	IgG_4	Monomers and aggregates	Prodromal to mild AD (CREAD and CREAD2 study), treatment for 100 weeks.	No meaningful changes in AD biomarkers and no improvement of clinical decline compared to placebo (CREAD and CREAD2).	(*22,23*)
Bapineuzumab (Janssen and Pfizer)	N-terminal sequence of Aβ (residues 1-5)	IgG_1	Monomers and aggregates	Mild-to-moderate AD with or without apolipoprotein E (*APOE*) ε4 allele, treatment for 78 weeks.	Reducing AD biomarkers in patients with *APOE* ε4 allele but no functional improvement in patients with or without *APOE* ε4 allele.	(*26*)
Aducanumab (Biogen and Eisai)	N-terminal sequence of Aβ (residues 3-7)	IgG_1	Mainly aggregates (soluble and insoluble)	Mild cognitive impairment or the mild dementia stage of AD (EMERGE and ENGAGE studies)	Reducing amyloid β plaques but inconsistency in reducing clinical decline compared to placebo.	(*15,27*)
Lecanemab (Biogen and Eisai)	N-terminal sequence (residues 1-16)	IgG_1	Mainly aggregates (soluble and insoluble)	Mild cognitive impairment or the mild dementia stage of AD (Clarity AD study), treatment for 18 months	Reducing amyloid burden and clinical decline compared to placebo.	(*30*)
Donanemab (Eli Lilly)	N-terminal modified Aβ peptide (Aβ3-42)	IgG_1	Plaque	Mild cognitive impairment or the mild dementia stage of AD (TRAILBLAZER-ALZ 2 study), treatment for 72 weeks	Reducing amyloid burden and slowing clinical progression compared to placebo.	(*31*)
Gantenerumab (Roche)	Both N-terminal and central regions of Aβ (conformational epitope; residues 3-11, 18-27)	IgG_1	Mainly aggregates (soluble and insoluble)	Mild cognitive impairment or mild dementia due to AD (GRADUATE I and II), treatment for 116 weeks.	Reducing amyloid plaque burden but no clinical improvement compared to placebo.	(*34*)

and γ-secretase, is a product consisting of 30-51 amino acid residues in length (*7,9*). The main forms of Aβ are $A\beta_{1-40}$ and $A\beta_{1-42}$, with additional N-terminally truncated products such as $A\beta_{3-42}$ (*10*). Aβ monomers are proposed to possess certain physiological functions, such as regulating learning and memory, angiogenesis, neurogenesis, repairing leaks in the blood-brain barrier, promoting recovery from injury, and acting as an antimicrobial peptide and tumor suppressor (*11,12*). However, due to excessive production or other unknown reasons, Aβ monomers aggregate abnormally, forming soluble oligomers and protofibrils that are highly neurotoxic (*13,14*). The protofibrils can further aggregate into insoluble fibrils and ultimately be deposited as plaques, which are considered pathological hallmarks of AD. The transition of Aβ monomers to plaques is thought to be a dynamic and reversible process, as reducing the levels of soluble Aβ can shift the equilibrium and lead to plaque dissolution (*7*). Aβ-directed antibodies aim to bind to Aβ and promote immune-mediated clearance. Depending on the antigen epitope targeted, the form of Aβ bound by the antibody also differs. Since the N-terminal sequence of Aβ is exposed after aggregation, antibodies targeting the epitope in this region can theoretically bind to all forms of Aβ (including monomers, oligomers, protofibrils, and amyloid fibrils) (*8*). That said, the central and C-terminal regions are buried within the aggregates, making antibodies targeting these regions primarily bind to Aβ monomers (*8*). Over the past 20 years, different antibodies designed to target various antigenic epitopes have been tested for their ability to clear Aβ and potentially slow or reverse the progression of AD. These successful or unsuccessful cases may provide valuable lessons and insights for the development of future Aβ-targeting drugs.

Typical antibodies targeting the C-terminal or central region of Aβ include ponezumab, solanezumab, and crenezumab (*15*). These antibodies bind to Aβ monomers, aiming to shift the equilibrium by reducing the quantity of Aβ monomers and consequently decreasing the quantity of highly cytotoxic forms of Aβ. Ponezumab, which targets the C-terminal sequence of Aβ (*16*), did not demonstrate a dose-response in terms of changes in AD biomarkers in cerebrospinal fluid and did not result in cognitive improvement in a phase 2 clinical trial involving patients with mild to moderate AD (*17*). As a result, further clinical research was discontinued. Solanezumab and crenezumab, both of which target the central region of Aβ, share some similarities in the amino acid composition of their Fab fragments (*18*). Solanezumab only binds to Aβ monomers, whereas crenezumab can also bind to the oligomer's lateral and edge residues (*18*). Four phase 3 clinical trials investigated the efficacy of solanezumab in patients in different stages of AD progression. EXPEDITION 1 and 2 included patients with mild to moderate AD, EXPEDITION 3 included patients with mild AD, and the A4 trial included asymptomatic or mildly symptomatic elderly individuals with biomarker evidence of brain amyloid deposition (*19-21*). Results indicated that solanezumab increased the concentration of $A\beta_{40}$ and $A\beta_{42}$ in plasma and cerebrospinal fluid, suggesting movement of Aβ within the central compartment and some transfer of Aβ to the periphery (*19-21*). However, solanezumab had no effect on removing deposited amyloid plaques and slowing disease progression in any of the studies (*19-21*). Two phase 3 clinical studies (CREAD and CREAD2) on the efficacy of crenezumab included participants with prodromal to mild AD (*22,23*). Results indicated that total $A\beta_{42}$ and $A\beta_{40}$ concentrations in plasma and cerebrospinal fluid significantly increased following the administration of crenezumab and remained elevated throughout the study (*22,23*). However, there were no significant changes in brain Aβ imaging, and crenezumab did not reduce clinical decline in participants (*22,23*). These research findings suggest that antibodies primarily targeting Aβ monomers may have limited efficacy in clearing amyloid plaques and slowing disease progression.

Antibodies targeting the N-terminal sequence of Aβ include bapineuzumab, aducanumab, lecanemab, and donanemab. Bapineuzumab has the ability to bind to all forms of Aβ, including monomers, oligomers, protofibrils, fibrils, and plaques (*24,25*). Two phase 3 clinical trial investigated the efficacy of bapineuzumab in mild to moderate AD patients with or without the apolipoprotein E (*APOE*) ε4 allele (*26*). Results indicated that bapineuzumab reduced AD biomarkers such as brain plaques and cerebrospinal fluid phosphorylated tau in *APOE* ε4 allele carriers but not in noncarriers (*26*). However, bapineuzumab did not improve clinical outcomes in patients either with or without the *APOE* ε4 allele (*26*). The failure of these trials prompts us to think that the deposition of Aβ in the brain and its pathological damage to neurons may occur much earlier than the onset of AD symptoms, and selecting patients in the middle to late stages of the disease for clinical trials may miss the optimal time window for anti-Aβ drug intervention. Two phase 3 clinical trials evaluating aducanumab (EMERGE and ENGAGE) included patients with mild cognitive impairment or the mild dementia stage of AD (*27*). Aducanumab demonstrated the ability to clear brain Aβ plaques and delayed disease progression in the EMERGE but not in the ENGAGE study (*27*). Aducanumab is the first drug based on the Aβ hypothesis to receive Accelerated Approval from the US Food and Drug Administration (FDA) in nearly two decades (*28*), but its efficacy still requires further confirmation in additional clinical trials. Lecanemab is another antibody that primarily targets aggregates of Aβ (mainly oligomers and protofibrils) (*29*). In a phase 3 clinical trial, lecanemab showed the ability to clear Aβ plaques and delay disease progression in patients with mild cognitive impairment or the mild dementia stage of AD (*30*). Based on robust

clinical data, lecanemab has received full FDA approval for the treatment of mild AD patients. Coincidentally, donanemab, an antibody targeting N-terminal modified Aβ peptides, has also shown efficacy in delaying disease progression in patients with mild cognitive impairment or the mild dementia stage of AD in a phase 3 clinical trial (TRAILBLAZER-ALZ 2) (*31*). It specifically targets $A\beta_{3\text{-}42}$ (*32*), which accumulates early in the deposition cascade, and it demonstrates the ability to effectively clear brain plaques (*10,31*). Results of clinical trials on aducanumab, lecanemab, and donanemab support the Aβ hypothesis and suggest that drugs targeting the N-terminal sequence and aggregated forms of Aβ, capable of plaque clearance, may be efficacious in early-stage AD patients.

Surprisingly, two recent phase III clinical trials, GRADUATE I and II, have demonstrated that gantenerumab, an antibody targeting the conformational epitopes of both the N-terminal and central sequences of Aβ and selectively binding to aggregated forms of Aβ (*33*), did not slow disease progression in patients with mild cognitive impairment or mild dementia due to AD, despite its reduction in cerebral Aβ plaque deposition (*34*). The reasons for the clinical trial failures are still unknown. Was gantenerumab's efficacy in clearing Aβ plaques insufficient, or did the recruited patients have more severe disease compared to studies of lecanemab and donanemab? Whatever the answer, these failures have raised new questions about the Aβ hypothesis.

In conclusion, recent trials have demonstrated that Aβ antibodies are efficacious in slowing disease progression, which to some extent dispels doubts surrounding the Aβ hypothesis. However, further experimental validation is still needed to confirm this hypothesis, particularly in terms of whether the strategies targeting Aβ will exhibit the same efficacy in additional clinical trials. Advances in research on the pathological mechanisms of AD and advances in early diagnostic techniques may shift the time window for drug intervention and offer a potential pathway for developing effective drugs to delay the onset and progression of AD in the future.

Funding: None.

Conflict of Interest: The authors have no conflicts of interest to disclose.

References

1. Scheltens P, De Strooper B, Kivipelto M, Holstege H, Chetelat G, Teunissen CE, Cummings J, van der Flier WM. Alzheimer's disease. Lancet. 2021; 397:1577-1590.
2. Xia J. Liquid-liquid phase separation: A new perspective to understanding aging and pathogenesis. Biosci Trends. 2022; 16:359-362.
3. Deng Y, Wang H, Gu K, Song P. Alzheimer's disease with frailty: Prevalence, screening, assessment, intervention strategies and challenges. Biosci Trends. 2023; 17:283-292.
4. Paudel P, Park CH, Jung HA, Yokozawa T, Choi JS. A systematic review on anti-Alzheimer's disease activity of prescription Kangen-karyu. Drug Discov Ther. 2020; 14:61-66.
5. World Health Organization. Global status report on the public health response to dementia. *https://iris.who.int/bitstream/handle/10665/344707/9789240038660-chi.pdf* (accessed November 21, 2023).
6. Zhou Y, Cheng Y, Li Y, Ma J, Wu Z, Chen Y, Mei J, Chen M. Soluble beta-amyloid impaired the GABA inhibition by mediating KCC2 in early APP/PS1 mice. Biosci Trends. 2021; 15:330-340.
7. Panza F, Lozupone M, Logroscino G, Imbimbo BP. A critical appraisal of amyloid-beta-targeting therapies for Alzheimer disease. Nat Rev Neurol. 2019; 15:73-88.
8. Wang Y, Yan T, Lu H, Yin W, Lin B, Fan W, Zhang X, Fernandez-Funez P. Lessons from anti-amyloid-beta immunotherapies in Alzheimer disease: Aiming at a moving target. Neurodegener Dis. 2017; 17:242-250.
9. Hampel H, Hardy J, Blennow K, *et al*. The amyloid-beta pathway in Alzheimer's disease. Mol Psychiatry. 2021; 26:5481-5503.
10. Demattos RB, Lu J, Tang Y, Racke MM, Delong CA, Tzaferis JA, Hole JT, Forster BM, McDonnell PC, Liu F, Kinley RD, Jordan WH, Hutton ML. A plaque-specific antibody clears existing beta-amyloid plaques in Alzheimer's disease mice. Neuron. 2012; 76:908-920.
11. Kent SA, Spires-Jones TL, Durrant CS. The physiological roles of tau and Abeta: implications for Alzheimer's disease pathology and therapeutics. Acta Neuropathol. 2020; 140:417-447.
12. Cho Y, Bae HG, Okun E, Arumugam TV, Jo DG. Physiology and pharmacology of amyloid precursor protein. Pharmacol Ther. 2022; 235:108122.
13. Tolar M, Hey J, Power A, Abushakra S. Neurotoxic soluble amyloid oligomers drive Alzheimer's pathogenesis and represent a clinically validated target for slowing disease progression. Int J Mol Sci. 2021; 22:6355.
14. Ono K, Condron MM, Teplow DB. Structure-neurotoxicity relationships of amyloid beta-protein oligomers. Proc Natl Acad Sci U S A. 2009; 106:14745-14750.
15. Arndt JW, Qian F, Smith BA, Quan C, Kilambi KP, Bush MW, Walz T, Pepinsky RB, Bussiere T, Hamann S, Cameron TO, Weinreb PH. Structural and kinetic basis for the selectivity of aducanumab for aggregated forms of amyloid-beta. Sci Rep. 2018; 8:6412.
16. La Porte SL, Bollini SS, Lanz TA, *et al*. Structural basis of C-terminal beta-amyloid peptide binding by the antibody ponezumab for the treatment of Alzheimer's disease. J Mol Biol. 2012; 421:525-536.
17. Landen JW, Cohen S, Billing CB, Jr., *et al*. Multiple-dose ponezumab for mild-to-moderate Alzheimer's disease: Safety and efficacy. Alzheimers Dement (N Y). 2017; 3:339-347.
18. Zhao J, Nussinov R, Ma B. Mechanisms of recognition of amyloid-beta (Abeta) monomer, oligomer, and fibril by homologous antibodies. J Biol Chem. 2017; 292:18325-18343.
19. Doody RS, Thomas RG, Farlow M, *et al*. Phase 3 trials of solanezumab for mild-to-moderate Alzheimer's disease. N Engl J Med. 2014; 370:311-321.
20. Honig LS, Vellas B, Woodward M, *et al*. Trial of solanezumab for mild dementia due to Alzheimer's disease. N Engl J Med. 2018; 378:321-330.
21. News. A4 Study Results Are Now Available. *https://*

atrinews.usc.edu/a4studyresults (accessed November 21, 2023). .
22. Ostrowitzki S, Bittner T, Sink KM, *et al*. Evaluating the safety and efficacy of crenezumab vs placebo in adults with early Alzheimer disease: Two phase 3 randomized placebo-controlled trials. JAMA Neurol. 2022; 79:1113-1121.
23. News. Roche's crenezumab fails to meet end points in autosomal dominant Alzheimer disease. *https://www.neurologylive.com/view/roche-crenezumab-fails-meet-end-points-autosomal-dominant-alzheimer-disease* (accessed November 21, 2023).
24. Miles LA, Crespi GA, Doughty L, Parker MW. Bapineuzumab captures the N-terminus of the Alzheimer's disease amyloid-beta peptide in a helical conformation. Sci Rep. 2013; 3:1302.
25. van Dyck CH. Anti-amyloid-beta monoclonal antibodies for Alzheimer's disease: Pitfalls and promise. Biol Psychiatry. 2018; 83:311-319.
26. Salloway S, Sperling R, Fox NC, *et al*. Two phase 3 trials of bapineuzumab in mild-to-moderate Alzheimer's disease. N Engl J Med. 2014; 370:322-333.
27. Dhillon S. Aducanumab: First approval. Drugs. 2021; 81:1437-1443.
28. Yang P, Sun F. Aducanumab: The first targeted Alzheimer's therapy. Drug Discov Ther. 2021; 15:166-168.
29. Tucker S, Moller C, Tegerstedt K, Lord A, Laudon H, Sjodahl J, Soderberg L, Spens E, Sahlin C, Waara ER, Satlin A, Gellerfors P, Osswald G, Lannfelt L. The murine version of BAN2401 (mAb158) selectively reduces amyloid-beta protofibrils in brain and cerebrospinal fluid of tg-ArcSwe mice. J Alzheimers Dis. 2015; 43:575-588.
30. van Dyck CH, Swanson CJ, Aisen P, *et al*. Lecanemab in early Alzheimer's disease. N Engl J Med. 2023; 388:9-21.
31. Sims JR, Zimmer JA, Evans CD, *et al*. Donanemab in early symptomatic Alzheimer disease: The TRAILBLAZER-ALZ 2 randomized clinical trial. JAMA. 2023; 330:512-527.
32. Iwatsubo T, Saido TC, Mann DM, Lee VM, Trojanowski JQ. Full-length amyloid-beta (1-42(43)) and amino-terminally modified and truncated amyloid-beta 42(43) deposit in diffuse plaques. Am J Pathol. 1996; 149:1823-1830.
33. Bohrmann B, Baumann K, Benz J, *et al*. Gantenerumab: A novel human anti-Abeta antibody demonstrates sustained cerebral amyloid-beta binding and elicits cell-mediated removal of human amyloid-beta. J Alzheimers Dis. 2012; 28:49-69.
34. Bateman RJ, Smith J, Donohue MC, *et al*. Two phase 3 trials of gantenerumab in early Alzheimer's disease. N Engl J Med. 2023; 389:1862-1876.

Received December 21, 2023; Accepted December 28, 2023.

**Address correspondence to:*
Jianjun Gao, Department of Pharmacology, School of Pharmacy, Qingdao University, Qingdao, Shandong, China.
E-mail: gaojj@qdu.edu.cn

DD&T
Drug Discoveries & Therapeutics

Guide for Authors

1. Scope of Articles

Drug Discoveries & Therapeutics (Print ISSN 1881-7831, Online ISSN 1881-784X) welcomes contributions in all fields of pharmaceutical and therapeutic research such as medicinal chemistry, pharmacology, pharmaceutical analysis, pharmaceutics, pharmaceutical administration, and experimental and clinical studies of effects, mechanisms, or uses of various treatments. Studies in drug-related fields such as biology, biochemistry, physiology, microbiology, and immunology are also within the scope of this journal.

2. Submission Types

Original Articles should be well-documented, novel, and significant to the field as a whole. An Original Article should be arranged into the following sections: Title page, Abstract, Introduction, Materials and Methods, Results, Discussion, Acknowledgments, and References. Original articles should not exceed 5,000 words in length (excluding references) and should be limited to a maximum of 50 references. Articles may contain a maximum of 10 figures and/or tables. Supplementary Data are permitted but should be limited to information that is not essential to the general understanding of the research presented in the main text, such as unaltered blots and source data as well as other file types.

Brief Reports definitively documenting either experimental results or informative clinical observations will be considered for publication in this category. Brief Reports are not intended for publication of incomplete or preliminary findings. Brief Reports should not exceed 3,000 words in length (excluding references) and should be limited to a maximum of 4 figures and/or tables and 30 references. A Brief Report contains the same sections as an Original Article, but the Results and Discussion sections should be combined.

Reviews should present a full and up-to-date account of recent developments within an area of research. Normally, reviews should not exceed 8,000 words in length (excluding references) and should be limited to a maximum of 10 figures and/or tables and 100 references. Mini reviews are also accepted, which should not exceed 4,000 words in length (excluding references) and should be limited to a maximum of 5 figures and/or tables and 50 references.

Policy Forum articles discuss research and policy issues in areas related to life science such as public health, the medical care system, and social science and may address governmental issues at district, national, and international levels of discourse. Policy Forum articles should not exceed 3,000 words in length (excluding references) and should be limited to a maximum of 5 figures and/or tables and 30 references.

Case Reports should be detailed reports of the symptoms, signs, diagnosis, treatment, and follow-up of an individual patient. Case reports may contain a demographic profile of the patient but usually describe an unusual or novel occurrence. Unreported or unusual side effects or adverse interactions involving medications will also be considered. Case Reports should not exceed 3,000 words in length (excluding references).

Communications are short, timely pieces that spotlight new research findings or policy issues of interest to the field of global health and medical practice that are of immediate importance. Depending on their content, Communications will be published as "Comments" or "Correspondence". Communications should not exceed 1,500 words in length (excluding references) and should be limited to a maximum of 2 figures and/or tables and 20 references.

Editorials are short, invited opinion pieces that discuss an issue of immediate importance to the fields of global health, medical practice, and basic science oriented for clinical application. Editorials should not exceed 1,000 words in length (excluding references) and should be limited to a maximum of 10 references. Editorials may contain one figure or table.

News articles should report the latest events in health sciences and medical research from around the world. News should not exceed 500 words in length.

Letters should present considered opinions in response to articles published in *Drug Discoveries & Therapeutics* in the last 6 months or issues of general interest. Letters should not exceed 800 words in length and may contain a maximum of 10 references. Letters may contain one figure or table.

3. Editorial Policies

For publishing and ethical standards, *Drug Discoveries & Therapeutics* follows the Recommendations for the Conduct, Reporting, Editing, and Publication of Scholarly Work in Medical Journals issued by the International Committee of Medical Journal Editors (ICMJE, *https://icmje.org/recommendations*), and the Principles of Transparency and Best Practice in Scholarly Publishing jointly issued by the Committee on Publication Ethics (COPE, *https://publicationethics.org/resources/guidelines-new/principles-transparency-and-best-practice-scholarly-publishing*), the Directory of Open Access Journals (DOAJ, *https://doaj.org/apply/transparency*), the Open Access Scholarly Publishers Association (OASPA, *https://oaspa.org/principles-of-transparency-and-best-practice-in-scholarly-publishing-4*), and the World Association of Medical Editors (WAME, *https://wame.org/principles-of-transparency-and-best-practice-in-scholarly-publishing*).

Drug Discoveries & Therapeutics will perform an especially prompt review to encourage innovative work. All original research will be subjected to a rigorous standard of peer review and will be edited by experienced copy editors to the highest standards.

Ethical Approval of Studies and Informed Consent: For all manuscripts reporting data from studies involving human participants or animals, formal review and approval, or formal review and waiver, by an appropriate institutional review board or ethics committee is required and should be described in the Methods section. When your manuscript contains any case details, personal information and/or images of patients or other individuals, authors must obtain appropriate written consent, permission and release in order to comply with all applicable laws and regulations concerning privacy and/or security of personal information. The consent form needs to comply with the relevant legal requirements of your particular jurisdiction, and please do not send signed consent form to *Drug Discoveries & Therapeutics* to respect your patient's and any other individual's privacy. Please instead describe the information clearly in the Methods (patient consent) section of your manuscript while retaining copies of the signed forms in the event they should be needed. Authors should also state that the study conformed to the provisions of the Declaration of Helsinki (as revised in 2013, *https://wma.net/what-we-do/medical-ethics/declaration-of-helsinki*). When reporting experiments on animals, authors should indicate whether the institutional and national guide for the care and use of laboratory animals was followed.

Reporting Clinical Trials: The ICMJE (*https:// icmje.org/recommendations/browse/publishing-and-editorial-issues/clinical-trial-registration.html*) defines a clinical trial as any research project that prospectively assigns people or a group of people to an intervention, with or without concurrent comparison or control groups, to study the relationship between a health-related intervention and a health outcome. Registration of clinical trials in a public trial registry

at or before the time of first patient enrollment is a condition of consideration for publication in *Drug Discoveries & Therapeutics*, and the trial registration number will be published at the end of the Abstract. The registry must be independent of for-profit interest and publicly accessible. Reports of trials must conform to CONSORT 2010 guidelines (*https://consort-statement.org/consort-2010*). Articles reporting the results of randomized trials must include the CONSORT flow diagram showing the progress of patients throughout the trial.

Conflict of Interest: All authors are required to disclose any actual or potential conflict of interest including financial interests or relationships with other people or organizations that might raise questions of bias in the work reported. If no conflict of interest exists for each author, please state "There is no conflict of interest to disclose".

Submission Declaration: When a manuscript is considered for submission to *Drug Discoveries & Therapeutics*, the authors should confirm that 1) no part of this manuscript is currently under consideration for publication elsewhere; 2) this manuscript does not contain the same information in whole or in part as manuscripts that have been published, accepted, or are under review elsewhere, except in the form of an abstract, a letter to the editor, or part of a published lecture or academic thesis; 3) authorization for publication has been obtained from the authors' employer or institution; and 4) all contributing authors have agreed to submit this manuscript.

Initial Editorial Check: Immediately after submission, the journal's managing editor will perform an initial check of the manuscript. A suitable academic editor will be notified of the submission and invited to check the manuscript and recommend reviewers. Academic editors will check for plagiarism and duplicate publication at this stage. The journal has a formal recusal process in place to help manage potential conflicts of interest of editors. In the event that an editor has a conflict of interest with a submitted manuscript or with the authors, the manuscript, review, and editorial decisions are managed by another designated editor without a conflict of interest related to the manuscript.

Peer Review: *Drug Discoveries & Therapeutics* operates a single-anonymized review process, which means that reviewers know the names of the authors, but the authors do not know who reviewed their manuscript. All articles are evaluated objectively based on academic content. External peer review of research articles is performed by at least two reviewers, and sometimes the opinions of more reviewers are sought. Peer reviewers are selected based on their expertise and ability to provide quality, constructive, and fair reviews. For research manuscripts, the editors may, in addition, seek the opinion of a statistical reviewer. Every reviewer is expected to evaluate the manuscript in a timely, transparent, and ethical manner, following the COPE guidelines (*https://publicationethics.org/files/cope-ethical-guidelines-peer-reviewers-v2_0.pdf*). We ask authors for sufficient revisions (with a second round of peer review, when necessary) before a final decision is made. Consideration for publication is based on the article's originality, novelty, and scientific soundness, and the appropriateness of its analysis.

Suggested Reviewers: A list of up to 3 reviewers who are qualified to assess the scientific merit of the study is welcomed. Reviewer information including names, affiliations, addresses, and e-mail should be provided at the same time the manuscript is submitted online. Please do not suggest reviewers with known conflicts of interest, including participants or anyone with a stake in the proposed research; anyone from the same institution; former students, advisors, or research collaborators (within the last three years); or close personal contacts. Please note that the Editor-in-Chief may accept one or more of the proposed reviewers or may request a review by other qualified persons.

Language Editing: Manuscripts prepared by authors whose native language is not English should have their work proofread by a native English speaker before submission. If not, this might delay the publication of your manuscript in *Drug Discoveries & Therapeutics*.

The Editing Support Organization can provide English proofreading, Japanese-English translation, and Chinese-English translation services to authors who want to publish in *Drug Discoveries & Therapeutics* and need assistance before submitting a manuscript. Authors can visit this organization directly at *https://www.iacmhr.com/iac-eso/support.php?lang=en. IAC-ESO* was established to facilitate manuscript preparation by researchers whose native language is not English and to help edit works intended for international academic journals.

Copyright and Reuse: Before a manuscript is accepted for publication in *Drug Discoveries & Therapeutics*, authors will be asked to sign a transfer of copyright agreement, which recognizes the common interest that both the journal and author(s) have in the protection of copyright. We accept that some authors (*e.g.*, government employees in some countries) are unable to transfer copyright. A JOURNAL PUBLISHING AGREEMENT (JPA) form will be e-mailed to the authors by the Editorial Office and must be returned by the authors by mail, fax, or as a scan. Only forms with a hand-written signature from the corresponding author are accepted. This copyright will ensure the widest possible dissemination of information. Please note that the manuscript will not proceed to the next step in publication until the JPA Form is received. In addition, if excerpts from other copyrighted works are included, the author(s) must obtain written permission from the copyright owners and credit the source(s) in the article.

4. Cover Letter

The manuscript must be accompanied by a cover letter prepared by the corresponding author on behalf of all authors. The letter should indicate the basic findings of the work and their significance. The letter should also include a statement affirming that all authors concur with the submission and that the material submitted for publication has not been published previously or is not under consideration for publication elsewhere. The cover letter should be submitted in PDF format. For an example of Cover Letter, please visit: Download Centre (*https://www.ddtjournal.com/downcentre)*.

5. Submission Checklist

The Submission Checklist should be submitted when submitting a manuscript through the Online Submission System. Please visit Download Centre (*https://www.ddtjournal.com/downcentre)* and download the Submission Checklist file. We recommend that authors use this checklist when preparing your manuscript to check that all the necessary information is included in your article (if applicable), especially with regard to Ethics Statements.

6. Manuscript Preparation

Manuscripts are suggested to be prepared in accordance with the "Recommendations for the Conduct, Reporting, Editing, and Publication of Scholarly Work in Medical Journals", as presented at *http://www.ICMJE.org*.

Manuscripts should be written in clear, grammatically correct English and submitted as a Microsoft Word file in a single-column format. Manuscripts must be paginated and typed in 12-point Times New Roman font with 24-point line spacing. Please do not embed figures in the text. Abbreviations should be used as little as possible and should be explained at first mention unless the term is a well-known abbreviation (*e.g.* DNA). Single words should not be abbreviated.

Title page: The title page must include 1) the title of the paper (Please note the title should be short, informative, and contain the major key words); 2) full name(s) and affiliation(s) of the author(s), 3) abbreviated names of the author(s), 4) full name, mailing address, telephone/fax numbers, and e-mail address of the corresponding author; 5) author contribution statements to specify the individual contributions of all authors to this manuscript, and 6) conflicts of interest (if you have an actual or potential conflict of interest to disclose, it must be included as a footnote on the title page of the manuscript; if no conflict of interest

exists for each author, please state "There is no conflict of interest to disclose").

Abstract: The abstract should briefly state the purpose of the study, methods, main findings, and conclusions. For article types including Original Article, Brief Report, Review, Policy Forum, and Case Report, a one-paragraph abstract consisting of no more than 250 words must be included in the manuscript. For Communications, Editorials, News, or Letters, a brief summary of main content in 150 words or fewer should be included in the manuscript. For articles reporting clinical trials, the trial registration number should be stated at the end of the Abstract. Abbreviations must be kept to a minimum and non-standard abbreviations explained in brackets at first mention. References should be avoided in the abstract. Three to six key words or phrases that do not occur in the title should be included in the Abstract page.

Introduction: The introduction should provide sufficient background information to make the article intelligible to readers in other disciplines and sufficient context clarifying the significance of the experimental findings.

Materials/Patients and Methods: The description should be brief but with sufficient detail to enable others to reproduce the experiments. Procedures that have been published previously should not be described in detail but appropriate references should simply be cited. Only new and significant modifications of previously published procedures require complete description. Names of products and manufacturers with their locations (city and state/country) should be given and sources of animals and cell lines should always be indicated. All clinical investigations must have been conducted in accordance with the Declaration of Helsinki (as revised in 2013, *https://wma.net/what-we-do/medical-ethics/declaration-of-helsinki*). All human and animal studies must have been approved by the appropriate institutional review board(s) and a specific declaration of approval must be made within this section.

Results: The description of the experimental results should be succinct but in sufficient detail to allow the experiments to be analyzed and interpreted by an independent reader. If necessary, subheadings may be used for an orderly presentation. All Figures and Tables should be referred to in the text in order, including those in the Supplementary Data.

Discussion: The data should be interpreted concisely without repeating material already presented in the Results section. Speculation is permissible, but it must be well-founded, and discussion of the wider implications of the findings is encouraged. Conclusions derived from the study should be included in this section.

Acknowledgments: All funding sources (including grant identification) should be credited in the Acknowledgments section. Authors should also describe the role of the study sponsor(s), if any, in study design; in the collection, analysis, and interpretation of data; in the writing of the report; and in the decision to submit the paper for publication. If the funding source had no such involvement, the authors should so state.

In addition, people who contributed to the work but who do not meet the criteria for authors should be listed along with their contributions.

References: References should be numbered in the order in which they appear in the text. Citing of unpublished results, personal communications, conference abstracts, and theses in the reference list is not recommended but these sources may be mentioned in the text. In the reference list, cite the names of all authors when there are fifteen or fewer authors; if there are sixteen or more authors, list the first three followed by *et al*. Names of journals should be abbreviated in the style used in PubMed. Authors are responsible for the accuracy of the references. The EndNote Style of *Drug Discoveries & Therapeutics* could be downloaded at **EndNote** (*https://www.ddtjournal.com/examples/Drug_Discoveries_Therapeutics.ens*).

Examples are given below:

Example 1 (Sample journal reference):

Nakata M, Tang W. Japan-China Joint Medical Workshop on Drug Discoveries and Therapeutics 2008: The need of Asian pharmaceutical researchers' cooperation. Drug Discov Ther. 2008; 2:262-263.

Example 2 (Sample journal reference with more than 15 authors):

Darby S, Hill D, Auvinen A, *et al*. Radon in homes and risk of lung cancer: Collaborative analysis of individual data from 13 European case-control studies. BMJ. 2005; 330:223.

Example 3 (Sample book reference):

Shalev AY. Post-traumatic stress disorder: Diagnosis, history and life course. In: Post-traumatic Stress Disorder, Diagnosis, Management and Treatment (Nutt DJ, Davidson JR, Zohar J, eds.). Martin Dunitz, London, UK, 2000; pp. 1-15.

Example 4 (Sample web page reference):

World Health Organization. The World Health Report 2008 – primary health care: Now more than ever. *https://apps.who.int/iris/handle/10665/43949* (accessed September 23, 2022).

Tables: All tables should be prepared in Microsoft Word or Excel and should be arranged at the end of the manuscript after the References section. Please note that tables should not in image format. All tables should have a concise title and should be numbered consecutively with Arabic numerals. If necessary, additional information should be given below the table.

Figure Legend: The figure legend should be typed on a separate page of the main manuscript and should include a short title and explanation. The legend should be concise but comprehensive and should be understood without referring to the text. Symbols used in figures must be explained. Any individually labeled figure parts or panels (A, B, *etc*.) should be specifically described by part name within the legend.

Figure Preparation: All figures should be clear and cited in numerical order in the text. Figures must fit a one- or two-column format on the journal page: 8.3 cm (3.3 in.) wide for a single column, 17.3 cm (6.8 in.) wide for a double column; maximum height: 24.0 cm (9.5 in.). Please make sure that artwork files are in an acceptable format (TIFF or JPEG) at minimum resolution (600 dpi for illustrations, graphs, and annotated artwork, and 300 dpi for micrographs and photographs). Please provide all figures as separate files. Please note that low-resolution images are one of the leading causes of article resubmission and schedule delays.

Units and Symbols: Units and symbols conforming to the International System of Units (SI) should be used for physicochemical quantities. Solidus notation (*e.g*. mg/kg, mg/mL, mol/mm^2/min) should be used. Please refer to the SI Guide *www.bipm.org/en/si/* for standard units.

Supplemental data: Supplemental data might be useful for supporting and enhancing your scientific research and *Drug Discoveries & Therapeutics* accepts the submission of these materials which will be only published online alongside the electronic version of your article. Supplemental files (figures, tables, and other text materials) should be prepared according to the above guidelines, numbered in Arabic numerals (*e.g*., Figure S1, Figure S2, and Table S1, Table S2) and referred to in the text. All figures and tables should have titles and legends. All figure legends, tables and supplemental text materials should be placed at the end of the paper. Please note all of these supplemental data should be provided at the time of initial submission and note that the editors reserve the right to limit the size

and length of Supplemental Data.

7. Online Submission

Manuscripts should be submitted to *Drug Discoveries & Therapeutics* online at *https://www.ddtjournal.com/login*. Receipt of your manuscripts submitted online will be acknowledged by an e-mail from Editorial Office containing a reference number, which should be used in all future communications. If for any reason you are unable to submit a file online, please contact the Editorial Office by e-mail at *office@ddtjournal.com*

8. Accepted Manuscripts

Page Charge: Page charges will be levied on all manuscripts accepted for publication in *Drug Discoveries & Therapeutics* (Original Articles / Brief Reports / Reviews / Policy Forum / Communications: $140 per page for black white pages, $340 per page for color pages; News / Letters: a total cost of $600). Under exceptional circumstances, the author(s) may apply to the editorial office for a waiver of the publication charges by stating the reason in the Cover Letter when the manuscript online.

Misconduct: *Drug Discoveries & Therapeutics* takes seriously all allegations of potential misconduct and adhere to the ICMJE Guideline (*https://icmje.org/recommendations*) and COPE Guideline (*https://publicationethics.org/files/Code_of_conduct_for_journal_editors.pdf*). In cases of suspected research or publication misconduct, it may be necessary for the Editor or Publisher to contact and share submission details with third parties including authors' institutions and ethics committees. The corrections, retractions, or editorial expressions of concern will be performed in line with above guidelines.

(As of December 2022)

Drug Discoveries & Therapeutics
Editorial and Head Office
Pearl City Koishikawa 603,
2-4-5 Kasuga, Bunkyo-ku,
Tokyo 112-0003, Japan.
E-mail: office@ddtjournal.com